MODELING THE POST-INJURY JOINT ENVIRONMENT FOR THE INVESTIGATION OF POST-TRAUMATIC OSTEOARTHRITIS

A Dissertation

Presented to the Faculty of the Graduate School

of Cornell University

In Partial Fulfillment of the Requirements for the Degree of

Doctor of Philosophy

by

Steven Ayala

December 2022

MODELING THE POST-INJURY JOINT ENVIRONMENT FOR THE INVESTIGATION OF POST-TRAUMATIC OSTEOARTHRITIS

Steven Ayala, Ph. D.

Cornell University 2022

Articular cartilage is the soft tissue found at the end of long bones within the joint capsule and plays an important role in load transmission and facilitating joint motion. However, traumatic injury delivered to joints generates extreme supraphysiologic shear and compressive forces which result in joint inflammation and significant damage to both cartilage tissue and chondrocytes. Chronic persistence of post-injury changes often results in the development of post-traumatic osteoarthritis (PTOA). Treatment options for cartilaginous injuries are limited due to the lack of vasculature or lymphatics, which limit the transport of anabolic cytokines to injured areas. Furthermore, development of disease modifying treatments is hindered by the lack of suitable PTOA models to conduct experimental trials upon as current models are unable to accurately model the post-injury joint environment, thereby limiting their translational relevance.

Thus, the overall goal of this thesis was to generate an ex vivo model of PTOA that could more closely capture the characteristics of an injured synovial joint. This was achieved by demonstrating that simultaneous compressive and shear forces delivered to cartilage generated a profile of chondrocyte damage that is more physiologically relevant to what is expected in vivo (Chapter 1). Secondly, by assessing changes in cartilage mechanical properties pre- and post-injury and relating

these changes to resulting chondrocyte damage, to evaluate chondrocyte sensitivity to mechanical loading (Chapter 2). Finally, the effect of negatively altering the lubricating qualities of synovial fluid on the relationship between local shear strains and cellular damage was also assessed (Chapter 3). Collectively, this work offers crucial insight into the mechanisms behind the early stages of PTOA pathogenesis and provides a physiologically relevant model to be utilized for future testing of potential PTOA therapeutics.

BIOGRAPHICAL SKETCH

Steven Ayala was born in New Brunswick NJ, in 1995 and grew up in Keyport, NJ. After graduating from Keyport High School in 2013, he went on to attend The College of New Jersey (TCNJ) through the assistance of TCNJ's Educational Opportunity Fund. During his time at TCNJ, Steven was a part of multiple on-campus organizations such as Delta Tau Delta fraternity, Community Advisors, The College Ambassador Program, and performed research under the advisement of Dr. Anthony G. Lau. During his time performing research with Dr. Lau, Steven worked projects investigating bone quality after exposure to low dose radiation and the biocompatibility of novel bone scaffolds using finite element analysis. In May 2017 Steven graduated from TCNJ *Magna Cum Laude* with a Bachelor of Science degree in biomedical engineering.

In the Fall of 2017 Steven was selected to receive a scholarship from the Alfred P. Sloan Foundation's Minority Ph.D. program to begin pursuing a PhD in biomedical engineering at Cornell University. Shortly after, Steven joined The Bonassar Research Group, led by Dr. Lawrence Bonassar, where he began performing research focused on developing models to study the injury response of cartilage. During his time at Cornell, Steven also served as the Live-In Advisor for Delta Kappa Epsilon fraternity from 2019 - 2022. Following graduation Steven plans on using his knowledge of biological sciences and transitioning into industry.

This dissertation is dedicated to my mentors, friends, family, and loving fiancée.

Without their support and guidance this work would not be possible.

ACKNOWLEDGMENTS

I'd like to begin by giving thanks to God for this opportunity I've been blessed with and the life I've been given. This journey has been exceptionally challenging and yet immensely rewarding. I also thank God for giving me the tenacity to keep moving forward every day. I'm reminded of Psalm 23:4, "Yea, though I walk through the valley of the shadow of death, I will fear no evil: for thou art with me; thy rod and thy staff they comfort me." Throughout my life these words have always served as a powerful source of strength. I'm grateful for the incredible people He has placed on my path through my graduate career who've guided me to reach this milestone in my life.

Next, I'd like to thank my advisor, Lawrence Bonassar, who has been an extraordinary mentor to me and has provided priceless guidance, insight, and support throughout my Cornell experience. In moments where I felt lost about what to do next with my research, had doubts in my talents and abilities, or simply needed to voice my concerns, Larry was always there to give me the wisdom I needed. Michelle Delco and Nelly Andarawis-Puri have also been amazing mentors and have played a crucial role as my thesis committee members, providing remarkable advice and encouragement throughout my studies. I'd also like to thank the Cornell BME administration, faculty, and staff for providing a welcoming environment that facilitated my growth into a professional researcher, and the Alfred P. Sloan Foundation for providing the funding that allowed me to begin my career here at Cornell.

I'd also like to give thanks to all my peers in the BME cohort, who I am proud to call my friends and colleagues, particularly Hania Koziol who has never failed to

make me laugh. Next, I'd like to thank the Delta Chi Chapter of Delta Kappa Epsilon at Cornell University for the pleasure of serving as their Live-In Advisor from 2019 - 2022. There was never a dull moment during my time at the house so thank you for providing me with countless laughs, stimulating debates, and amazing memories. I give special thanks to all past and present members of the Bonassar Research Group: Eddie Bonnevie, Chris DiDomenico, Ben Cohen, Alex Boys, Jill Middendorf, Nicole Diamantides, Stephen Sloan, Becka Irwin, Liz Feeney, Marianne Lintz, Jongkil Kim, Leigh Slyker, Sean Kim, Karan Vishwanath, Eric Yoon, Rachel Yerden, Sera Lopez, Alicia Matavosian, Alikhan Fidai, Caroline Thompson, Aiyana Fortin, Emily Jiang, and Jared Matthews. You all have made my time at Cornell an incredible experience and I'm honored to call you all my friends, I look forward to staying in touch and hearing all about your future achievements as you become trailblazers in your respective fields.

I'd like to thank all my friends from home who have been some of my biggest supporters. You all made every phone call, weekend trip, and vacation a cherished memory. Thank you for always being there for me; I can't wait to make more memories with you all in the years to come. To my dear mother and father, thank you for raising me into the man I am today, for all the sacrifices you've made for me, and for always believing in me. To my brothers: Brian, Matthew, Adrian, and Isaac, I love you guys more than words can describe. To my stepmother, grandparents, aunts, uncles, cousins, and the Kelly, Crawbuck, and Field family, thank you for always cheering me on and giving me strength.

Last and certainly not least, I would like to thank my loving fiancée, Liz Kelly,

for her unending support throughout my PhD. Thank you for all the phone calls, letters, pizza dates, personal photoshoots, lazy Sundays, vacations, pep talks, hard truths, long drives, and amazing memories we've shared. Thank you for believing in me every step of the way, you motivate me to achieve my full potential. I couldn't imagine my life without you. I vow to repay your unfaltering love and encouragement over these years by becoming your husband and doing my part to bring about a happy life for us and our future family.

TABLE OF CONTENTS

LIST OF FIGURES

PI and n = 3 for groups with PI.

Figure 4.S2. Depth-dependent shear modulus of cartilage samples. n = 8.

LIST OF TABLES

CHAPTER 1

An Introduction to Post-Traumatic Osteoarthritis

Structure and Function of Articular Cartilage

Articular cartilage is the soft tissue found at the end of long bones and function as a low-friction and highly durable wear-resistant surface to transmit loads and facilitate joint movement (Figure 1.1).[1] Articular cartilage is composed of hyaline cartilage, the most abundant type of cartilage in the human body, and is able to support up to 2.5-5 times body weight during normal movement.[2] Articular cartilage is able to achieve this functionality due to its highly specialized extracellular matrix (ECM), which contains cells called chondrocytes.[3] However, unlike most tissues, articular cartilage lacks presence of blood vessels, nerves, or lymphatics thus limiting transport of nutrients and growth factors to cells. Therefore, transport of metabolites through the ECM to chondrocytes is primarily directed by interstitial fluid flow that is generated during cyclic compression.[4]

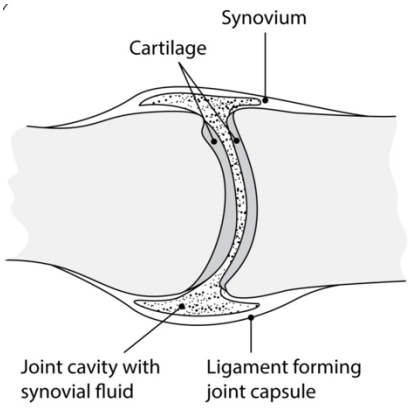

Figure 1.1. Normal, healthy synovial joint. Figure adapted from Tamer[5]

The ECM of articular cartilage is primarily composed of water (65-80%), collagen (10-20%), proteoglycans (10-20%), and other glycoproteins, lipids,

carbohydrates, and noncollagenous proteins (<5%).[6] Water content within articular cartilage varies spatially with water concentration being highest at the cartilage surface and decreases towards the subchondral bone. The presence of water within the ECM causes the mechanics of articular cartilage to behave with properties of both a solid and fluid, thus being referred to as a viscoelastic material.[7] Dissolved within the water are ions such as sodium, calcium, potassium, and chloride that are circulated to chondrocytes via interstitial fluid flow, along with growth factors, cytokines, and enzymes necessary for metabolism.[4,8] Collagen is the most prevalent structural macromolecule in the ECM, composing roughly two-thirds of the dry weight of articular cartilage.[3,6,9] The most abundant type of collagen within the collagen network is type II representing 90-95% of the ECM collagen and types I, III, IV, V, IX, and XI representing the remaining collagen.[10] The collagen within the network exist as fibers that behave as ropes resisting tensile forces, however they buckle under compressive loads due their slender nature. These collagen fibers together form the collagen network and are responsible for providing tensile and shear stiffness to the articular cartilage.[6,11]

The final major component that comprises articular cartilage are proteoglycans which account for roughly 30% of the dry weight.[1,4,7,8] Proteoglycans are protein polysaccharides that consist of a protein core with 1 or more negatively charged glycosaminoglycans (GAG) chains that are covalently attached to the core. These chains extend out from the core and remain distanced from one another due to charge repulsion. Proteoglycan chains fill the spaces between collagen fibers and are thus restrained by the collagen network from free expansion.[12] Proteoglycans preserve fluid

and ionic charge balance in articular cartilage through its negative charge that attracts cations and water into the cartilage matrix, generating a selling pressure.[1,13,14] Conversely to water content, proteoglycan content is lowest at the cartilage surface and increases towards the subchondral bone. During cartilage compression, water flows out through the articular surface and proteoglycans inside the matrix are pushed closer together. By decreasing the distance between mutually charged glycosaminoglycan side chains repulsive forces are greatly increased, in turn generating resistance to compressive loads.[8,15]

The components of the articular cartilage are organized in a highly organized matrix whose contents and mechanical properties vary depth-dependently and is characterized by a distinct zonal arrangement (Figure 1.2).[16] The zones that comprise the articular cartilage are the superficial zone, middle zone, and deep zone with each zone containing a specific morphology, organization of chondrocytes, and biochemical content. The surface zone of the cartilage comprises the top 10-20% of the cartilage thickness containing tightly packed collagen fibers aligned parallel to the articular surface and a dense population of small and flat chondrocytes.[7,17,18] Due to the impermeability of the subchondral bone, fluid flow exudes out of the articular cartilage primarily from the surface zone and to some extent the middle zone.[19] The orientation of collagen fibers in this region allows for articular cartilage to resist shear deformations caused by joint articulation.[6,20,21] The surface also acts as a protective layer for the rest of the cartilage by dissipating energy via increased compliance compared to the tissue bulk.[22–24] Disruption of the surface layer can result in reduced surface mechanics, increased tissue permeability, and greater stress on the ECM. The

middle zone of articular cartilage represents 40-60% of tissue thickness and contains greater proteoglycan content, thicker collagen fibers that exist in an ambiguous orientation, and sparsely distributed rounded chondrocytes.[20,25] Within the middle zone of the articular cartilage the compressive and shear stiffness of the ECM significantly increases compared to the surface, providing structural integrity to the matrix.[22,26] Finally, the deep zone accounts for the final ~30% of articular cartilage thickness and contains the thickest collagen fibers, greatest proteoglycan content, and lowest water content.[27,28] This region contains the lowest chondrocyte density throughout the articular cartilage, which are arranged in columns called chondrons that are parallel to collagen fibers and perpendicular to the articular surface.[1,7,20,29] The deep zone of articular cartilage provides the greatest resistance to compressive forces given orientation of collagen fibes.[7,20,30] Despite the robustness of articular cartilage, degenerative stimuli can potentially alter its zonal structure, biochemical components, and mechanical functionality, causing development of joint disease.

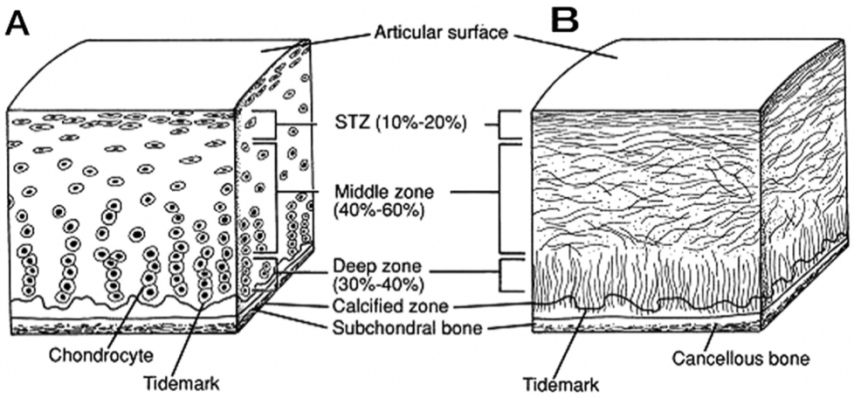

Figure 1.2. Schematic, cross-sectional diagram of healthy articular cartilage: A, cellular organization in the zones of articular cartilage; B, collagen fiber architecture. Figure adapted from Fox et al.[3]

Post-Traumatic Osteoarthritis

Osteoarthritis (OA) is the most common joint disease and is categorized by progressive degradation of the articular cartilage, changes to the subchondral bone, and inflammation of the joint capsule and synovium that ultimately leads to joint failure.[31,32] Estimates indicate this condition affects 46.4 million adults in the US alone and causes a financial burden of over $100 billion per year in healthcare costs.[33,34] OA is a disease with varying phenotypes, each with their own mechanism of development. Prior studies have indicated six variables that lead to distinct clinical phenotypes: aging, chronic inflammation, obesity/metabolic syndrome, bone and cartilage metabolism, minimal joint disease, and cartilage injury.[35–37] This thesis will focus specifically on the phenotype of OA that is caused by traumatic cartilage injury, which is known as post-traumatic osteoarthritis (PTOA).

PTOA represents 12% of all OA cases and is an especially debilitating form of OA due to the patient population being generally younger and more active compared to those who develop idiopathic OA.[34,38–40] PTOA is caused by momentary supraphysiologic shear and compressive forces delivered to articular cartilage during joint trauma, which may produce osteochondral lesions and joint inflammation.[41–44] High impact loading is typically responsible for PTOA development, which may occur during incidents such as sports injuries, falling, and traffic accidents. Loads that are classified as impacts are determined by rate of loading, rather than solely impact magnitude, which may be as high as 30 times faster than physiological loading rates.[41] There are five common injuries that are associated with placing patients at greater risks of developing PTOA which are: anterior cruciate ligament rupture, meniscal

tearing, shoulder dislocation, patellar dislocation, and ankle sprains (Figure 1.3).[38,45–49] Each of these injury modalities generates joint inflammation along with a cascade of catabolic processes that result in damage to chondrocytes and the ECM; however PTOA development occurs through long-term perpetuation of catabolic processes.[50]

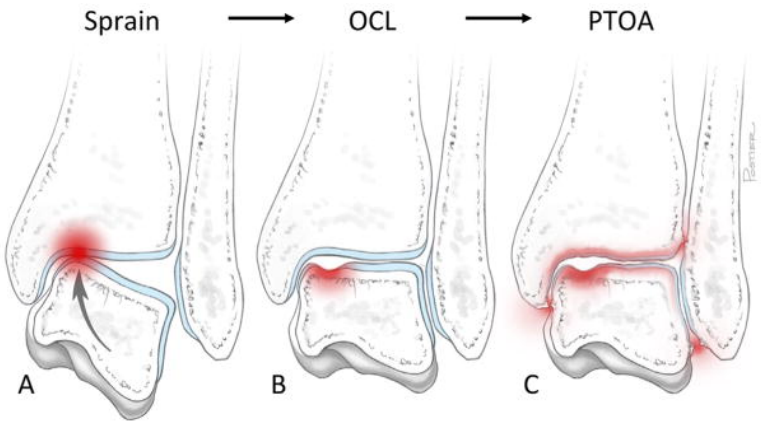

Figure 1.3. The proposed mechanism of posttraumatic osteoarthritis after a severe ankle sprain. (A) During a typical lateral ankle sprain (inversion) the medial aspect of the talus likely impacts the tibial plafond, which may result in (B) a talar osteochondral lesion. Direct trauma to the articular surface can initiate progressive, irreversible joint destruction culminating in (C) late-stage posttraumatic osteoarthritis years to decades after the original injury. Figure adapted from Delco et al.[51]

Consequences of Traumatic Injury to Cartilage

Mechanical injury subjects the ECM and chondrocytes of articular cartilage to supraphysiological compression, which causes immediate chondrocyte necrosis and rupturing of the articular surface.[52,53] In the minutes to hours following the initial insult, several pro-inflammatory cytokines are released and transported through the synovial fluid, including: interleukin (IL)-1β, IL-6, IL-8, tumor necrosis factor (TNFα), matrix metalloproteinases (MMP)-1, MMP-13, aggrecanases, nitric oxide, and other reactive oxygen species (ROS) (Figure 1.4).[43,52,54–56] These cytokines promote PTOA development through various biological pathways for example: ILs

and TNFα has been shown to inhibit collagen II and GAG synthesis as well as increase caspase activity leading to chondrocyte apoptosis, MMPs cause degradation of type II collagen and the ECM, aggrecanases which catabolize aggrecan, and finally ROS increase oxidative stress and trigger mitochondria (MT) mediated apoptosis and cell death.[57–63] These processes are intended to remove debris and microbes around the injury site before tissue repair can take place, however prolonged inflammation results in these cytokines acting synergistically to create a viscous cycle of cartilage destruction.[64] Studies show that synovial fluid concentration of these cytokines is highest 0-1 days post injury but may remain significantly elevated up to four weeks after traumatic injury, and can stay elevated even after one year.[65–72] Multiple factors can affect the duration of inflammation such as reinjury, which restarts the release of pro-inflammatory mediators with continued exposure leading to PTOA pathogenesis.[54] Additionally, joint instability may also extend the inflammatory process by altering joint kinematics and cause abnormal and injurious loading of the joint surface.[38] Nevertheless, once inflammation subsides the cartilage tissue will begin the healing process, however its lack of vascularity severely limits its regenerative capacity.[43]

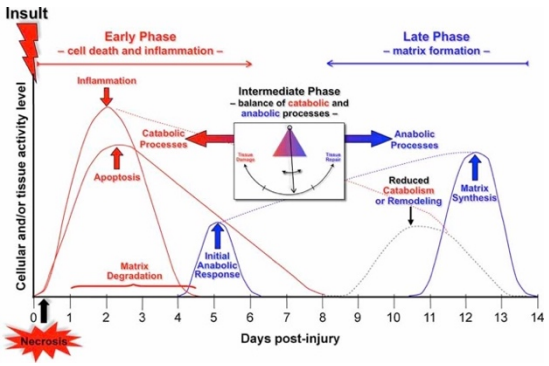

Figure 1.4. This conceptual framework depicts the immediate cellular responses to acute joint trauma and facilitates the identification of targets for early interventions. Catabolic and anabolic processes are involved in the response to the injury and overlap with one another. Figure adapted from Anderson et al.[43]

The cartilage healing process commences with the recruitment of cells to the area that secrete anti-inflammatory factors and trigger anabolic processes such as: macrophages, dendritic cells, and T cells.[57] M2 macrophages stimulate Th2 cells to release IL-10, transforming growth factor (TGF)-β1, IL-1 receptor antagonist, and other cytokines which act to inhibit inflammation, reduce chondrocyte apoptosis, and promote cartilage repair.[73,74] TGF-β1 release is particularly noteworthy due to its role as a key mediator of chondrocyte homeostasis by stimulating collagen type II and GAG deposition, and modulating chondrogenic enzymes.[75,76] Additionally, immature dendritic cells are activated post-injury to promote mesenchymal stem cell (MSC) chondrogenic differentiation, and T cells inhibit production of pro-inflammatory cytokines while also releasing IL-4 and IL-5 to reduce inflammation.[77,78] This healing effect maybe aided by penetration of the subchondral bone if sufficient damage was delivered during injury to allow exposure of its vascularity to the defect site to deliver nutrients to the cartilage.[56,79] During the healing process a rudimentary repair matrix is laid down in the form of a transitional tissue between hyaline cartilage and fibrous ligaments known as fibrocartilage and hypertrophic cartilage, containing high levels of type I and X collagen respectively, thick collagen fibers, and poor ground substance of cartilaginous tissues.[80,81] While this structure may fill defect sites, reports have shown this provisional matrix displays mixed clinical results compared to hyaline cartilage.[82]

A large factor for the inferiority of fibrocartilage compared to hyaline cartilage is the difference in mechanical properties between both tissue types.[83–85] This mismatch of mechanical properties often generates stress concentrations at the

interface of these two tissues due to insufficient integration.[86,87] Fibrocartilage has shown to have lower compressive stiffness than hyaline cartilage, making it unable to withstand the compressive loads that are generated in during articulation leading to eventual deterioration to the repair matrix and surrounding areas.[88,89] Furthermore, repair sites typically possess rough and incongruent surfaces that causes abnormal local pressures that may exceed the load bearing capacities of both hyaline cartilage and fibrocartilage leading to additional surface fibrillation.[90] These limitations of fibrocartilage may ultimately mean the scar tissue formed during healing is predisposed to further damage over the long-term. Unfortunately, there currently exists no way to promote the growth of hyaline cartilage into defect sites of injured joints. However, research is being done to investigate possible treatments for PTOA ranging from: surgical interventions, tissue engineered devices, and disease-modifying therapies.[91–93]

Existing Treatments for Post-Traumatic Osteoarthritis

Despite the poor intrinsic repair capacities of native articular cartilage, there have been several advancements made in surgical techniques to treat cartilage fracture and osteochondral lesions. The first major category of surgical intervention for the treatment of OA is joint arthroplasty: joints with late-stage OA will have all or portions of cartilage removed along with a small amount of underlying bone and have a prosthetic device made of metal, ceramic, and/or heavy-duty plastic attached to the bone (Figure 1.5).[94,95] Rather than addressing underlying cartilage degeneration, joint arthroplasty primarily seeks to treat patient joint pain and restore lost functionality by

providing a new articulating surface, free of osteochondral defects and bone spurs, to facilitate joint motion.[96,97] Typically, joint arthroplasty show low rates of medical complications, low mortality rates, and revision rates of approximately 4%-25% over 10 years and 8%-45% over 15 years.[98,99] Unfortunately, this procedure is not ideal for PTOA treatment due to a younger patient population with more active demands, compared to the generally elderly population of arthroplasty patients, which may result in higher occurrences of revision over the patient's lifetime.[96,100]

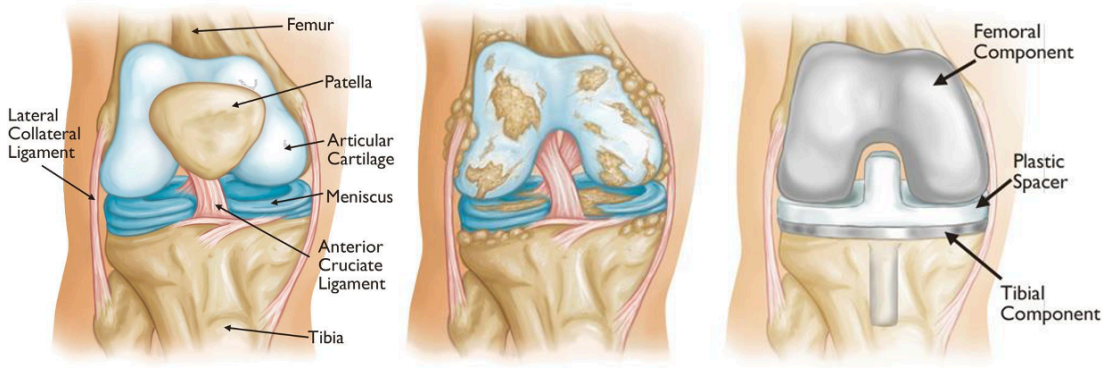

Figure 1.5. (Left) Normal knee anatomy (Middle) Severe osteoarthritis (Right) Arthritic cartilage has been removed and resurfaced with metal implants on the femur and tibia, and a plastic spacer in between metal implants. Figure adapted from American Academy of Orthopaedic Surgeons[101]

The next series of surgical interventions used for PTOA treatment involve the filling of osteochondral defects through stimulation of fibrocartilage development or transplantation of osteochondral grafts. To stimulate infiltration of blood into defect sites to trigger fibrocartilage formation, surgeons drill into the underlying subchondral bone to expose its vascularity in an operation known as microfracture.[102–104] Autologous chondrocyte isolation (ACI) and platelet-rich plasma (PRP) represent alternative approaches to microfracture, where a chondral biopsy is sourced from a minor load-bearing area to culture chondrocytes (ACI) or platelets are extracted from

peripheral venous blood (PRP) for later transplantation into the defect site.[82,105–107] While microfracture, ACI, and PRP produce fibrocartilage infill and satisfactory short to midterm clinical outcomes, long-term outcomes have shown mixed results.[108–111] As stated previously, this is due to the decreased compressive stiffness and decreased shear resistance compared to hyaline cartilage.[112] However, techniques such as osteochondral autograft transplantation (OAT) involve harvesting osteochondral plug(s) from non-weight bearing areas of the knee to fill osteochondral defects.[113,114] The benefit of this technique is that native hyaline cartilage is used to fill defect sites rather than using fibrocartilage, however it is also limited by the amount of donor tissue available and is therefore ideal on lesions smaller than 4 cm^2.[115] Studies have reported osteochondral transplantation may display improved clinical outcomes compared to techniques relying on fibrocartilage infill.[82,116,117] Despite promising initial results, long-term results for OAT also show eventual progression towards PTOA.[118] Therefore, research has focused on developing tissue engineering strategies to develop graft materials that can be used as a biological scaffold to promote cartilage regeneration.[119]

Tissue engineering strategies to treat OCLs typically involve creation of a three-dimensional scaffolds that is cultured with autologous chondrocytes or stem cells for later implantation into the defect site.[120] The goal of this technique is to recreate the native architecture and functionality of hyaline cartilage, which requires materials able to support and facilitate the growth and expansion of seeded cells while also remaining stiff enough to support physiologic loads. To achieve this goal multiple types of scaffold material have been tested, including hydrogels, decellularized

cartilage matrix, hyaluronic acid, collagen, and synthetic polymers.[121–124] While these scaffolds have shown promising results, there are still advancements that need to be made with this technology before being implemented clinically. Specifically, the stiffness of scaffolds must be improved to support physiologic loads so uneven wear of the surrounding tissue is avoided and biochemical composition must more closely match that of hyaline cartilage to better mimic its biological and mechanical functions.[125,126]

Future treatment for PTOA involves the development of disease modifying drugs that seek to modulate catabolic biological processes to impede disease progression during early stages of cartilage degeneration.[127] Clinical management of PTOA typically involves a combination of pharmacological and non-pharmacological treatment options that are aimed at treating patient symptomology such as pain and reduced joint mobility rather than treating underlying disease pathogenesis.[128] Biologic agents tested so far include bone morphogenic protein (BMP)-7, MMP inhibitors, caspase inhibitors, TNF inhibitors, antioxidants such as SS-31, bisphosphonates, and gene therapies.[129–134] Currently, none of these potential therapeutics have met regulatory approval for clinical use due to disappointing outcomes in clinical trials.[52] In order to overcome this obstacle existing models of PTOA need to be improved to better model the post-injury joint environment and increase their translational relevance.

Research Objectives

The primary goal of this thesis project was to generate an ex vivo model of

PTOA that could more closely mimic the environment of an injured synovial joint. The primary hypotheses examined in this project were: (1) post-injury cartilage articulation will lead to a synergistic increase in chondrocyte damage in a depth-dependent manner throughout the tissue (Chapter 2), (2) chondrocytes possess an intrinsic sensitivity to shear loading which is altered after injury due to a reduction in cartilage mechanical properties (Chapter 3), and finally (3) poor lubricating synovial fluid will can alter chondrocyte sensitivity to strain by increasing depth-dependent shear strains experienced by cartilage tissue, leading to exacerbated adverse cellular response (Chapter 4).

Specific Aims

Specific Aim 1 (Chapter 2)

Evaluate the effect of combined mechanical loading on chondrocytes via traumatic injury followed by articulation on cartilage tissue

Traditional models of PTOA typically involve a single cycle of rapid impact loading followed by assessment of cellular and/or tissue level damage found in the cartilage tissue through various types of techniques. However, PTOA pathogenesis in vivo is complicated due to continued movement of the injured joint post-injury. these Single impact PTOA models fail to capture the mechanical environment of an injured joint, where joint articulation subjects injured cartilage tissue to continuous shear loading. The goal of this project was to determine the effect of shear loading on injured cartilage tissue and observe the depth-dependent cellular response of chondrocytes embedded within the cartilage matrix. Therefore, cartilage explants were

harvested from the femoral condyle of neonatal bovine knee joints and subjected to either rapid impact injury, repetitive sliding, or rapid impact injury followed by repetitive sliding. After being subjected to mechanical injury, cartilage explants were fluorescently stained to assess the health of chondrocytes within the extracellular matrix. Explants were stained for cell viability, caspase activity (apoptosis), and mitochondria polarization.

All groups demonstrated significantly greater chondrocyte damage at the articular surface compared to control samples, while the impact and combined loading group experienced significant middle zone damage compared to control and slid only. Surface zone chondrocyte damage propagated until ~200 μm, for mostly all groups and stains before reaching a plateau of damage that remained relatively constant within the middle zone. Surface zone damage for all injured groups was ~90% or greater for cell death and MT depolarization and 1000 apoptotic cells/mm^2. Middle zone damage for the slid group was minimally different from controls, while the impact group showed ~40% cell death, and 32% MT depolarization and impact and slid group showed ~50% cell death, and 62% MT depolarization. The interaction between both loading modalities caused significant increases in MT depolarization, indicating the MT are highly sensitive to mechanical loading with increased exposure leading to enhanced depolarization. Overall, the hierarchy of chondrocyte damage magnitude, from least to greatest, between groups was: control, slid only, impact only, and combined loading. Results show that compared to either impact or sliding alone, explants that were both impacted and slid experienced higher magnitudes of damage spanning greater tissue depths.

Specific Aim 2 (Chapter 3)

Determine the relationship between chondrocyte damage and local tissue strains in talar and femoral condylar cartilage, both before and after injury

The next advancement that was completed for the custom PTOA model developed in Chapter 2 was to detect changes in tissue mechanics due to injury. Assessing the change in mechanical properties of injured cartilage is essential because chondrocytes behave as mechanotransducers and generate biological responses to mechanical stimuli. Measuring changes in tissue stiffness and shear strains after injury and relating these to cellular damage allows for determination of the sensitivity of chondrocytes to mechanical stimulation. Cartilage tissue from the talar dome of the ankle joint was studied in addition to femoral condyle cartilage for this project because evidence suggests that the ankle joint is more susceptible to developing PTOA compared to the knee joint due to differences in mechanical properties. Therefore, a secondary aim of this project was to determine which joint would experience greater magnitudes of cellular and tissue level damage after injury. Cartilage explants from the femoral condyle and talar dome were subjected to the combined loading PTOA model developed in Chapter 2 as well as tested on a tissue deformation imaging stage to measure depth-dependent shear modulus and shear strain.

Femoral condylar cartilage and talar cartilage showed unique spatial patterns of cellular response after injury through combined loading. Condylar cartilage showed similar behavior to that found in Chapter 2, while talar cartilage comparatively lower surface zone response but an increased damage within the middle zone. This finding

was consistent with histological evaluation, which showed that talar cartilage displayed less surface fracturing after injury compared to femoral condylar cartilage. However, elastography measurements showed nonsignificant changes in the local shear modulus or local shear strains for the femoral condyle, while the shear strains generated at the surface of the talus increased by a factor of four. The shear strains at the articular surface of the condyle were ~12%, both before and after injury, however talar shear strains at the surface increased from ~4% to 18%. Chondrocyte sensitivity to shear strain was a positive linear relationship. Furthermore, comparing chondrocyte sensitivities showed that injury cause significant changes in sensitivity, and that chondrocytes of the knee and ankle possess inherent differences in sensitivity to mechanical loads.

Specific Aim 3 (Chapter 4)

Determine the effect of degraded synovial fluid on the relationship between cellular damage and local shear strains

The final advancement that was achieved for the combined loading PTOA model during this thesis project was to incorporate synovial fluid degradation, which occurs in vivo after traumatic injury. While PTOA pathogenesis begins after significant injury, joint inflammation, also known as synovitis, is a crucial factor in the manifestation of the disease. The release of inflammatory cytokines triggers multiple biological responses including: destruction of the cartilage matrix, death of chondrocytes, and depletion of the lubricating macromolecules in synovial fluid. The main molecules responsible for the lubricating qualities of synovial fluid are lubricin

and hyaluronic acid. Degradation of the synovial fluid, particularly lubricin and HA, is concerning in the context of PTOA because synovial fluid is responsible for stimulating the release of anabolic cytokines by chondrocytes, decreasing the friction between cartilage surfaces in the joint, and decreasing shear loads generated during articulation. Therefore, synovitis was simulated within the combined loading PTOA model by treating synovial fluid with either trypsin or hyaluronidase to remove lubricin or HA. These enzymatically degraded lubricants were used within the model developed in Chapters 2 and 3 and then compared to the results of normal synovial fluid. Testing lubricin and HA depleted synovial fluid allows us to infer what the effect of synovitis is on the progression of PTOA and if it changes the sensitivity of chondrocytes to mechanical damage.

Lubricin depleted and HA depleted synovial fluid were tested on femoral condylar cartilage samples via the combined loading PTOA model described in Chapters 2 and 3 then compared to results of control synovial fluid. Degraded synovial fluid generated similar levels of surface zone damage as normal synovial fluid but greater damage within the middle zone. Additionally, lubricin depleted and HA depleted synovial fluid produced significantly greater shear strains within the top 150 μm of cartilage tissue compared to standard synovial fluid. Degraded synovial fluid produced an average of 20% shear strain at the surface, while standard synovial fluid produced ~12%. While there existed minimal differences between the sensitivities of lubricin depleted and HA depleted synovial fluid, both degraded synovial fluids produced significant changes in the sensitivity of chondrocytes to shear strains compared to normal synovial fluid.

References

1. Ulrich-Vinther M, Maloney MD, Schwarz EM, et al. 2003. Articular cartilage biology. J Am Acad Orthop Surg 11(6):421–430.
2. Wang ML, Peng ZX. 2015. Wear in human knees. Biosurface and Biotribology 1(2):98–112.
3. Sophia Fox AJ, Bedi A, Rodeo SA. 2009. The basic science of articular cartilage: Structure, composition, and function. Sports Health 1(6):461–468.
4. Suh JK, Scherping S, Marii T, et al. 1995. Basic science of articular cartilage injury and repair. Operative Techniques in Sports Medicine 3(2):78–86.
5. Tamer TM. 2013. Hyaluronan and synovial joint: function, distribution and healing. Interdisciplinary Toxicology 6(3):111 [cited 2022 Jun 13] Available from: /pmc/articles/PMC3967437/.
6. Bhosale AM, Richardson JB. 2008. Articular cartilage: Structure, injuries and review of management. British Medical Bulletin 87(1):77–95.
7. Eschweiler J, Horn N, Rath B, et al. 2021. The Biomechanics of Cartilage — An Overview.
8. Mansour JM. 2013. Biomechanics of cartilage. Kinesiology: The Mechanics and Pathomechanics of Human Movement: Second Edition :69–83.
9. Lane JM, Weiss C. 1975. Review of articular cartilage collagen research. Arthritis & Rheumatism 18(6):553–562.
10. Eyre DR, Weis MA, Wu JJ. 2006. Articular cartilage collagen: An irreplaceable framework? European Cells and Materials 12:57–63.
11. Eyre DR. 2004. Collagens and cartilage matrix homeostasis. Clinical

Orthopaedics and Related Research 427(SUPPL.):118–122.

12. Kuettner KE, Kimura JH. 1985. Proteoglycans: An overview. Journal of Cellular Biochemistry 27(4):327–336.

13. Knudson CB, Knudson W. 2001. Cartilage proteoglycans. Seminars in Cell and Developmental Biology 12(2):69–78.

14. Emanuel KS, Kellner LJ, Peters MJM, et al. 2022. The relation between the biochemical composition of knee articular cartilage and quantitative MRI: a systematic review and meta-analysis. Osteoarthritis and Cartilage 30(5):650–662.

15. Roughley PJ, Lee ER. 1994. Cartilage proteoglycans: Structure and potential functions. Microscopy Research and Technique 28(5):385–397.

16. Dijkgraaf LC, de Bont LGM, Boering G, Liem RSB. 1995. Normal cartilage structure, biochemistry, and metabolism. Journal of Oral and Maxillofacial Surgery 53(8):924–929.

17. Rolauffs B, Williams JM, Grodzinsky AJ, et al. 2008. Distinct horizontal patterns in the spatial organization of superficial zone chondrocytes of human joints. Journal of Structural Biology 162(2):335–344.

18. Umlauf D, Frank S, Pap T, Bertrand J. 2010. Cartilage biology, pathology, and repair. Cellular and Molecular Life Sciences 67(24):4197–4211.

19. Mow VC, Ateshian GA. 1997. Lubrication and wear of diarthrodial joints. Basic orthopaedic biomechanics 2:275–315.

20. Xia Y, Momot KI, Chen Z, et al. 2017. Introduction to Cartilage. In: New Developments in NMR. p 3–43.

21. Wong BL, Bae WC, Chun J, et al. 2008. Biomechanics of cartilage articulation: Effects of lubrication and degeneration on shear deformation. Arthritis and Rheumatism 58(7):2065–2074.

22. Henak CR, Ross KA, Bonnevie ED, et al. 2016. Human talar and femoral cartilage have distinct mechanical properties near the articular surface. Journal of Biomechanics 49(14):3320–3327.

23. Bartell LR, Xu MC, Bonassar LJ, Cohen I. 2018. Local and global measurements show that damage initiation in articular cartilage is inhibited by the surface layer and has significant rate dependence. Journal of Biomechanics 72:63–70.

24. Jasin HE. 1995. Structure and function of the articular cartilage surface. Scandinavian Journal of Rheumatology 24(S101):51–55 [cited 2022 Jun 12].

25. Decker RS, Koyama E, Pacifici M. 2015. Articular Cartilage: Structural and Developmental Intricacies and Questions. Current Osteoporosis Reports 13(6):407–414.

26. Treppo S, Koepp H, Quan EC, et al. 2000. Comparison of biomechanical and biochemical properties of cartilage from human knee and ankle pairs. Journal of Orthopaedic Research 18(5):739–748.

27. Bloebaum RD, Wilson AS, Martin WN. 2021. A Review of the Collagen Orientation in the Articular Cartilage. Cartilage 13(2):367S-374S.

28. Wong M, Carter DR. 2003. Articular cartilage functional histomorphology and mechanobiology: A research perspective. Bone 33(1):1–13.

29. Decker RS. 2016. Articular cartilage: structural and developmental intricacies

and questions.13(6):407–414.

30. Mostakhdemin M, Nand A, Ramezani M. 2021. Articular and artificial cartilage, characteristics, properties and testing approaches—a review. Polymers (Basel) 13(12):1–25.

31. Ashford S, Williard J. 2014. Osteoarthritis: A review. Nurse Practitioner 39(5):1–8.

32. Lozada CJ, Diamond HS. 2021. Osteoarthritis. Medscape Rheumatology :1–59.

33. Helmick CG, Felson DT, Lawrence RC, et al. 2008. Estimates of the prevalence of arthritis and other rheumatic conditions in the United States. Part I. Arthritis and Rheumatism 58(1):15–25.

34. Brown TD, Johnston RC, Saltzman CL, et al. 2006. Posttraumatic osteoarthritis: A first estimate of incidence, prevalence, and burden of disease. Journal of Orthopaedic Trauma 20(10):739–744.

35. Vina ER, Kwoh CK. 2018. Epidemiology of osteoarthritis: Literature update. Current Opinion in Rheumatology 30(2):160–167.

36. Martel-Pelletier J, Barr AJ, Cicuttini FM, et al. 2016. Osteoarthritis. [cited 2022 Jun 14] Available from: www.nature.com/nrdp.

37. Neogi T, Zhang Y. 2013. Epidemiology of OA. Rheum Dis Clin North Am 39(1):1.

38. Carbone A, Rodeo S. 2017. Review of current understanding of post-traumatic osteoarthritis resulting from sports injuries. Journal of Orthopaedic Research 35(3):397–405.

39. Murphy L, Schwartz TA, Helmick CG, et al. 2008. Lifetime risk of symptomatic knee osteoarthritis. Arthritis Care and Research 59(9):1207–1213.

40. Thomas AC, Hubbard-Turner T, Wikstrom EA, Palmieri-Smith RM. 2017. Epidemiology of posttraumatic osteoarthritis. Journal of Athletic Training 52(6):491–496.

41. Aspden RM, Jeffrey JE, Burgin L V. 2002. Letter to the editor. Osteoarthritis and Cartilage 10(7):588–589.

42. Ayala S, Fortier LA, Delco ML, et al. 2020. Cartilage articulation enhances chondrocyte injury and death after impact injury. Journal of Orthopaedic Research 28(December):S192–S193 Available from: https://pubmed.ncbi.nlm.nih.gov/33274781/.

43. Anderson DD, Chubinskaya S, Guilak F, et al. 2011. Post-traumatic osteoarthritis: Improved understanding and opportunities for early intervention. Journal of Orthopaedic Research 29(6):802–809.

44. Anderson DD, Chubinskaya S, Guilak F, et al. 2011. Post-traumatic osteoarthritis: Improved understanding and opportunities for early intervention. Journal of Orthopaedic Research 29(6):802–809 [cited 2022 Jun 14] Available from: https://onlinelibrary.wiley.com/doi/full/10.1002/jor.21359.

45. Lohmander LS, Englund PM, Dahl LL, Roos EM. 2007. The long-term consequence of anterior cruciate ligament and meniscus injuries: Osteoarthritis. American Journal of Sports Medicine 35(10):1756–1769.

46. Plath JE, Aboalata M, Seppel G, et al. 2015. Prevalence of and risk factors for

dislocation arthropathy: Radiological long-term outcome of arthroscopic bankart repair in 100 shoulders at an average 13-year follow-up. American Journal of Sports Medicine 43(5):1084–1090.

47. Sugimoto K, Takakura Y, Okahashi K, et al. 2009. Chondral injuries of the ankle with recurrent lateral instability: An arthroscopic study. Journal of Bone and Joint Surgery 91(1):99–106.

48. Harrington KD. 1979. Degenerative arthritis of the ankle secondary to long-standing lateral ligament instability. JBJS 61(3).

49. Fithian DC, Paxton EW, Stone M Lou, et al. 2004. Epidemiology and natural history of acute patellar dislocation. American Journal of Sports Medicine 32(5):1114–1121.

50. Lieberthal J, Sambamurthy N, Scanzello CR. 2015. Inflammation in joint injury and post-traumatic osteoarthritis. Osteoarthritis and Cartilage 23(11):1825–1834 [cited 2022 Jun 14].

51. Delco ML, Kennedy JG, Bonassar LJ, Fortier LA. 2017. Post-traumatic osteoarthritis of the ankle: A distinct clinical entity requiring new research approaches. Journal of Orthopaedic Research 35(3):440–453.

52. Riegger J, Brenner RE. 2020. Pathomechanisms of posttraumatic osteoarthritis: Chondrocyte behavior and fate in a precarious environment. International Journal of Molecular Sciences 21(5).

53. Kurz B, Lemke AK, Fay J, et al. 2005. Pathomechanisms of cartilage destruction by mechanical injury. Annals of Anatomy 187(5–6):473–485.

54. Lieberthal J, Sambamurthy N, Scanzello CR. 2015. Inflammation in joint

injury and post-traumatic osteoarthritis. Osteoarthritis and Cartilage 23(11):1825–1834.

55. Mazor M, Best TM, Cesaro A, et al. 2019. Osteoarthritis Biomarker Responses and Cartilage Adaptation to Exercise: A Review of Animal and Human Models. Scandinavian Journal of Medicine & Science in Sports (December 2018):1–11.

56. Furman BD, Olson SA, Guilak F. 2006. The development of posttraumatic arthritis after articular fracture. Journal of Orthopaedic Trauma 20(10):719–725.

57. Li M, Yin H, Yan Z, et al. 2022. The immune microenvironment in cartilage injury and repair. Acta Biomaterialia 140:23–42.

58. Goldring MB, Otero M, Plumb DA, et al. 2011. Roles of inflammatory and anabolic cytokines in cartilage metabolism: Signals and multiple effectors converge upon MMP-13 regulation in osteoarthritis. European Cells and Materials 21:202–220.

59. Swärd P, Frobell R, Englund M, et al. 2012. Cartilage and bone markers and inflammatory cytokines are increased in synovial fluid in the acute phase of knee injury (hemarthrosis) - a cross-sectional analysis. Osteoarthritis and Cartilage 20(11):1302–1308.

60. Stevens AL, Wishnok JS, White FM, et al. 2009. Mechanical injury and cytokines cause loss of cartilage integrity and upregulate proteins associated with catabolism, immunity, inflammation, and repair. Molecular and Cellular Proteomics 8(7):1475–1489 [cited 2022 Jun 15].

61. Punzi L, Galozzi P, Luisetto R, et al. 2016. Post-traumatic arthritis: overview on pathogenic mechanisms and role of inflammation. RMD Open 2(2):e000279.

62. Delco ML, Bonnevie ED, Szeto HS, et al. 2018. Mitoprotective therapy preserves chondrocyte viability and prevents cartilage degeneration in an ex vivo model of posttraumatic osteoarthritis. Journal of Orthopaedic Research .

63. Delco ML, Bonnevie ED, Bonassar LJ, Fortier LA. 2018. Mitochondrial dysfunction is an acute response of articular chondrocytes to mechanical injury. Journal of Orthopaedic Research .

64. Woodell-May JE, Sommerfeld SD. 2020. Role of Inflammation and the Immune System in the Progression of Osteoarthritis. Journal of Orthopaedic Research 38(2):253–257 [cited 2022 Jun 16] Available from: https://onlinelibrary.wiley.com/doi/full/10.1002/jor.24457.

65. Catterall JB, Stabler T v., Flannery CR, Kraus VB. 2010. Changes in serum and synovial fluid biomarkers after acute injury (NCT00332254). Arthritis Research and Therapy 12(6):1–9 [cited 2022 Jun 16] Available from: https://arthritis-research.biomedcentral.com/articles/10.1186/ar3216.

66. Lohmander LS, Ionescu M, Jugessur H, Poole AR. 1999. Changes in joint cartilage aggrecan after knee injury and in osteoarthritis. Arthritis and Rheumatism 42(3):534–544.

67. Lohmander LS, Saxne T, Heinegard DK. 1994. Release of cartilage oligomeric matrix protein (COMP) into joint fluid after knee injury and in osteoarthritis. Annals of the Rheumatic Diseases 53(1):8–13.

68. Stefan Lohmander L, Neame PJ, Sandy JD. 1993. The structure of aggrecan fragments in human synovial fluid. evidence that aggrecanase mediates cartilage degradation in inflammatory joint disease, joint injury, and osteoarthritis. Arthritis & Rheumatism 36(9):1214–1222.

69. Lohmander LS, Hoerrner LA, Lark MW. 1993. Metalloproteinases, tissue inhibitor, and proteoglycan fragments in knee synovial fluid in human osteoarthritis. Arthritis & Rheumatism 36(2):181–189.

70. Harkey MS, Luc BA, Golightly YM, et al. 2015. Osteoarthritis-related biomarkers following anterior cruciate ligament injury and reconstruction: a systematic review. Osteoarthritis and Cartilage 23(1):1–12.

71. Cameron M, Buchgraber A, Passler H, et al. 1997. The natural history of the anterior cruciate ligament-deficient knee. Changes in synovial fluid cytokine and keratan sulfate concentrations. American Journal of Sports Medicine 25(6):751–754.

72. Marks PH, Donaldson MLC. 2005. Inflammatory cytokine profiles associated with chondral damage in the anterior cruciate ligament-deficient knee. Arthroscopy - Journal of Arthroscopic and Related Surgery 21(11):1342–1347.

73. Wang N, Liang H, Zen K. 2014. Molecular mechanisms that influence the macrophage M1-M2 polarization balance. Frontiers in Immunology 5(NOV):614.

74. van Tiel ST, Utomo L, de Swart J, et al. 2016. Imaging inflammation in the knee joint with 111IN-octreoscan. Osteoarthritis and Cartilage 24:S320.

75. Gasser O, Schifferli JA. 2004. Activated polymorphonuclear neutrophils

disseminate anti-inflammatory microparticles by ectocytosis. Blood 104(8):2543–2548.

76. Headland SE, Jones HR, Norling L V., et al. 2015. Neutrophil-derived microvesicles enter cartilage and protect the joint in inflammatory arthritis. Science Translational Medicine 7(315).

77. Schulze-Koops H, Kalden JR. 2001. The balance of Th1/Th2 cytokines in rheumatoid arthritis. Best Practice and Research: Clinical Rheumatology 15(5):677–691.

78. Alahdal M, Zhang H, Huang R, et al. [date unknown]. Potential efficacy of dendritic cell immunomodulation in the treatment of osteoarthritis.

79. O'Driscoll SW. 1998. The healing and regeneration of articular cartilage. Journal of Bone and Joint Surgery 80(12):1795–1812.

80. Benjamin M, Ralphs JR. 2004. Biology of Fibrocartilage Cells. International Review of Cytology 233:1–45.

81. Armiento AR, Alini M, Stoddart MJ. 2019. Articular fibrocartilage - Why does hyaline cartilage fail to repair? Advanced Drug Delivery Reviews 146:289–305.

82. Horas U, Pelinkovic D, Herr G, et al. 2003. Autologous chondrocyte implantation and osteochondral cylinder transplantation in cartilage repair of the knee joint. A prospective, comparative trial. Journal of Bone and Joint Surgery 85(2):185–192.

83. Charalambous CP. 2014. Articular Cartilage. Part II: Degeneration and Osteoarthrosis, Repair, Regeneration, and Transplantation. In: Banaszkiewicz

PA, Kader DF, editors. Classic Papers in Orthopaedics. London: Springer London. p 389–391.

84. Shah MR, Kaplan KM, Meislin RJ, Bosco JA. 2007. Patient Evaluation Articular Cartilage Restoration of the Knee. Bulletin of the NYU Hospital for Joint Diseases 65(1):51–60 [cited 2022 Jun 18].

85. Boos MA, Lamandé SR, Stok KS. 2022. Multiscale Strain Transfer in Cartilage. Frontiers in Cell and Developmental Biology 10:178 [cited 2022 Jun 18].

86. Albright JA, Misra RP. 1983. Mechanisms of Resorption and Remodeling of Cartilage. In: HALL BK, editor. Cartilage. Academic Press. p 49–86 Available from: https://www.sciencedirect.com/science/article/pii/B9780123195036500086.

87. Zhong D, Zhang M, Yu J, Luo ZP. 2018. Local tensile stress in the development of posttraumatic osteoarthritis. BioMed Research International 2018.

88. Athanasiou KA, Shah AR, Hernandez RJ, LeBaron RG. 2001. Basic science of articular cartilage repair. Clinics in Sports Medicine 20(2):223–247.

89. Benjamin M, Evans EJ. 1990. Fibrocartilage. J Anat 171:1–15.

90. Brown TD, Anderson DD, Nepola J v., et al. 1988. Contact stress aberrations following imprecise reduction of simple tibial plateau fractures. Journal of Orthopaedic Research 6(6):851–862 [cited 2022 Jun 19] Available from: https://onlinelibrary.wiley.com/doi/full/10.1002/jor.1100060609.

91. Newman AP. 1998. Articular cartilage repair. American Journal of Sports

Medicine 26(2):309–324 [cited 2022 Jun 18] Available from: https://journals.sagepub.com/doi/10.1177/03635465980260022701?url_ver=Z39.88-2003.

92. Szeto HH. 2014. First-in-class cardiolipin-protective compound as a therapeutic agent to restore mitochondrial bioenergetics. British Journal of Pharmacology 171(8):2029–2050.

93. Middendorf JM, Shortkroff S, Dugopolski C, et al. 2017. In vitro culture increases mechanical stability of human tissue engineered cartilage constructs by prevention of microscale scaffold buckling. Journal of Biomechanics 64:77–84 Available from: https://doi.org/10.1016/j.jbiomech.2017.09.007.

94. Elbardesy H, Awad AK, McLeod A, et al. 2021. Does bicompartmental knee arthroplasty hold an advantage over total knee arthroplasty? Systematic review and meta-analysis. SICOT J 7 [cited 2022 Jun 19] Available from: https://pubmed.ncbi.nlm.nih.gov/34241595/.

95. Ma J xiong, He W wei, Kuang M jie, et al. 2017. Efficacy of bicompartmental knee arthroplasty (BKA) for bicompartmental knee osteoarthritis: A meta analysis. International Journal of Surgery 46:53–60 [cited 2022 Jun 19].

96. Taylor CEV, Murray CM, Stanton TR. 2022. Patient perspectives of pain and function after knee replacement: a systematic review and meta-synthesis of qualitative studies. PAIN Reports 7(3):e1006.

97. Zhao J long, Zeng L feng, Pan J ke, et al. 2022. Comparisons of the Efficacy and Safety of Total Knee Arthroplasty by Different Surgical Approaches: A Systematic Review and Network Meta-analysis. Orthop Surg 14(3):472–485

[cited 2022 Jun 19] Available from: https://pubmed.ncbi.nlm.nih.gov/35128816/.

98. Shen G, Shen D, Fang Y, et al. 2022. Clinical Outcomes of Revision Total Knee Arthroplasty after High Tibial Osteotomy and Unicompartmental Knee Arthroplasty: A Systematic Review and Meta-Analysis. Orthop Surg [cited 2022 Jun 19] Available from: https://pubmed.ncbi.nlm.nih.gov/35611758/.

99. Curlewis K, Leung B, Sinclair L, et al. 2022. Systemic medical complications following joint replacement: a review of the evidence. https://doi.org/10.1308/rcsann.2022.0012 [cited 2022 Jun 19] Available from: https://publishing.rcseng.ac.uk/doi/10.1308/rcsann.2022.0012.

100. Evans JP, Evans JT, Mohammad HR, et al. 2022. How long does an elbow replacement last? A systematic review and meta-analysis of case-series and national registry reports with more than 10 years of follow-up. Acta Orthop 93:495–502 [cited 2022 Jun 19] Available from: https://pubmed.ncbi.nlm.nih.gov/35642497/.

101. Foran JRH. 2020. Total Knee Replacement - AAOS. [cited 2022 Jun 19] Available from: https://orthoinfo.aaos.org/en/treatment/total-knee-replacement.

102. Insall J. 1974. The Pridie Debridement Operation for Osteoarthritis of the Knee. Clinical Orthopaedics and Related Research® 101 Available from: https://journals.lww.com/clinorthop/Fulltext/1974/06000/The_Pridie_Debridement_Operation_for.9.aspx.

103. Seo S-S, Kim C-W, Jung D-W. 2011. Management of Focal Chondral Lesion in the Knee Joint. Knee Surgery & Related Research 23(4):185–196 Available

from: http://www.jksrr.org/journal/view.html?doi=10.5792/ksrr.2011.23.4.185.

104. Tyler TF, Lung JY. 2012. Rehabilitation following osteochondral injury to the knee. Current Reviews in Musculoskeletal Medicine 5(1):72–81.

105. Brittberg M, Lindahl A, Nilsson A, et al. 1994. Treatment of deep cartilage defects in the knee with autologous chondrocyte transplantation. N Engl J Med 331(14):889–895 [cited 2022 Jun 19] Available from: https://pubmed.ncbi.nlm.nih.gov/8078550/.

106. Becerra J, Andrades JA, Guerado E, et al. 2010. Articular cartilage: Structure and regeneration. Tissue Engineering - Part B: Reviews 16(6):617–627 [cited 2022 Jun 12] Available from: www.liebertpub.com.

107. Irwin RM, Bonassar LJ, Cohen I, et al. 2019. The clot thickens: Autologous and allogeneic fibrin sealants are mechanically equivalent in an ex vivo model of cartilage repair. PLoS ONE 14(11):1–17.

108. Shimozono Y, Coale M, Yasui Y, et al. 2018. Subchondral Bone Degradation After Microfracture for Osteochondral Lesions of the Talus: An MRI Analysis. American Journal of Sports Medicine 46(3):642–648.

109. Zengerink M, Struijs PAA, Tol JL, van Dijk CN. 2010. Treatment of osteochondral lesions of the talus: A systematic review. Knee Surgery, Sports Traumatology, Arthroscopy 18(2):238–246 [cited 2022 Jun 19] Available from: https://pubmed.ncbi.nlm.nih.gov/19859695/.

110. Shapiro F, Koide S, Glimcher MJ. 1993. Cell origin and differentiation in the repair of full-thickness defects of articular cartilage. J Bone Joint Surg Am 75(4):532–553 [cited 2022 Jun 19] Available from:

https://pubmed.ncbi.nlm.nih.gov/8478382/.

111. Migliorini F, Cuozzo F, Cipollaro L, et al. 2022. Platelet-rich plasma (PRP) augmentation does not result in more favourable outcomes in arthroscopic meniscal repair: a meta-analysis. Journal of Orthopaedics and Traumatology 23(1) [cited 2022 Jun 19] Available from: https://pubmed.ncbi.nlm.nih.gov/35129728/.

112. Hirahara AM, Mueller KW. 2015. BioCartilage: A New Biomaterial to Treat Chondral Lesions. Sports Medicine and Arthroscopy Review 23(3):143–148.

113. Branam GM, Saber AY. 2021. Osteochondral Autograft Transplantation. StatPearls Publishing, Treasure Island (FL). Available from: http://europepmc.org/abstract/MED/32809490.

114. Badekas T, Takvorian M, Souras N. 2013. Treatment principles for osteochondral lesions in foot and ankle. International Orthopaedics 37(9):1697–1706.

115. Toker B, Erden T, Çetinkaya S, et al. 2020. Long-term results of osteochondral autograft transplantation of the talus with a novel groove malleolar osteotomy technique. Jt Dis Relat Surg 31(3):509–515 [cited 2022 Jun 19] Available from: https://pubmed.ncbi.nlm.nih.gov/32962583/.

116. Attmanspacher W, Dittrich V, Stedtfeld HW. 2000. [Experiences with arthroscopic therapy of chondral and osteochondral defects of the knee joint with OATS (Osteochondral Autograft Transfer System)]. Zentralblatt fur Chirurgie 125(6):494–499 Available from: http://europepmc.org/abstract/MED/10919241.

117. Barber FA, Chow JCY. 2001. Arthroscopic osteochondral transplantation: Histologic results. Arthroscopy 17(8):832–835 [cited 2022 Jun 19] Available from: https://pubmed.ncbi.nlm.nih.gov/11600980/.

118. Gudas R, Gudaite A, Pocius A, et al. 2012. Ten-year follow-up of a prospective, randomized clinical study of mosaic osteochondral autologous transplantation versus microfracture for the treatment of osteochondral defects in the knee joint of athletes. American Journal of Sports Medicine 40(11):2499–2508 [cited 2022 Jun 19] Available from: https://journals.sagepub.com/doi/10.1177/0363546512458763?url_ver=Z39.88-2003&rfr_id=ori%3Arid%3Acrossref.org&rfr_dat=cr_pub++0pubmed.

119. Dong X, Li C, Zhang M, et al. 2022. Multifunctional injectable hydrogel for effective promotion of cartilage regeneration and protection against osteoarthritis: combined chondroinductive, antioxidative and anti-inflammatory strategy. Sci Technol Adv Mater 23(1):361–375 [cited 2022 Jun 20] Available from: https://pubmed.ncbi.nlm.nih.gov/35693891/.

120. Jia L, Zhang P, Ci Z, et al. 2022. Acellular cartilage matrix biomimetic scaffold with immediate enrichment of autologous bone marrow mononuclear cells to repair articular cartilage defects. Materials Today Bio 15(March):100310 Available from: https://doi.org/10.1016/j.mtbio.2022.100310.

121. Kessler MW, Grande DA. 2008. Tissue engineering and cartilage. Organogenesis 4(1):28 [cited 2022 Jun 20] Available from: /pmc/articles/PMC2634176/.

122. Hoffman AS. 2012. Hydrogels for biomedical applications ☆. Advanced Drug Delivery Reviews 64:18–23 [cited 2022 Jun 21] Available from: http://dx.doi.org/10.1016/j.addr.2012.09.010.

123. Hoon Jeon Y, Hyun Choi J, Kyung Sung J, et al. [date unknown]. Original Articles Different Effects of PLGA and Chitosan Scaffolds on Human Cartilage Tissue Engineering.

124. Solchaga LA, Dennis JE, Goldberg VM, Caplan AI. 1999. Hyaluronic acid-based polymers as cell carriers for tissue-engineered repair of bone and cartilage. J Orthop Res 17(2):205–213 [cited 2022 Jun 21] Available from: https://pubmed.ncbi.nlm.nih.gov/10221837/.

125. Dong X, Premaratne ID, Bernstein JL, et al. 2021. Three-Dimensional-Printed External Scaffolds Mitigate Loss of Volume and Topography in Engineered Elastic Cartilage Constructs. Cartilage 13(2_suppl):1780S-1789S [cited 2022 Jun 21] Available from: https://pubmed.ncbi.nlm.nih.gov/34636646/.

126. Kim J, Boys AJ, Estroff LA, Bonassar LJ. 2021. Combining TGF-β1 and Mechanical Anchoring to Enhance Collagen Fiber Formation and Alignment in Tissue-Engineered Menisci. ACS Biomaterials Science and Engineering 7(4):1608–1620 [cited 2022 Jun 21].

127. Tonge DP, Pearson MJ, Jones SW. 2014. The hallmarks of osteoarthritis and the potential to develop personalised disease-modifying pharmacological therapeutics. Osteoarthritis and Cartilage 22(5):609–621.

128. Oo WM, Yu SPC, Daniel MS, Hunter DJ. 2018. Disease-modifying drugs in osteoarthritis: current understanding and future therapeutics. Expert Opinion

on Emerging Drugs 23(4):331–347.

129. Pascual Garrido C, Hakimiyan AA, Rappoport L, et al. 2009. Anti-apoptotic treatments prevent cartilage degradation after acute trauma to human ankle cartilage. Osteoarthritis and Cartilage 17(9):1244–1251 Available from: http://dx.doi.org/10.1016/j.joca.2009.03.007.

130. Mitchell W, Ng E, Tamucci J, et al. 2019. Molecular Mechanism of Action of Mitochondrial Therapeutic SS-31 (Elamipretide): Membrane Interactions and Effects on Surface Electrostatics.31.

131. Laslett LL, Kingsbury SR, Hensor EMA, et al. 2014. Effect of bisphosphonate use in patients with symptomatic and radiographic knee osteoarthritis: Data from the Osteoarthritis Initiative. Annals of the Rheumatic Diseases 73(5):824–830.

132. Bingham CO, Buckland-Wright JC, Garnero P, et al. 2006. Risedronate decreases biochemical markers of cartilage degradation but does not decrease symptoms or slow radiographic progression in patients with medial compartment osteoarthritis of the knee: Results of the two-year multinational knee osteoarthritis structural arthritis study. Arthritis and Rheumatism 54(11):3494–3507 [cited 2022 Jun 21].

133. Persson MSM, Sarmanova A, Doherty M, Zhang W. 2018. Conventional and biologic disease-modifying anti-rheumatic drugs for osteoarthritis: a meta-analysis of randomized controlled trials. Rheumatology (Oxford) 57(10):1830–1837 [cited 2022 Jun 21] Available from: https://pubmed.ncbi.nlm.nih.gov/29917100/.

134. Cook SD, Patron LP, Salkeld SL, Rueger DC. 2003. Repair of Articular Cartilage Defects with Osteogenic Protein-1 (BMP-7) in Dogs.

CHAPTER 2

Cartilage Articulation Exacerbates Chondrocyte Damage and Death After Impact Injury

Abstract

Post-traumatic osteoarthritis (PTOA) is typically initiated by momentary supraphysiologic shear and compressive forces delivered to articular cartilage during acute joint injury and develops through subsequent degradation of cartilage matrix components and tissue remodeling. PTOA affects 12% of the population who experience osteoarthritis and is attributed to over $3 billion dollars annually in healthcare costs. It is currently unknown whether articulation of the joint post-injury helps tissue healing or exacerbates cellular dysfunction and eventual death. We hypothesize that post-injury cartilage articulation will lead to increased cartilage damage. Our objective was to test this hypothesis by mimicking the mechanical environment of the joint during and post-injury and determining if subsequent joint articulation exacerbates damage produced by initial injury. We use a model of PTOA that combines impact injury and repetitive sliding with confocal microscopy to quantify and track chondrocyte viability, apoptosis, and mitochondrial depolarization in a depth-dependent manner. Cartilage explants were harvested from neonatal bovine knee joints and subjected to either rapid impact injury (17.34 ± 0.99 MPa, 21.6 ± 2.45 GPa/s), sliding (60 min at 1 mm/s, under 15% axial compression), or rapid impact injury followed by sliding. Explants were then bisected and fluorescently stained for cell viability, caspase activity (apoptosis), and mitochondria polarization. Results show that compared to either impact or sliding alone, explants that were both impacted

and slid experienced higher magnitudes of damage spanning greater tissue depths.

Ayala S, Delco ML, Fortier LA, Cohen I, Bonassar LJ. Cartilage articulation exacerbates chondrocyte damage and death after impact injury. J Orthop Res. 2021 Oct;39(10):2130-2140.

Introduction

Clinically, 12% of osteoarthritis is post-traumatic (PTOA) affecting approximately 5.6 million individuals in the United States and attributed to over $3 billion dollars annually in healthcare costs.[1–3] PTOA is initiated by momentary supraphysiologic shear and compressive forces created during physical trauma that results in cartilage damage and subsequent joint inflammation.[4–6] Typically, patients who develop PTOA are young, active, and have suffered some type of traumatic injury such as anterior cruciate ligament (ACL) rupture, meniscus tear, or shoulder dislocation.[4,7–10] Such patients typically require surgical intervention early in life and often suffer rapid OA progression caused by damage to chondrocytes and/or extracellular matrix.[8,11]

There are numerous cellular responses that occur as a consequence of injury, and some, like mitochondrial (MT) pathways towards cell death, may be amenable to intervention. For mitochondria in particular, depolarization occurs minutes after injury and leads to bioenergetic failure of the cell through decreased ATP production.[12] MT depolarization also leads to increases in oxidative stress, inflammation, caspase activation and excess reactive oxygen species production, resulting in apoptosis and cell death respectively.[13,14] Studies have also shown that MT dysfunction results in decreased collagen II secretion by chondrocytes, which may increase cartilage degeneration in the pathogenesis of OA.[15] In patients with later-stage OA, chondrocytes experience down-regulation of superoxide dismutase 2 resulting in increased MT DNA strand breaks as well as reduced activities of complexes II and III resulting in decreased energy production.[16,17] While mitochondrial repolarization is

possible, prolonged depolarization past an unknown threshold of time leads to mitochondrial damage and depending on the severity can induce cell death by apoptosis or necrosis if the damage is extensive.[18,19] While there are promising new chemical interventions to halt the progression of mitochondrial and other biochemical processes, [20,21] the current standard of care is to prescribe rehabilitation therapy to improve supporting musculature strength, joint functionality, and decrease pain[22–24]

It is unknown, however, if movement soon after joint injury is beneficial or detrimental to long term outcome and the development PTOA. Complete immobilization of knee joints has been noted to be beneficial for up to 2 weeks post-surgery by decreasing rate of apoptosis and increasing rate of proliferation.[25] However, immobilization of longer than 2 weeks or shorter than 1 week has been noted to cause further damage within the joint by increasing rate of apoptosis, decreasing rate of proliferation, and decreasing glycosaminoglycan content.[26]

Since the timeline of cartilage damage to PTOA is not fully understood, it is unclear if movement of an injured joint may further damage chondrocytes.[27] Previous work modeled initiation of PTOA in cartilage tissue through ACL transection, meniscal destabilization, delivering impact injury, or shear strain through sliding.[28–33] While each of these techniques have the potential to cause cellular injury, it is unknown if damage would be exacerbated by impact and subsequently sliding injured cartilage.[12,30–32] This type of loading modality would be possible after articulating joints that have endured falls, sports injury, or traumatic injury.[34,35] These combined mechanical forces would more closely simulate the mechanical environment of an injured joint that is subject to continued use after trauma. Based on previous work that

showed sliding alone can damage tissue[30], we hypothesize that sliding previously impacted tissue will lead to a synergistic increase in chondrocyte damage in a depth-dependent manner throughout the tissue. The results of this study will reveal what regions of the cartilage tissue are most damaged following injury and if prior injury leaves the cartilage predisposed to continued arthritic degeneration.

Materials and Methods

Tissue Harvest and Preparation

Cartilage from the femoral condyles of 6 neonatal (i.e. skeletally immature) bovids (sex unknown; Gold Medal Packing, Rome, NY) was harvested, rinsed with 1X Dulbecco's phosphate buffered saline (DPBS) containing antibiotics (100 U/ml penicillin-streptomycin, Mediatech, Manassas, VA) and sectioned into cylindrical plugs using 6 mm diameter biopsy punches (Integra, York, PA) using sterile practices. Explants were trimmed, while keeping the articular surface intact, to 2 mm in depth using a custom jig and blades lubricated with bovine synovial fluid (Lampire, Pipersville, PA) to minimize shear force and limit chondrocyte death preceding testing. Prior to injury, explants were incubated overnight in media (phenol red-free DMEM containing 1% FBS, HEPES 0.025 ml/ml, penicillin 100 U/ml, streptomycin 100 U/ml, and 2.5 mM glucose) at 37 °C, 5% CO_2.

Cartilage Impact Protocol

Cartilage explants were subjected to injury using a previously described, spring-loaded impactor system.[29,36] A single cycle of unconfined compression was delivered to the articular surface of explants using a 12 mm diameter cylindrical impacting head. All impacts were delivered, over a loading time of ~ 1ms, at a peak

stress of 17.34 ± 0.99 MPa and peak stress rate of 21.6 ± 2.45 GPa/s (10 mm internal spring compression). While loading magnitudes of this nature have been seen in previous studies to cause failure of the anterior cruciate ligament[37], this impacting protocol was chosen to deliver impact trauma resulting in pathological cell death without fibrillation or full thickness cracking.[5,32,38] Impact force was measured at 50 kHz using a load cell mounted in parallel to the impacting missile (PCB Piezotronics, Depew, NY). A linear variable differential transducer (LVDT; RDP Electronics, Pottstown PA) was mounted in parallel with the impacting tip to measure the deformation of the cartilage plugs.

Cartilage Sliding Protocol

Impacted and non-impacted cartilage explants were slid against a polished glass counterface (McMaster Carr, Elmhurst IL) in a custom-built tribometer.[30,39] Explants were submerged in a lubricating bath of bovine synovial fluid (Lampire, Pipersville, PA). Before sliding, explants were compressed to 15% axial strain and allowed to equilibrate for 60 min.[40] Some level of static compression is required for these experiments to ensure that there is not slippage between the plug and the glass counterface.[41] Our previous work has investigated a wide variety of static compressions and sliding speeds[40,42] and has shown that 15% compression followed by sliding[30] is quite reliable at producing cell death, apoptosis, and mitochondrial depolarization. Explants were slid for 60 min at 1 mm/s as actuated by a lead screw-driven stage actuated by a micro-stepper motor (MDrive Plus, Schneider Electric, Rueil-Malmaison, France)[30].

Study Design

Cartilage explants were randomly assigned to one of 4 treatment groups ($n \geq 7$/group), uninjured control, sliding, impact, and impact followed by sliding. At time zero, explants in the sliding group were mounted onto the tribometer and allowed to stress relax for 1 h before beginning to slide. At t = 2 h, impact and impact & sliding groups were impacted; immediately following impact, explants in group impact & sliding were mounted onto the tribometer and allowed to stress relax for 1 h before beginning to slide. After group impact & sliding completed sliding, t = 4 h, all explants in each of the four treatment groups were axially bisected into hemicylinders, with each hemicylinder being stained for either cell viability, mitochondrial polarization, or caspase activity. Imaging of explants began at t = 7 h, after 3 h post-injury of the impact & sliding group.

Fluorescent Staining and Imaging

Cylindrical samples were axially bisected into hemicylinders and stained either for 30 min with 1 μl/ml Calcein AM and 1 μl/ml ethidium homodimer (Thermo Fisher Scientific, Waltham, MA), 30 min with CellEvent Caspase-3/7 Green (Thermo Fisher Scientific, Waltham, MA) following manufacturer instructions, or MitoTracker Green (200 nM; Thermo Fisher Scientific, Waltham, MA) for 20 min followed by addition of tetramethylrhodamine methyl ester perchlorate (10 nM; Thermo Fisher Scientific, Waltham, MA) for 20 min. After staining, all explants were rinsed in DPBS for 5 min. Cartilage explants were imaged on a Zeiss LSM880 confocal/multiphoton inverted microscope to determine the cellular responses to rapid impact injury, repeated frictional shear, or the combination of both.

Confocal images were captured and imported into ImageJ to create a

composite image (550 μm wide by 725 μm depth). Depth-dependent cellular responses were quantified using Fiji (NIH, Bethesda, MD) a custom MATLAB program (MathWorks, Inc, Natick, MA).[30,31,43] Global tissue responses were reported as percentage cell death (100 * total red cells/total red and green cells), percent cells with depolarized MT (100 * total green cells/total cells colocalizing red and green), and number of caspase-positive cells normalized to the area of the composite image, 0.39875 mm^2. Depth-dependent results were calculated by segmenting each image into 18 depth dependent bins (~40 μm depth by 550 μm wide) with all bins using the same image analysis outcomes. The number of caspase-positive cells were normalized to the area of the bin, 0.022153 mm^2.

Statistical Analysis

Two-way ANOVAs were performed to compare the effects of impact, sliding, and performing both in succession. Differences were considered statistically significant at $p \leq 0.05$, for both global tissue and depth-dependent results. Comparisons between groups were performed using Tukey's HSD method. Depth-dependent results were fit to a stretched exponential curve where the results of each stain were plotted as a function of x, distance away from the cartilage articular surface, given by:

$$y(x) = P + (Y_o - P)e^{-(x/\lambda)^d}$$

Where, Y_o represents the magnitude of damage at the articular surface, P represents the magnitude of damage in the middle zone of the tissue, λ represents the depth from the articular surface at the mid-point of the transition from the highest to lowest magnitude in the model, and d is a fitting parameter controlling the slope of the

transition.

Parameters for cell death and MT depolarization were subjected to the constraints: 100% ≥ Y_o and $P \geq 0\%$, $\lambda \geq 50$, and $d \geq 0$; while parameters from number of apoptotic cells were subjected to the constraints: highest number of apoptotic cells in an individual bin ≥ Y_o and $P \geq 0$, $\lambda \geq 50$, and $d \geq 0$. These constraints were placed on the model in order to constrict values to non-zero results between 0% - 100%, and to ensure that λ was not smaller the bin size used to track depth dependent results. Goodness of fit between the data and the model was characterized by the R^2 values attained by plotting the data against the values obtained through the model. Two-way ANOVAs and Tukey's HSD tests were then used to compare the values of P, Y_o, and λ between all groups for each of the three stains used. Nonlinear modeling and statistical analyses and were performed using GraphPad Prism 7 software.

Results

Experiments

Our study entailed a detailed comparison of cartilage damage as a function of mechanical loading (Figure 1). To conduct this study, we harvested cartilage explants and subjected them to one of four loading conditions as outlined by the timelines in Figure 1: control, slid, impacted, or impacted & slid. Following these protocols, tissues were bisected and stained to assess cell death, apoptosis, and MT depolarization using procedures described in the Methods section.

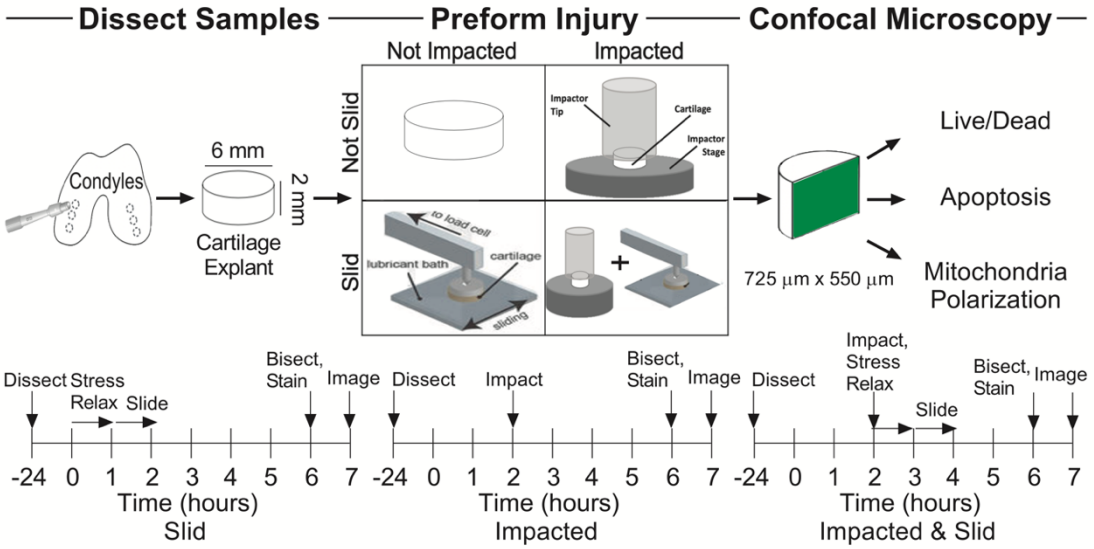

Figure 2.1. Experimental design and methods.

Confocal Images

Confocal microscopy of the tissue samples (Figure 2) indicated clear spatial patterns of tissue response with magnitude of damage increasing in order of least to greatest for the control (left column), slid (left-middle column), impact (right-middle column), and impacted & slid (right column) conditions. We observed that cell death (red) was concentrated at the surface and penetrated deeper into the tissue for the impacted and impacted & slid conditions. We also observed that the deeper regions of the tissue contained a combination of live and dead cells in the impacted & slid condition. Similarly, we observe that caspase activity (green in Figure 2B), often a precursor to apoptosis, increases both in magnitude and depth as we vary the condition from control to impacted & slid (note that the white dots are image artifacts that arise from image tiling). Finally, we find that mitochondrial depolarization (green in Figure 2C) also increased in magnitude and depth as we varied the conditions from control to impacted & slid. Here too, we observed a greater mixing of polarized and depolarized

mitochondrial populations for the impacted and impacted & slid conditions. We used a newly developed algorithm to quantify these observed spatial patterns as described in Methods, and report these measurements below.

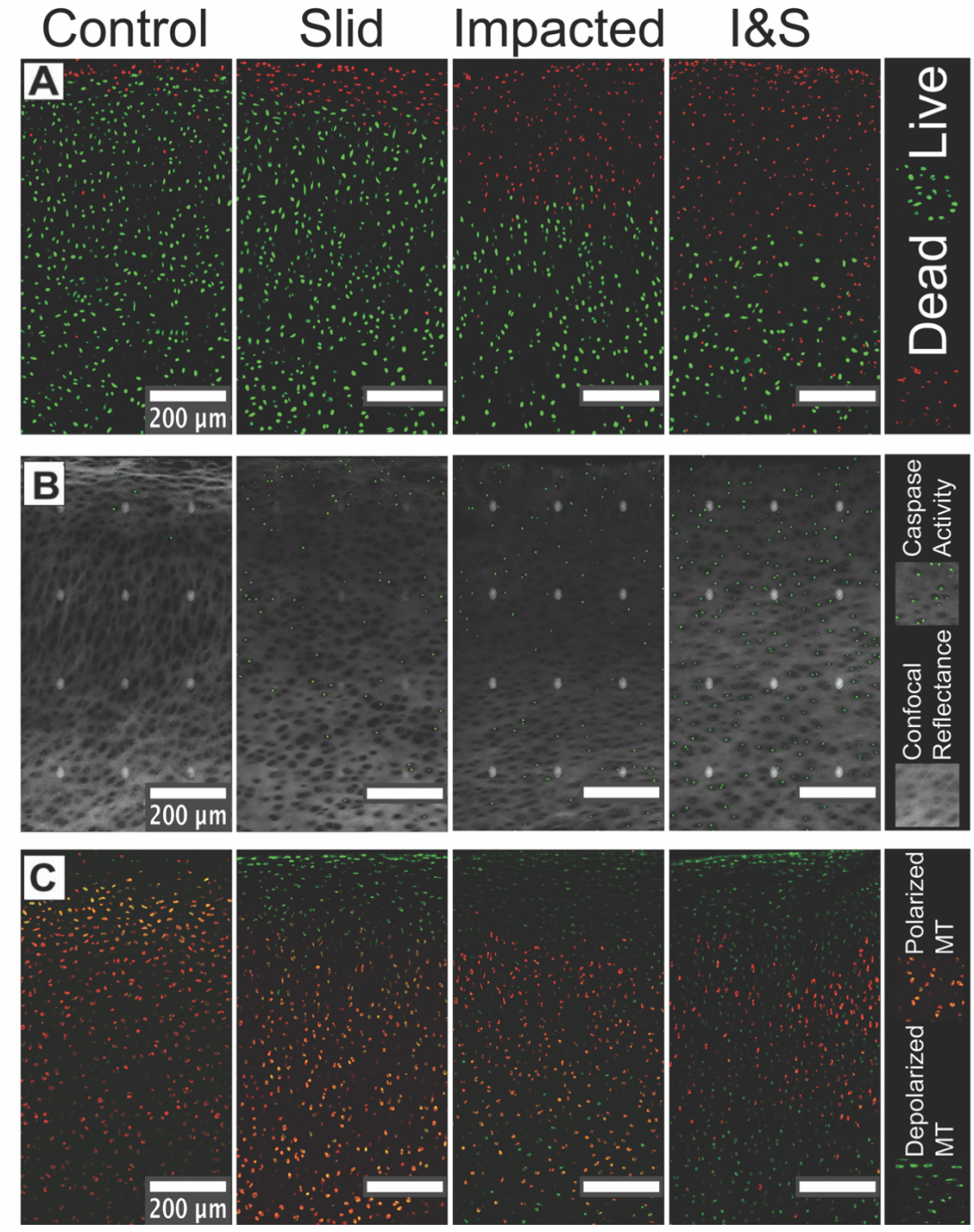

Figure 2.2. Representative confocal images of each group used tested during study.

Global Tissue Analysis

Measurements of cell death, caspase activity, and mitochondrial polarization averaged over the entire imaging region showed clear progression of damage as the condition varied from control, to slid, impacted, and impacted & slid. However, we observed a high degree of sample to sample variations due to differences in extent of localization of damage between conditions. Despite these variations, clear patterns in cell damage were noted based on type of injury. Cell death measurements showed the impacted & slid condition reached the highest magnitude of damage at 63.0% cell death, with impacted at a similar level of 51.9% ($p = 0.0802$). Slid induced the lowest amount of cell death of all loading modalities at 26.5%, however was still greater than that of the control group ($p = 0.0006$). Caspase activity followed a similar trend as cell death with impacted & slid achieving the greatest response at 747 apoptotic cells/mm^2, with impacted at a similar magnitude of 616 apoptotic cells/mm^2 ($p > 0.05$). However, the response of slid, 525 apoptotic cells/mm^2, was similar to that of controls and the other loading modalities ($p > 0.05$). Finally, assessments of MT depolarization showed that impacted & slid led to the highest magnitude of response at 69.6%. This result was higher than that of impacted at 44.8% ($p = 0.0008$) or slid at 18.1% ($p < 0.0001$). Impacted & slid led to an increase of MT depolarization greater than impacted or slid (Figure 3C) ($p = 0.016$ for interaction via two-way ANOVA). The degree of variation in the measurements averaged over the entire region of interest suggests that depth dependent data may be more appropriate for statistically distinguishing magnitude of damage across the different loading conditions.

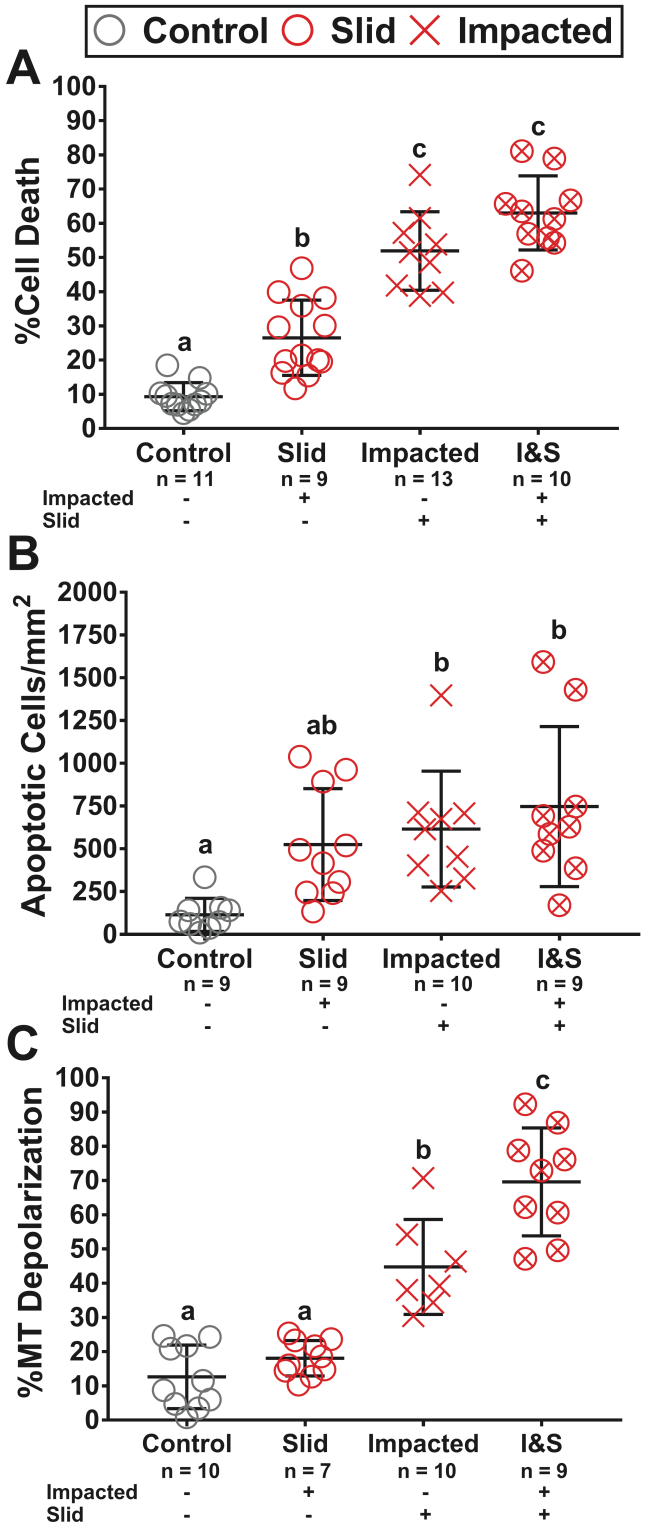

Figure 2.3. Global tissue analysis results.

Depth-Dependent Tissue Analysis

Indeed, we find that reporting the outcomes as a function of depth by segmenting the region of interest into bins ~40 μm in depth enables us to further distinguish the outcomes due to the different loading conditions and observe clear differences in surface and middle zone responses (Figure 4A-C). Again, we detect a similar order of tissue response as seen in our global analysis with magnitude of damage increasing in order of least to greatest: control (grey circle), slid (red circle), impacted (red x), and impacted & slid (red circle with x). This hierarchy of tissue response was observed in both the cartilage surface and middle zones. Cell death, apoptosis, and MT polarization showed minimal damage in the control samples beyond a depth of 100 μm. However, all loading conditions produced greater cell death compared to controls within the surface zone ($p < 0.0264$), while impacted and impacted & slid showed greater cell death than controls throughout the middle zone as well ($p < 0.0473$). Apoptosis measurements revealed slid and impacted induced greater response compared to controls within the surface zone up to depths of 260 μm, while impacted & slid induced greater damage up to depths of 540 μm. Finally, MT depolarization in the slid group was minimal past 100 μm and was only greater than controls up to depths of 60 μm (Figure 4C). Impacted and impacted & slid caused MT depolarization greater than controls throughout the surface zone ($p < 0.0027$). However, impacted & slid propagated MT depolarization greater than controls throughout the entire middle zone ($p < 0.0001$)

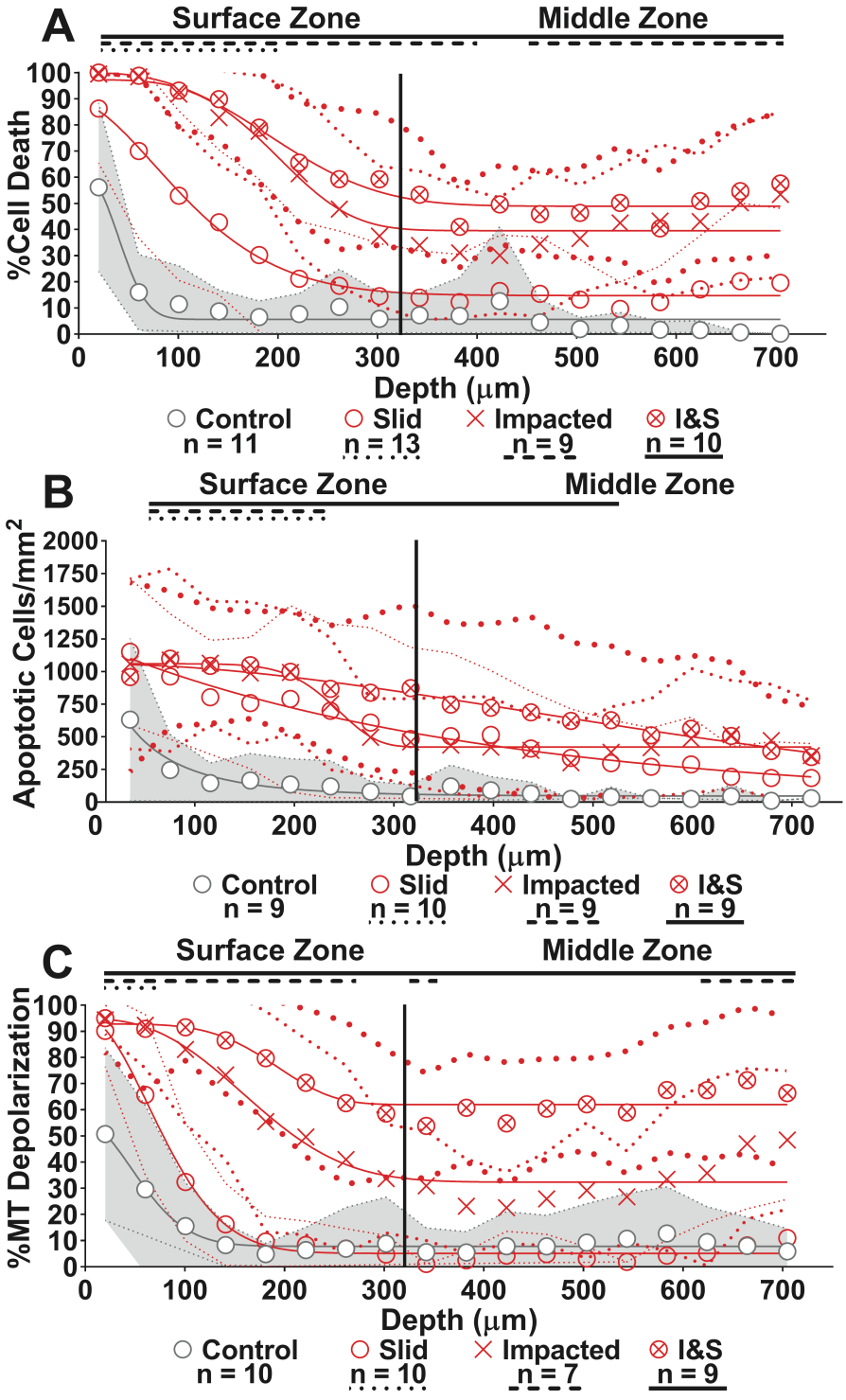

Figure 2.4. Depth-dependent analysis results with nonlinear curve fit.

To quantify and compare the degree of damage reached at the articular surface

and middle zone across conditions, we use nonlinear modeling via fits (Methods) to a stretched exponential plus an offset: $y(x) = P + (Y_o - P)*e^{-(x/\lambda)^d}$ (solid curves in Figure 4). In this model, Y_o represents the magnitude of damage at the articular surface, P represents the magnitude of damage in the middle zone of the tissue, λ represents the depth from the articular surface at the mid-point of the transition from the highest to lowest magnitude in the model, and d is a fitting parameter controlling the slope of the transition. The detailed results for the fits are reported in Table 1. The range of goodness of fit for all models ranged between 0.8915 - 0.9896. We report the dependence of the parameters Y_o, P, and λ on the testing condition in Figure 5.

$y(x) = (Y_o - P)*e^{-(x/\lambda)^d} + P$											
Stain/Group		N	Y_o	SEM	P	SEM	λ	SEM	d	SEM	R^2
Live/Dead	Control	11	61.7	53.3	5.64	1.04	50.0	41.2	2.44	7.38	0.9141
	Slid	9	88.6	8.6	14.74	2.05	134.8	16.8	1.64	0.47	0.9844
	Impacted	13	97.3	5.3	39.57	2.51	218.6	16.6	3.74	1.44	0.9353
	I&S	10	100.0	4.7	48.92	2.13	225.3	19.0	2.74	0.87	0.9529
Apoptosis	Control	9	928.9	645.2	46.48	24.69	50.0	53.7	0.79	0.61	0.9321
	Slid	9	1161.1	235.7	0.00	390.77	389.5	232.8	0.99	0.51	0.9753
	Impacted	10	1059.0	76.1	421.74	43.67	235.8	18.8	7.10	5.09	0.9689
	I&S	9	1054.8	137.1	45.29	2261.70	665.0	1379.7	1.77	2.12	0.9609
MT Depolarization	Control	10	55.0	10.7	7.81	1.34	70.3	14.8	1.85	1.10	0.9689
	Slid	7	95.4	6.0	5.10	1.11	94.7	6.2	1.88	0.33	0.9896
	Impacted	10	94.7	8.3	32.33	3.17	191.8	23.6	2.57	1.13	0.9176
	I&S	9	92.8	4.9	61.96	2.26	205.1	24.9	4.46	3.28	0.8915

Table 2.1. Results from fitting experimental data to stretched exponential model. Live/Dead and MT Depolarization are reported as percentages while Apoptosis is reported as # of cells/mm^2. SEM represents standard error of the mean and R^2 represents the correlation between the model values and experimental values.

For all injury groups, the magnitude of damage at the articular surface, Y_o, was high and reached a minimum of 88.6% cell death, 1055 apoptotic cells/mm^2, and 92.8% MT depolarization. The magnitude of damage was not significantly different between slid, impacted, and impacted & slid at the articular surface (Figure 5A, 5D,

and 5G). Cell death and apoptosis at the surface were similar between injured and control samples ($p > 0.05$), while MT depolarization at the surface was lower in controls than injured groups ($p < 0.012$).

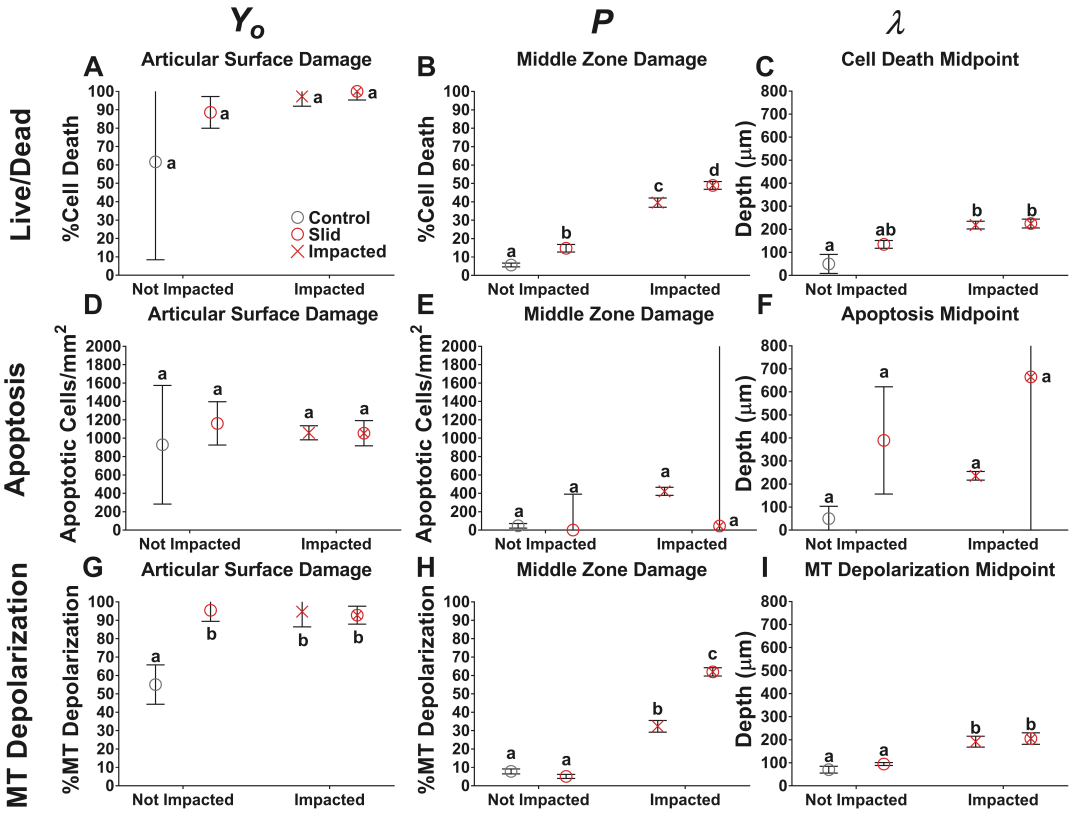

Figure 2.5. Comparison of parameters from nonlinear model.

The magnitude of damage reached at the middle zone, *P*, was minimally affected in the slid condition and was only higher than controls in cell death ($p = 0.025$) (Figure 5B). For apoptosis, none of the groups were different from one another ($p > 0.05$), however impacted had the highest damage with 422 apoptotic cells/mm^2 present at the middle zone (Figure 5E). For cell death and MT depolarization, impacted & slid had the highest levels of damage at the middle zone, followed by impacted. Impacted & slid caused 48.9% cell death and 62.0% MT depolarization at

the middle zone while impacted caused 39.6% cell death and 32.3% MT depolarization and was statistically higher in both cases ($p < 0.0119$) (Figure 5B and 5H). The combination of impacting and sliding was again additive for cell death and greater than additive for MT depolarization ($p < 0.0001$ for interaction via two-way ANOVA).

The stretched exponential model revealed that for all outcome measures, the mid-point of damage, λ, of impacted & slid occurred deeper into the tissue compared to either slid or impacted ($p < 0.05$). The mid-point of impacted & slid and was not reached until a minimum depth of 205 μm (Figure 5I) and a maximum depth of 665 μm (Figure 5F). For cell death and MT depolarization the midpoint of impacted & slid was similar to impacted ($p > 0.05$) and higher than the midpoint of slid ($p = 0.005$) (Figure 5C and 5I). Impacted groups having the deepest midpoints of damage indicates that impact is most responsible for propagating cell death and MT depolarization into deeper regions of cartilage. For apoptosis, the midpoint of slid damage, occurred at a depth of 389 μm, while the midpoint for impacted occurred at a depth of 235 μm ($p > 0.05$) (Figure 5F). While not significantly different, slid groups having deeper midpoints for apoptosis may indicate that sliding is most responsible for propagating damage into deeper regions of the cartilage, rather than impact. Overall, the hierarchy of greatest cause of cellular damage was impacted & slid, followed by impacted, followed by sliding. This model showed of the three outcome measures, MT depolarization was observed most frequently following injury. MT depolarization reached the highest amount of response globally and throughout the depth of the tissue. Following MT depolarization, cell death was next most affected while

apoptosis showed the least amount of response from mechanical injury.

Discussion

In this paper, we developed a new and robust *ex vivo* model of PTOA to more closely mimic the mechanical environment in cartilage after articular injury. We've also developed a statistical method able to characterize results by evaluating degree of injury in a global and depth-dependent manner. Using this model, we observed the combined effects of two types of loading experienced in joints during and after trauma, namely rapid compression and cyclic shear. Our results show that while both impact injury and sliding motion affect the health of chondrocytes, sliding previously impacted tissue led to aggravated chondrocyte damage throughout the depth of the cartilage. Assessments of cell death and apoptosis, looking at the global tissue and spatially through the depth, show that combining both loading modalities had an additive effect. Traumatic injury seems to impair the protective qualities of the surface region and prime chondrocytes for further damage that is propagated by the shear loading caused by sliding motion. The results of this study would imply that those who receive injuries associated with PTOA development, such as anterior cruciate ligament rupture and meniscus tears, would be susceptible to exacerbating their injury by articulating injured joints shortly after initial injury.[4]

Our results showed that damage is primarily concentrated at the articular surface and indicates that impacting, sliding, or both will cause the cartilage surface to be most affected. Damage generated by injury was seen to drop to half its maximum at about halfway through the surface zone. The severe decline of damage at the surface zone shows that the surface acts as a protective layer to limit damage propagation

deeper into the tissue.[30,31] Previous studies have shown the surface acts as the primary shear energy dissipating region with damage to this region exacerbating the effect of shear stress elsewhere in the tissue, which is consistent with the results of this study.[44–46] The protective nature of cartilage could be due to its inhomogeneous nature where the superficial layer is more compliant than the bulk, which results in the strain, and therefore the majority of cellular damage, being concentrated at the surface.[46,47] Next, the cellular damage caused by sliding motion is consistent with previous studies showing that the shear strain produced, at physiologic sliding speeds, similar levels of chondrocyte death at the superficial layer.[30] Minor superficial cracking without fibrillation was observed at the cartilage surface, which may be responsible for the increased damage in cartilage that was impacted prior to sliding is due to the integrity of the superficial layer being compromised, making it resemble cartilage samples in previous studies where the surface is removed prior to impact.[31,45] This shows the need of an alternative shear energy dissipation mechanism once the surface becomes compromised. Lubrication of the cartilage sliding surfaces has been shown to assist in this function with alteration to the lubricant's lubricating properties being capable of mitigating or agitating cell death.[48] Our results show that the heterogeneity of cartilage result in significant differences in the strains experienced throughout the tissue, which affects the patterns of cellular damage that occurs as a consequence to injury.

The combination of impacting & sliding caused a synergistic increase of MT depolarization, particularly past the surface zone in deeper regions of the tissue. Synergistic increase in MT depolarization may indicate that the MT are highly sensitive to mechanical injury. Recent evidence suggests that MT dysfunction is

central to chondrocyte's response to trauma and is related to local tissue mechanics; increased friction leads to in increased tissue strain and results in increased MT depolarization.[20,30] A possible mechanism for this synergy is that impact injury damages cartilage such that further loading causes higher strains within the injured joint. In particular, it has been demonstrated that impact injury causes cracking of the cartilage matrix, which in turn may cause a positive feedback loop of abnormal stresses around the crack that further propagates it.[49,50] Higher strains could be the result of a loss in cartilage stiffness due the presence of microcracks present throughout the tissue that grow in size as the tissue is further articulated. While temporary joint immobilization may provide limited benefits, it is possible that delayed sliding of cartilage tissue with damaged collagen networks will induce similar levels of cell damage as immediate sliding due to the limited capability of collagen repair by chondrocytes. Cartilage self-repair occurs to a limited degree with fibrocartilage[51], which possess inferior mechanical properties to normal cartilage tissue, meaning once the extracellular matrix becomes compromised, the cartilage will experience increased strains and is therefore predisposed to exacerbated cellular damage

There are several limitations to consider when interpreting these data such as using neonatal cartilage tissue, which may be more susceptible to damage compared to mature tissue.[52,53] Due to cartilage becoming more stiff with age, particularly within the deep zone, use of neonatal cartilage may have resulted in cartilage damage that is more pronounced than would be seen in mature tissue.[54] Neonatal cartilage was selected for use due to higher levels of chondrocytes present within the cartilage

matrix, its consistency and reproducibility as a tissue source.[55,56] Many groups have also used neonatal cartilage to study PTOA in particular, which further validates its use as a tissue source for this study.[57] Also, unlike other forms of OA, PTOA generally develops in younger populations that are more active, which may make the use of neonatal cartilage as a tissue source appropriate when studying PTOA.[58] Furthermore, impacting cartilage explants using a flat tip that covers the surface, without subchondral bone underneath, affects the boundary conditions of the impact and may change the thresholds for damage from what would be experienced in vivo. The loading profile used, static compression at 15% strain for 1 hour, was also limited in its physiologic relevancy due to joint motion being able to produce larger and less stable strains on cartilage. In addition, subjecting cartilage explants to the combined loading of sliding and a constant 15% compression may contribute to the increased cellular damage observed in this study. Also, while using polished glass as the counterface during the sliding process may mimic the joint environment, further studies may aim to use an *in vivo* model where cartilage on cartilage articulation is present. Next, use of Calcein AM and ethidium homodimer results in indirect measurements of cell death via cell membrane permeability whereas techniques such as TUNEL staining would directly measure cell death occurring via apoptosis.[59] As such, cell death data presented above may not truly be cell death in the absence of TUNEL staining and future work may seek to add TUNEL staining to the staining protocol. Furthermore, the difficulty of reproducing environmental conditions that result in physiologic MT oxygen consumption, membrane potential, or respiratory chain complex activity[12,15] *ex vivo* is further indication that *in vivo* studies would be

beneficial.

In summary, this study demonstrated, both globally and in a depth-dependent manner, that mechanical injury followed by repetitive sliding exacerbated cellular damage compared to either injury or sliding alone. A possible mechanism for reducing the level of MT depolarization and cell death would be to decrease the shear load experienced at the articular surface through viscosupplementation of the lubricating fluid, which is supported by results from previous studies.[47,48,60] Our results reveal a concentration of damage at the cartilage articular surface, which persisted at a high magnitude throughout the middle zone in cartilage that was impacted and slid. At the middle zone, the MT in particular saw a high degree of damage, leaving a sizable population of viable chondrocytes with MT depolarization. The population of cells with MT depolarization represents a possible mechanism by which damage spreads to other areas of the tissue and joint. As such, viable cells experiencing MT depolarization represents a potential target for treatment through therapeutics that are able to specifically target the MT to restore its bioenergetic function.[21,61,62]

References

1. Brown TD, Johnston RC, Saltzman CL, et al. 2006. Posttraumatic osteoarthritis: A first estimate of incidence, prevalence, and burden of disease. J. Orthop. Trauma 20(10):739–744.
2. Thomas AC, Hubbard-Turner T, Wikstrom EA, Palmieri-Smith RM. 2017. Epidemiology of posttraumatic osteoarthritis. J. Athl. Train. 52(6):491–496.
3. Dell'Isola A, Allan R, Smith SL, et al. 2016. Identification of clinical phenotypes in knee osteoarthritis: a systematic review of the literature. BMC Musculoskelet. Disord. 17(1):1–12.
4. Carbone A, Rodeo S. 2017. Review of current understanding of post-traumatic osteoarthritis resulting from sports injuries. J. Orthop. Res. 35(3):397–405.
5. Aspden RM, Jeffrey JE, Burgin L V. 2002. Letter to the editor. Osteoarthr. Cartil. 10(7):588–589.
6. Murphy L, Schwartz TA, Helmick CG, et al. 2008. Lifetime risk of symptomatic knee osteoarthritis. Arthritis Care Res. 59(9):1207–1213.
7. Rodeo S, Joseph A B, Lotz M. 2017. Special Issue: Injury and post-traumatic osteoarthritis. J. Orthop. Res. 35(3):395–396.
8. Whittaker JL, Roos EM. 2019. A pragmatic approach to prevent post-traumatic osteoarthritis after sport or exercise-related joint injury. Best Pract. Res. Clin. Rheumatol. 33(1):158–171 Available from: https://doi.org/10.1016/j.berh.2019.02.008.
9. Whittaker JL, Woodhouse LJ, Nettel-Aguirre A, Emery CA. 2015. Outcomes associated with early post-traumatic osteoarthritis and other negative health

consequences 3-10 years following knee joint injury in youth sport. Osteoarthr. Cartil. 23(7):1122–1129 Available from: http://dx.doi.org/10.1016/j.joca.2015.02.021.

10. Lieberthal J, Sambamurthy N, Scanzello CR. 2015. Inflammation in joint injury and post-traumatic osteoarthritis. Osteoarthr. Cartil. 23(11):1825–1834 Available from: http://dx.doi.org/10.1016/j.joca.2015.08.015.
11. Anderson DD, Chubinskaya S, Guilak F, et al. 2011. Post-traumatic osteoarthritis: Improved understanding and opportunities for early intervention. J. Orthop. Res. 29(6):802–809.
12. Delco ML, Bonnevie ED, Bonassar LJ, Fortier LA. 2018. Mitochondrial dysfunction is an acute response of articular chondrocytes to mechanical injury. J. Orthop. Res. .
13. Delco ML, Bonnevie ED, Szeto HS, et al. 2018. Mitoprotective therapy preserves chondrocyte viability and prevents cartilage degeneration in an ex vivo model of posttraumatic osteoarthritis. J. Orthop. Res. .
14. Lõpez De Figueroa P, Lotz MK, Blanco FJ, Caramés B. 2015. Autophagy activation and protection from mitochondrial dysfunction in human chondrocytes. Arthritis Rheumatol. 67(4):966–976.
15. Liu H, Li Z, Cao Y, et al. 2019. Effect of chondrocyte mitochondrial dysfunction on cartilage degeneration: A possible pathway for osteoarthritis pathology at the subcellular level. Mol. Med. Rep. 20(4):3308–3316.
16. Maneiro E, Martín MA, De Andres MC, et al. 2003. Mitochondrial respiratory activity is altered in osteoarthritic human articular chondrocytes. Arthritis

Rheum. 48(3):700–708.

17. Gavriilidis C, Miwa S, Von Zglinicki T, et al. 2013. Mitochondrial dysfunction in osteoarthritis is associated with down-regulation of superoxide dismutase 2. Arthritis Rheum. 65(2):378–387.

18. Gerencser AA, Chinopoulos C, Birket MJ, et al. 2012. Quantitative measurement of mitochondrial membrane potential in cultured cells: Calcium-induced de- and hyperpolarization of neuronal mitochondria. J. Physiol. 590(12):2845–2871.

19. Zorova LD, Popkov VA, Plotnikov EY, et al. 2018. Mitochondrial membrane potential. Anal. Biochem. 552:50–59.

20. Bartell LR, Fortier LA, Bonassar LJ, et al. 2019. Mitoprotective therapy prevents rapid, strain-dependent mitochondrial dysfunction after articular cartilage injury. J. Orthop. Res. (December):1–11 Available from: http://dx.doi.org/10.1002/jor.24567.

21. Szeto HH, Liu S. 2018. Cardiolipin-targeted peptides rejuvenate mitochondrial function, remodel mitochondria, and promote tissue regeneration during aging. Arch. Biochem. Biophys. 660(October):137–148.

22. Sweeney EA, Howell DR, James DA, et al. 2018. Returning to Sport after Gymnastics Injuries. Curr. Sports Med. Rep. 17(11):376–390.

23. Hinman RS, Heywood SE, Day AR. 2007. Aquatic Physical Therapy for Hip and Knee Osteoarthritis: Results of a Single-Blind Randomized Controlled Trial. Phys. Ther. 87(1):32–43.

24. G.D. Deyle, N.E. Henderson, R.L. Matekel, M.G. Ryder, M.B. Garber and

SCA. 2000. Effectiveness of Manual Physical Therapy and Exercise in Osteoarthritis of the Knee. A Randomized, Controlled Trial. Ann. Intern. Med. 132(3):173–181.

25. Mutsuzaki H, Nakajima H, Sakane M. 2018. Extension of knee immobilization delays recovery of histological damages in the anterior cruciate ligament insertion and articular cartilage in rabbits. J. Phys. Ther. Sci. 30(1):140–144.

26. Mutsuzaki H, Nakajima H, Wadano Y, et al. 2017. Influence of knee immobilization on chondrocyte apoptosis and histological features of the anterior cruciate ligament insertion and articular cartilage in rabbits. Int. J. Mol. Sci. 18(2).

27. Tyler TF, Lung JY. 2012. Rehabilitation following osteochondral injury to the knee. Curr. Rev. Musculoskelet. Med. 5(1):72–81.

28. Pauly HM, Larson BE, Coatney GA, et al. 2015. Assessment of cortical and trabecular bone changes in two models of post-traumatic osteoarthritis. J. Orthop. Res. 33(12):1835–1845.

29. Bonnevie ED, Delco ML, Fortier LA, et al. 2015. Characterization of tissue response to impact loads delivered using a hand-held instrument for studying articular cartilage injury. Cartilage 6(4):226–232.

30. Bonnevie ED, Delco ML, Bartell LR, et al. 2018. Microscale frictional strains determine chondrocyte fate in loaded cartilage. J. Biomech. 74:72–78.

31. Bartell LR, Fortier LA, Bonassar LJ, Cohen I. 2015. Measuring microscale strain fields in articular cartilage during rapid impact reveals thresholds for chondrocyte death and a protective role for the superficial layer. J. Biomech.

48(12):3440–3446 Available from: http://dx.doi.org/10.1016/j.jbiomech.2015.05.035.

32. Bonnevie ED, Delco ML, Galesso D, et al. 2017. Sub-critical impact inhibits the lubricating mechanisms of articular cartilage. J. Biomech. 53:64–70.

33. Steineman BD, Laprade RF, Santangelo KS, et al. 2017. Early osteoarthritis after untreated anterior meniscal root tears: An in vivo animal study. Orthop. J. Sport. Med. 5(4):1–14.

34. Exler Y. 1991. Patella fracture: Review of the literature and five case presentations. J. Orthop. Sports Phys. Ther. 13(4):177–183.

35. Boeth H, Duda GN, Heller MO, et al. 2013. Anterior cruciate ligament-deficient patients with passive knee joint laxity have a decreased range of anterior-posterior motion during active movements. Am. J. Sports Med. 41(5):1051–1057.

36. Alexander PG, Song Y, Taboas JM, et al. 2013. Development of a Spring-Loaded Impact Device to Deliver Injurious Mechanical Impacts to the Articular Cartilage Surface. Cartilage 4(1):52–62.

37. Noyes FR, Grood ES. 1976. The strength of the anterior cruciate ligament in humans and rhesus monkeys: Age related and species related changes. J. Bone Jt. Surg. - Ser. A 58(8):1074–1082.

38. D'Lima DD, Hashimoto S, Chen PC, et al. 2001. Human chondrocyte apoptosis in response to mechanical injury. Osteoarthr. Cartil. 9(8):712–719.

39. Gleghorn JP, Jones ARC, Flannery CR, Bonassar LJ. 2009. Boundary mode lubrication of articular cartilage by recombinant human lubricin. J. Orthop. Res.

27(6):771–777.

40. Bonnevie ED, Galesso D, Secchieri C, et al. 2015. Elastoviscous transitions of articular cartilage reveal a mechanism of synergy between lubricin and hyaluronic acid. PLoS One 10(11):1–15.

41. Buckley MR, Bergou AJ, Fouchard J, et al. 2010. High-resolution spatial mapping of shear properties in cartilage. J. Biomech. 43(4):796–800 Available from: http://dx.doi.org/10.1016/j.jbiomech.2009.10.012.

42. Gleghorn JP, Bonassar LJ. 2008. Lubrication mode analysis of articular cartilage using Stribeck surfaces. J. Biomech. 41(9):1910–1918.

43. Johannes Schindelin, Ignacio Arganda-Carreras, Erwin Frise, Verena Kaynig, Mark Longair, Tobias Pietzsch, Stephan Preibisch, Curtis Rueden, Stephan Saalfeld, Benjamin Schmid, Jean-Yves Tinevez, Daniel James White, Volker Hartenstein, Kevin Eliceiri PT. 2012. Fiji: an open-source platform for biological-image analysis. Nat. Methods 9:676–682.

44. Kaleem B, Maier F, Drissi H, Pierce DM. 2017. Low-energy impact of human cartilage : predictors for microcracking the network of collagen. Osteoarthr. Cartil. 25(4):544–553 Available from: http://dx.doi.org/10.1016/j.joca.2016.11.009.

45. Bartell LR, Xu MC, Bonassar LJ, Cohen I. 2018. Local and global measurements show that damage initiation in articular cartilage is inhibited by the surface layer and has significant rate dependence. J. Biomech. 72:63–70.

46. Buckley MR, Bonassar LJ, Cohen I. 2013. Localization of viscous behavior and shear energy dissipation in articular cartilage under dynamic shear loading. J.

Biomech. Eng. 135(3):1–9.

47. Wong BL, Bae WC, Chun J, et al. 2008. Biomechanics of cartilage articulation: Effects of lubrication and degeneration on shear deformation. Arthritis Rheum. 58(7):2065–2074.

48. Waller KA, Zhang LX, Elsaid KA, et al. 2013. Role of lubricin and boundary lubrication in the prevention of chondrocyte apoptosis. Proc. Natl. Acad. Sci. U. S. A. 110(15):5852–5857.

49. Zhong D, Zhang M, Yu J, Luo ZP. 2018. Local tensile stress in the development of posttraumatic osteoarthritis. Biomed Res. Int. 2018.

50. Sadeghi H, Lawless BM, Espino DM, Shepherd DET. 2018. Effect of frequency on crack growth in articular cartilage. J. Mech. Behav. Biomed. Mater. 77(August):40–46.

51. Wang KH, Wan R, Chiu LH, et al. 2018. Effects of collagen matrix and bioreactor cultivation on cartilage regeneration of a full-thickness critical-size knee joint cartilage defects with subchondral bone damage in a rabbit model. PLoS One 13(6):1–15.

52. Kurz B, Lemke A, Kehn M, et al. 2004. Influence of Tissue Maturation and Antioxidants on the Apoptotic Response of Articular Cartilage after Injurious Compression. Arthritis Rheum. 50(1):123–130.

53. Levin AS, Chen CTC, Torzilli PA. 2005. Effect of tissue maturity on cell viability in load-injured articular cartilage explants. Osteoarthr. Cartil. 13(6):488–496.

54. Gannon AR, Nagel T, Bell AP, et al. 2015. Postnatal changes to the mechanical

properties of articular cartilage are driven by the evolution of its Collagen network. Eur. Cells Mater. 29:105–123.

55. Mauch KA, Katwal AB, Seyedin M. 2013. The Potential of Human Allogeneic Juvenile Chondrocytes for Restoration of Articular Cartilage. Am. J. od Sport. Med. 38(7):1324–1333.

56. Adkisson HD, Milliman C, Zhang X, et al. 2010. Immune evasion by neocartilage-derived chondrocytes: Implications for biologic repair of joint articular cartilage. Stem Cell Res. 4(1):57–68 Available from: http://dx.doi.org/10.1016/j.scr.2009.09.004.

57. Torre OM, Das R, Berenblum RE, et al. 2018. Neonatal mouse intervertebral discs heal with restored function following herniation injury. FASEB J. 32(9):4753–4762.

58. Buckwalter JA, Anderson DD, Brown TD, et al. 2013. The Roles of Mechanical Stresses in the Pathogenesis of Osteoarthritis: Implications for Treatment of Joint Injuries. Cartilage 4(4):286–294.

59. Ziegler U, Groscurth P. 2004. Morphological features of cell death. News Physiol. Sci. 19(3):124–128.

60. Flannery CR, Zollner R, Corcoran C, et al. 2009. Prevention of cartilage degeneration in a rat model of osteoarthritis by intraarticular treatment with recombinant lubricin. Arthritis Rheum. 60(3):840–847.

61. Szeto HH. 2014. First-in-class cardiolipin-protective compound as a therapeutic agent to restore mitochondrial bioenergetics. Br. J. Pharmacol. 171(8):2029–2050.

62. Zhao K, Zhao GM, Wu D, et al. 2004. Cell-permeable peptide antioxidants targeted to inner mitochondrial membrane inhibit mitochondrial swelling, oxidative cell death, and reperfusion injury. J. Biol. Chem. 279(33):34682–34690.

CHAPTER 3

Articular Chondrocytes from the Knee and Ankle Have Differential Sensitivities to Shear Strain

Abstract

Traumatic injury delivered to synovial joints typically results in development of focal defects and proinflammatory changes in cartilage tissue, eventually leading to development of post traumatic osteoarthritis (PTOA). However, there exist disparate incidence rates of PTOA between joints. For example, 80% of all OA cases in the ankle are attributed to PTOA whereas only 10% of knee OA cases are attributed to PTOA. We hypothesize that differences in rates of PTOA between knee and ankle cartilage is due to inherent differences in mechanical properties and chondrocyte sensitivity to mechanical loads. Therefore, our objective was to compare the effect of injury on the spatial patterns of cellular response between knee and ankle cartilage and relate these responses to changes in tissue mechanical properties. Cartilage explants from the talar dome of the ankle and femoral condyle of the knee were subjected to our ex vivo model of PTOA which combines rapid impact injury and repetitive cartilage articulation. Explants were bisected and fluorescently stained to assess global and depth-dependent cell death, caspase activity, and mitochondrial depolarization. Explants were also tested via confocal elastography to determine the local shear strain and shear modulus profile. Results showed that chondrocyte response differed between joints, with knee cartilage showing greater damage within the surface region. Additionally, ankle cartilage experienced a greater decrease in shear modulus post-injury compared knee, causing depth-dependent shear strain to

significantly increase. Furthermore, we overserved that knee and ankle chondrocytes possess inherent differences in sensitivity to shear strain.

Ayala S, Delco ML, Fortier LA, Cohen I, Bonassar LJ. Articular Chondrocytes from the Knee and Ankle Have Differential Sensitivities to Shear Strain. In preparation to be submitted to Journal of Biomechanics. 2022.

Introduction

Posttraumatic osteoarthritis (PTOA) accounts for ~10% of all knee OA cases compared to ~80% of ankle OA cases.[1–3] This discrepancy indicates a need to directly study PTOA pathogenesis in ankle cartilage to elucidate distinct mechanisms by which degeneration propagates after injury. Disparities in PTOA incidence rates between knee and ankle cartilage may be partially attributed to differences in chondrocyte organization, biochemical composition, and mechanical properties between both joints.[3–5] Examples of such differences between knee and ankle cartilage include the talar dome possessing chondrocytes predominately arranged in circular clusters, whereas chondrocytes of the femoral condyles are arranged in columns.[4] Additionally, ankle cartilage contains increased proteoglycan and sulfated glycosaminoglycan content compared to knee cartilage, which results in ankle cartilage possessing ten times greater stiffness at the articular surface.[3,6–8] Lower stiffness in knee cartilage would lead to higher shear strains, which are known to correlate with cell damage and death.[9] However, the relationship between shear strain and subsequent chondrocyte damage after traumatic injury has yet to be studied, for either knee or ankle cartilage.

Traumatic joint injury involves rapid supraphysiologic shear and compressive forces delivered to cartilage tissue, which cause damage to chondrocytes and the surrounding matrix. Such damage includes: mitochondrial (MT) depolarization; increases in reactive oxygen species; caspase activity; apoptosis and cell death.[10–12] Additionally, traumatic cartilage injury has been shown to cause cracking of the articular surface, damage to the collagen network, and formation of focal defects.[13–15]

Once cartilage integrity has been compromised, subsequent tissue loading leads to enhanced cartilage degradation.[14,16,17] Injured cartilage tissue displays inferior mechanical properties, which alters loading on chondrocytes and promotes further catabolic activity.[18,19]

Several studies have developed models that use ankle cartilage to understand PTOA initiation, propagation, and treatment. One group found that human talar cartilage explants contained greater glycosaminoglycan and hydroxyproline content resulting in greater stiffness compared to knee cartilage.[6] Another group used a drop-tower system on a human ankle joint and investigated resulting cell death patterns along fracture-edges of the talar dome.[20] Finally, a model using caspase inhibitors on human talar cartilage subjected to a single pressure-controlled impact injury was used to impede apoptosis and cell death post-injury.[21] However, the catalog of studies that currently exists does not clarify the origin of PTOA prevalence disparities between the knee and ankle. Previous results from our group on knee cartilage injury showed that shear loading after impact increased chondrocyte damage, particularly in the middle zone.[17] However, it is unknown if similar trends are observed in ankle cartilage after injury.

Elucidating the mechanisms by which knee and ankle cartilage experience disparate rates of PTOA requires an understanding of the relationship between chondrocyte damage post-injury and the shear strains that generate such damage. By investigating cellular damage along with changes in cartilage mechanics post-injury, we can detect and compare the sensitivity of chondrocytes from knee and ankle cartilage to mechanical injury. Our group has presented an ex vivo PTOA model that

utilizes rapid impact injury followed by subsequent to more closely mimic the mechanical environment of the injured knee joint.[9,16,17,22] A great benefit of our model is that we can investigate PTOA pathogenesis on global and local levels in cartilage tissue from any joint, including the ankle.

We hypothesize that ankle cartilage will experience a larger reduction in mechanical properties post-injury compared to knee cartilage, resulting in an increase in shear strain and subsequent chondrocyte death, apoptosis, and MT depolarization. Such differences would have important implications on the discrepancy in PTOA prevalence between the knee and ankle. Therefore, the objective of this study is to utilize our custom model of PTOA to determine the relationship between shear strain and cellular response for cartilage from the talar dome and compare these data to results from the femoral condyle. Specifically, we will: a) spatially map cell death, apoptosis, and MT depolarization in knee and ankle cartilage after traumatic injury; b) examine the effect of traumatic injury on the shear strain and shear modulus profiles of knee and ankle cartilage; c) and compare the sensitivity of chondrocytes to loading by examining the relationship between chondrocyte damage and shear strain. The results of this study will reveal the underlying mechanisms that result in cartilage degeneration for the knee and ankle joint.

Materials and Methods

Sample Preparation

Cartilage from the femoral condyle and ipsilateral talar dome of the knee and ankle joint of twelve neonatal (i.e., skeletally immature) bovids (sex unknown; Gold Medal Packing) was sterilely harvested, rinsed with Dulbecco's phosphate-buffered

saline (DPBS) containing antibiotics (100 U/ml penicillin-streptomycin, Mediatech) and sectioned into cylindrical plugs using 6mm diameter biopsy punches (Integra). Explants from the femoral condyle were trimmed, while keeping the articular surface intact, to 2 mm in depth. Explants from the talus were full thickness samples, each about 1 mm in height. Cuts were performed using a custom jig and blades lubricated with bovine synovial fluid (Lampire) to limit chondrocyte death preceding testing. Before injury, explants tested via confocal microscopy were incubated overnight in media (phenol red-free DMEM containing 1% FBS, HEPES 0.025 ml/ml, penicillin 100 U/ml, streptomycin 100 U/ml, and 2.5 mM glucose) at 37°C, 5% CO_2.

Combined loading model of PTOA

Cartilage explants were subjected to injury using a previously described, spring-loaded impactor system.[13,23] A single cycle of unconfined compression was delivered to the articular surface of explants using a 12 mm diameter cylindrical impacting tip. All impacts were delivered, over a loading time of ~ 1 ms, at a peak stress of 17.34 ± 0.99 MPa and peak stress rate of 21.6 ± 2.45 GPa/s. Loading magnitudes of this nature have been seen in previous studies to cause failure of the anterior cruciate ligament, however this loading protocol was chosen to deliver injurious compression resulting in pathological chondrocyte death and damage without full thickness cracking.[24–27] Following traumatic injury, impacted and non-impacted cartilage explants were slid against a polished glass counterface (McMaster Carr) in a custom-built tribometer.[9,28–31] Explants were submerged in a lubricating bath of bovine synovial fluid (Lampire), compressed to 15% axial strain, allowed to equilibrate for 60 min, then slid for 60 min at 1mm/s.[30] This loading regimen is known to be reliable at

producing cell death, apoptosis, and mitochondrial depolarization.[9,17,30,31]

Confocal elastography

A setup mimicking the tribometer configuration was mounted on a 3i Marianas Spinning Disk Confocal Microscope to measure depth-dependent shear modulus and shear strains of cartilage explants.[32] Shear strains were tracked in a similar manner to previous studies that measured depth-dependent shear properties.[33,34] Cylindrical femoral condylar and talar cartilage explants were axially bisected into hemicylinders that were stained for 1 h in 14 μg/ml 5-dichlorotriazinyl-aminofluorescein (5-DTAF, Molecular Probes, Grand Island, NY) followed by a 30 min DPBS wash. Samples were then mounted via their deep zone to a tissue deformation imaging stage (TDIS) as previously described.[35,36] Samples were submerged in a lubricating bath of bovine synovial fluid (Lampire) and compressed to 15% axial strain against polished glass using a micrometer stage and allowed to stress relax for 30 min. In a similar manner to shearing performed on the tribometer, the glass slide was reciprocated against the cartilage surface using a piezoelectric positioning stage at a magnitude of 5% of sample thickness at 1 Hz. Videos were captured at 20 frames per second throughout the tissue depth to track the depth-dependent properties of the cartilage tissue. Depth-dependent shear deformations were tracked by analyzing the displacement of the tissue between frames via a custom MATLAB code. The maximum local shear strains were calculated through differentiation of the local displacements as previously described.[37,38]

Confocal microscopy

Imaging of explants began 3 h post-injury. Cylindrical samples were axially

bisected into hemicylinders and stained either for 30 min with 1 μl/ml Calcein AM and 1 μl/ml ethidium homodimer (Thermo Fisher Scientific), 30 min with CellEvent Caspase-3/7 Green (Thermo Fisher Scientific) following manufacturer instructions, or MitoTracker Green (200 nM; Thermo Fisher Scientific) for 20 min followed by addition of tetramethylrhodamine methyl ester perchlorate (10 nM; Thermo Fisher Scientific) for 30 min. After staining, all explants were rinsed in DPBS for 30 min. Cartilage explants were imaged on a Zeiss LSM880 confocal/multiphoton inverted microscope to determine the cellular response of talar and femoral condylar cartilage to rapid impact injury followed by repeated frictional shear.

Confocal images were captured and imported into ImageJ to create a composite image (550 μm wide vs 725 μm depth). Depth-dependent cellular responses were quantified using Fiji (NIH) a custom MATLAB program (MathWorks, Inc.).[16,39] Global tissue responses were reported as percent cell death, percent cells with depolarized MT, and number of caspase-positive cells normalized to the area of composite image: 0.39882 mm^2. Depth-dependent results were calculated by segmenting each image into eighteen ~40 μm bins with all bins using the same image analysis outcomes. The number of caspase-positive cells were normalized to the area of the bin, 0.022 mm^2.

Histology

To reveal the extent of surface damage caused by our PTOA model, injured and control samples were fixed in buffered 10% formalin for ~48 h before being placed in 70% ethanol, embedded in paraffin, and mounted on slides. Slides were stained with either Safranin-O or picrosirius red to visualize glycosaminoglycan and

collagen content, respectively.[25,40] Picrosirius red and Safranin-O samples were imaged under brightfield on a light microscope with a 4x objective. Picrosirius red stained slides were also viewed under crossed polarizers to view collagen architecture and organization. Images were obtained with a SPOT RT camera (Diagnostic Instruments, Sterling Heights, MI) attached to a Nikon Eclipse TE2000-S microscope (Nikon Instruments, Melville, NY).

Statistical analysis

Two-way ANOVAs were performed to compare the effect of our custom PTOA model on the spatial patterns of cellular response between talar and femoral condylar cartilage. Differences were considered statistically significant at $p \leq 0.05$, for both global tissue and depth-dependent results. Comparisons between groups were performed using Tukey's HSD method. Depth-dependent results were fit to a previously described stretched exponential model where the results of each stain were plotted as a function of distance away from the cartilage articular surface.[17] Goodness of fit between the data and the model was characterized by R^2 values. Two-way ANOVAs and Tukey's HSD tests were then used to compare the values of our nonlinear model between all groups for each of the three stains used.

Depth-dependent shear strains were plotted against depth-dependent results for each cell damage metric, with coefficient of determination, represented by R^2 values, being calculated by modeling the data to a line of best fit. Differences of slopes for each category were tested using an interaction model, p-values associated with the interactions were Bonferroni adjusted, differences were considered statistically significant at $p \leq 0.05$. Nonlinear modeling, correlation plots, and statistical analyses

were performed using GraphPad Prism & software.

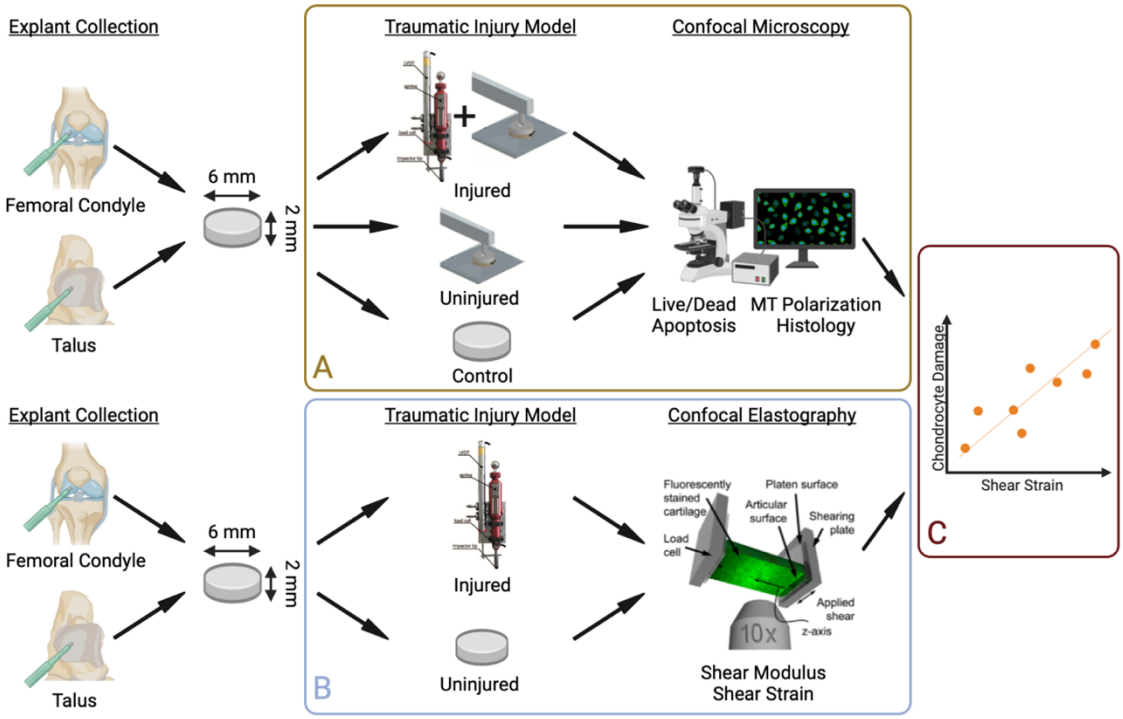

Figure 3.1. Experimental design and methods. Section A describes the techniques used to spatially map chondrocyte behavior in knee and ankle cartilage after traumatic injury. Section B centers on elucidating the effect of traumatic injury on the mechanical properties of knee and ankle cartilage. Section C involves overlaying the results of Sections A and B to derive chondrocyte sensitivity to shear strain.

Results

Confocal Microscopy

Global tissue analysis of cell death, apoptotic activity, and MT polarization in knee and ankle cartilage revealed that traumatic injury generated significant chondrocyte damage compared to control samples. Cartilage from the knee and ankle experienced a roughly 4-fold increase in cell death (10.70% to 43.79% and 7.17% to 33.56%, respectively) and MT depolarization (13.35% to 46.81% and 9.62% to 39.66%, respectively) due to injury (Figure 2 A,E) ($p < 0.0007$). Traumatic injury also generated significantly greater levels of apoptosis in knee cartilage resulting in an

average of 487.70 apoptotic cells/mm^2 (Figure 2C) (p = 0.0003), whereas ankle cartilage experienced a non-significant increase after injury.

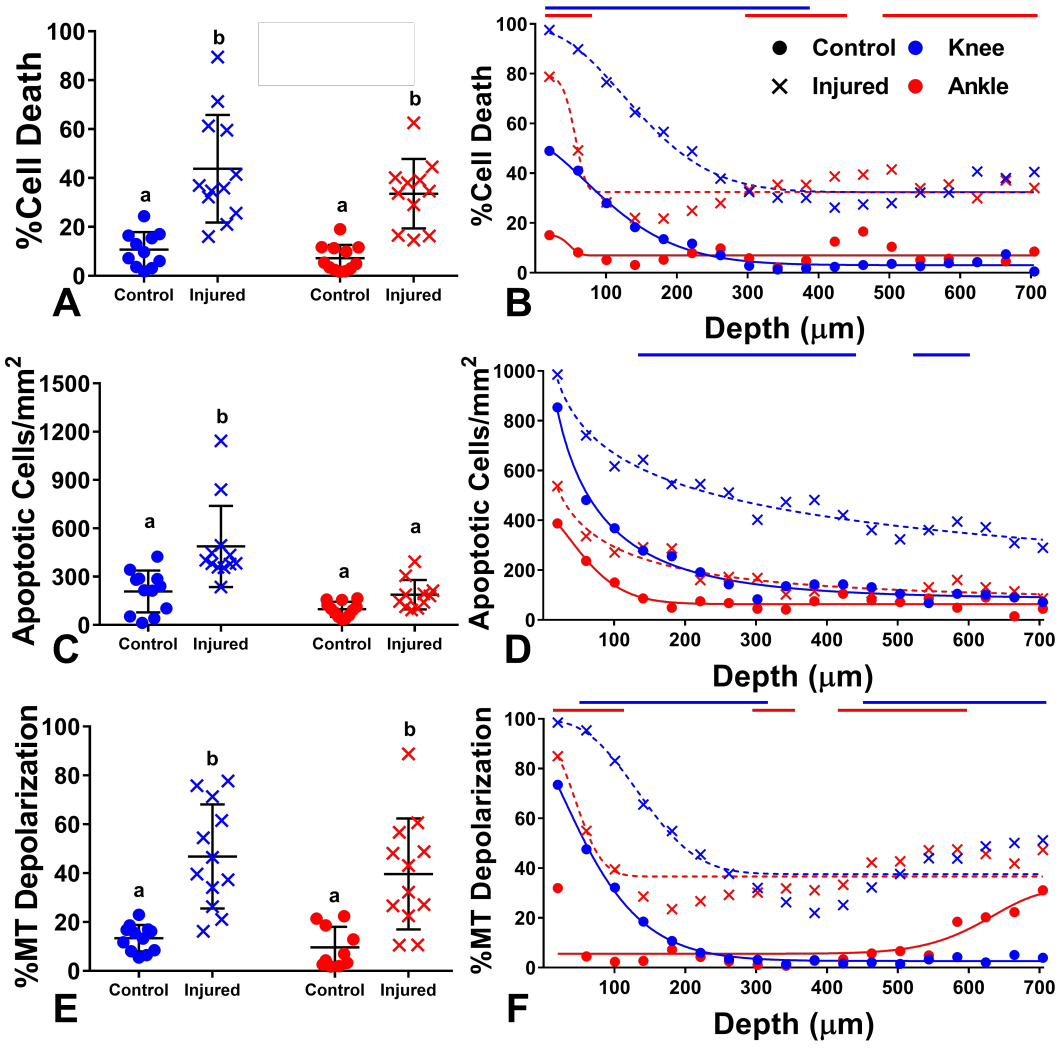

Figure 3.2. Global tissue analysis results along with depth-dependent analysis results with nonlinear curve fit. Groups with different letters denote significant difference, lines indicate area of significant difference between injured cartilage and its respective control. n = 10-12.

Additionally, we observed distinct spatial patterns of chondrocyte damage between the knee and ankle (Figure 2B,D,F). Again, we note significantly increased levels of chondrocyte damage in traumatically injured cartilage samples, compared to

controls, of both the knee and ankle at both the surface and middle zone. Injury induced significantly greater death in knee cartilage from the articular surface up to 380 μm ($p < 0.0220$), whereas injury induced significantly greater chondrocyte death in ankle cartilage from the surface up to 60 μm, 300 to 420 μm, and 500 to 700 μm ($p < 0.0477$) (Figure 2B). The difference between the cell death generated in injured knee cartilage was significantly greater than injured ankle cartilage between 60 μm and 180 μm ($p < 0.0025$). Apoptosis measurements showed injured knee cartilage displayed greater levels of response compared to its control group from 140 to 420 μm, and 540 to 580 μm ($p < 0.0428$) (Figure 2D). Interestingly, injured ankle cartilage did not show significantly greater apoptosis at any depth of the region of interest compared to controls. Injured knee cartilage displayed greater apoptosis compared to injured ankle cartilage from the articular surface up to 140 μm, 220 to 260 μm, and 340 to 420 μm ($p < 0.0302$). Lastly, traumatic injury induced significantly greater MT depolarization in knee cartilage compared to control samples from 60 to 300 μm, and 460 to 700 μm ($p < 0.0343$) (Figure 2F). Injured ankle cartilage showed greater MT depolarization from the articular surface to 100 μm, 300 to 340 μm, and 420 to 580 μm compared to controls ($p < 0.0461$). MT depolarization in injured knee cartilage was greater than injured ankle cartilage from 60 to 180 μm.

Histological analysis of cartilage samples via picrosirius red and Safranin-O can be found in Supplemental Figure 1. These data showed that injury produced more fibrillation and proteoglycan loss near the cartilage surface and caused disruption of the collagen matrix, in knee cartilage compared to ankle cartilage. Additionally, in

Supplemental Figure 2 experimental data of cell death, apoptosis, and MT depolarization was fit to a stretched exponential plus an offset: $y(x) = P+(Y_o - P)*e^{-(x/\lambda)^{\wedge}d}$ (solid and dashed curves in Figure 2B,D,F). The main result from this analysis was that our nonlinear model had greater difficulty fitting ankle cartilage data whereas knee cartilage showed results consistent to prior studies. The goodness of fit, measured by R^2, for all models ranged between 0.2282 and 0.9962 and further results are reported in Supplemental Table 1.

Confocal Elastography

Traumatic injury to ankle cartilage resulted in significantly greater shear strains up to 40 μm ($p < 0.0287$) that reached 18.12%, which was almost four times greater shear strain seen at the articular surface of uninjured ankle cartilage 4.82% (Figure 3A). This trend was not seen in injured knee cartilage which had shear strains that remained largely similar across the region of interest ($p > 0.05$). Using shear strain data in combination with measured loads we calculated depth-dependent shear modulus (Figure 3B). From shear modulus analysis we noted an increase in stiffness between the surface region and the bulk of the cartilage that is consistent with prior studies.[7] While, statistical evaluation describe differences between groups as nonsignificant we note several trends such as the stiffness of ankle cartilage decreases as a consequence of injury while knee cartilage remains mostly unchanged after injury. Changes in material properties of cartilage after injury are most apparent when observing depth-dependent shear strain results.

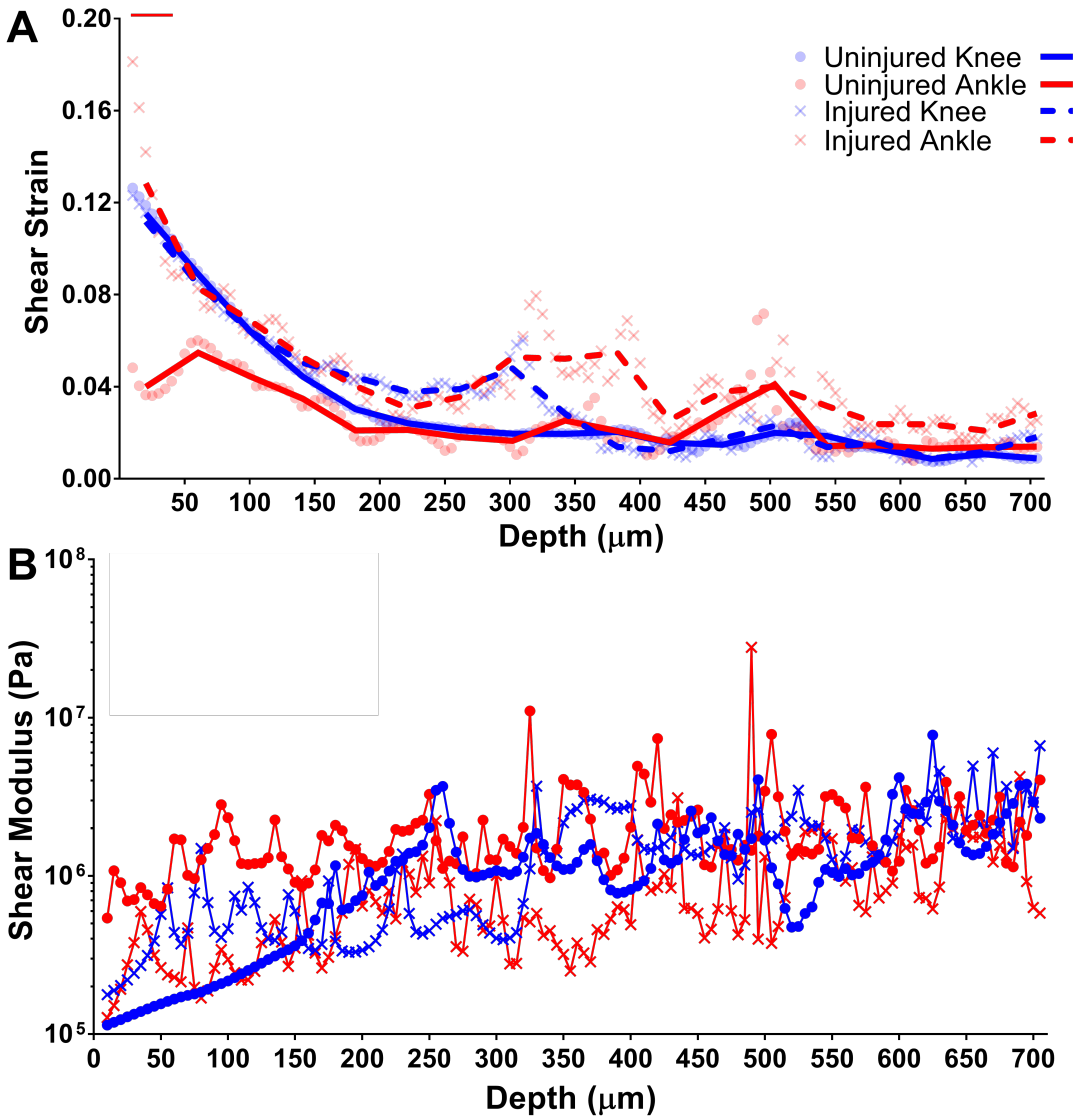

Figure 3.3. A) Depth-dependent shear strain results with transparent points representing raw data while overlayed lines represent shear strains averaged across 6 adjacent depths, lines above indicate areas of significant difference between injured groups and their respective control with n = 8. B) Depth-dependent shear modulus results, n = 8.

We combined spatial maps of cellular damage and shear strain of both injured (Figure 2) and uninjured cartilage (Figure S3) to assess the sensitivity of chondrocytes to cell death, apoptosis, and MT depolarization. The data was fit to a linear regression where the slope of the regression represents the sensitivity of cellular damage to shear

strain. Additionally, the sensitivity of cellular damage to shear strain was compared across all groups for each metric used. Further detail for the linear regression results is reported in Table 1. Supplemental Figure 3 displays cartilage samples that were solely sheared on the tribometer system, which more closely represents the shear strains generated in the tissue compared to the unmanipulated control samples of Figure 2. Supplemental Figure 3 did not show significant differences between solely slid knee and ankle cartilage samples at either the global or local level. However, uninjured ankle cartilage showed nominally lower cellular damage compared to uninjured knee cartilage from the articular surface up to 400 μm.

$y(x) = mx + b$									
Stain/Group		N_x	N_y	m	SEM	b	SEM	R^2	Slope Comparison
Live/Dead	Knee Uninjured	8	8	983.20	118.10	-1.42	4.98	0.8126	a
	Ankle Uninjured	8	8	791.20	159.40	-5.05	4.46	0.6062	ab
	Knee Injured	8	12	712.20	82.11	20.69	3.69	0.8246	a
	Ankle Injured	8	11	345.40	83.56	20.02	4.41	0.5165	b
	Knee	8	8/12	873.10	83.76	8.47	3.65	0.7616	a
	Ankle	8	8/11	551.80	78.71	5.73	3.33	0.5911	b
	Uninjured	8	8	978.80	92.23	-5.52	3.30	0.7681	a
	Injured	8	12/11	483.80	80.39	21.24	3.94	0.5158	b
Apoptosis	Knee Uninjured	8	8	9248.00	926.10	27.99	39.05	0.8617	a
	Ankle Uninjured	8	8	6663.00	1926.00	0.00	53.89	0.4278	ab
	Knee Injured	8	12	5745.00	604.80	282.80	27.20	0.8494	b
	Ankle Injured	8	11	3737.00	573.90	15.64	30.32	0.7261	b
	Knee	8	8/12	7779.00	745.60	141.90	32.50	0.7620	a
	Ankle	8	8/11	3577.00	662.40	50.27	28.00	0.4618	b
	Uninjured	8	8	9127.00	872.40	-15.08	31.21	0.7630	a
	Injured	8	12/11	3554.00	1170.00	192.60	57.40	0.2133	b
MT Depolarization	Knee Uninjured	8	8	967.30	80.13	-1.85	3.38	0.9011	a
	Ankle Uninjured	8	8	680.10	321.80	1.22	9.00	0.2183	ab
	Knee Injured	8	12	663.90	114.40	25.97	5.15	0.6778	ab
	Ankle Injured	8	12	328.70	106.20	25.29	5.61	0.3743	b
	Knee	8	8/12	848.60	89.73	10.61	3.91	0.7246	a

	Ankle	8	8/12	535.20	114.50	10.31	4.84	0.3910	b
	Uninjured	8	8	935.60	102.90	-3.03	3.68	0.7087	a
	Injured	8	12	454.90	91.49	26.44	4.49	0.4210	b

Table 3.1. Results from fitting shear strain vs chondrocyte fate data to linear regression model. Live/Dead and MT Depolarization are reported as percentages while Apoptosis is reported as # of cells/mm^2. SEM represents standard error of the mean and R^2 represents the correlation between the linear regression and experimental values. Rows that shared colors had slopes compared via two-way ANOVA.

Injured and uninjured samples showed a significant difference between their sensitivity for cell death, apoptosis, and MT depolarization (Figure 4A,B,C). Correlation strength, R^2, for data separated by injury status ranged from 0.2133 - 0.7681 and we noted that shear strain was a stronger predictor of cell death, apoptosis, and MT depolarization for knee compared to ankle. For cell death measurements, uninjured samples had a sensitivity of 978.80 while injured samples had 483.80 (p = 0.0001) showing a high degree of significance (Figure 4A). Similar results were seen with apoptosis and MT depolarization, which both showed injured cartilage samples had significantly lower ($p < 0.0009$) sensitivity to cellular damage compared their uninjured counterpart (Figure 4B,C). Next, we grouped data by solely joint location to observe whether knee and ankle cartilage had differences in chondrocyte sensitivity to shear strain (Figure 4D,E,F). We noted that grouping cellular damage vs shear strain data by joint location yields correlations that vary from 0.3910 to 0.7620, with stronger correlations once again belonging to the knee cartilage group. For cell death (873.10 vs 551.80), apoptosis (7779 vs 3577), and MT depolarization (848.60 vs 535.20), we saw knee and ankle chondrocytes have significantly different sensitivities ($p < 0.0342$) to shear strain with knee chondrocytes displaying higher sensitivity in all cases.

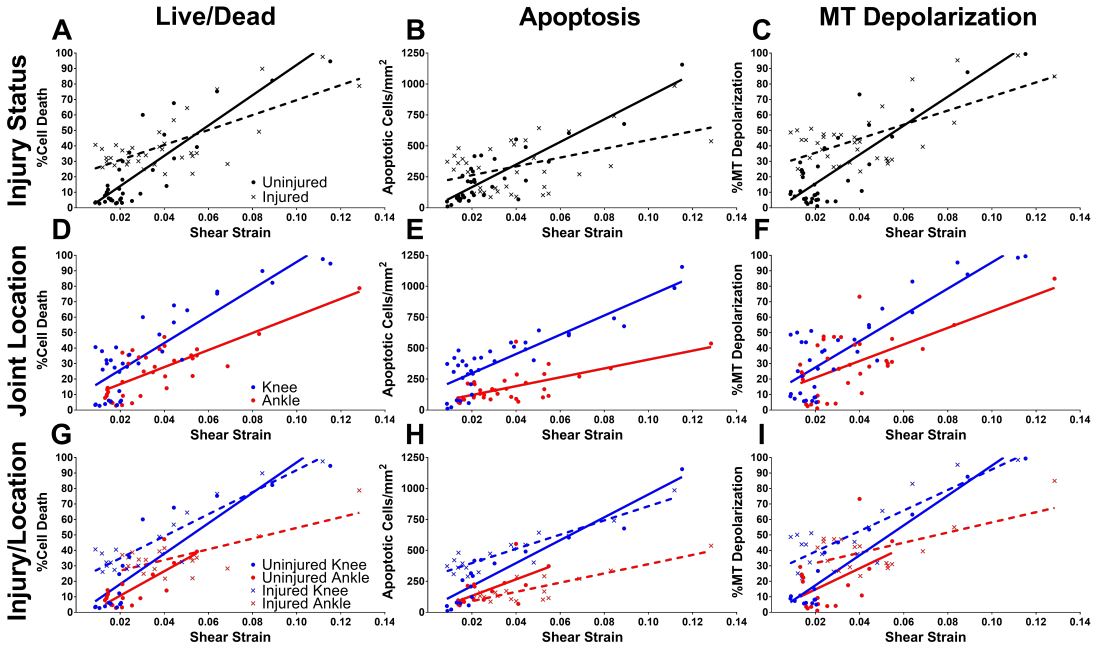

Figure 3.4. Correlation plots of shear strain against cellular responses grouped by injury status and joint location, joint location, or injury status, y axis n = 8-12, x axis n = 8.

The final group comparison made between correlations of cellular damage vs shear strain was between groups separated by both injury status and joint location (Figure 4G,H,I). Correlation strength between shear strain and cellular damage ranged from 0.2183 to 0.9011, with ankle results having lower correlations compared to the knee. In the case of cell death, injured ankle chondrocytes had a lower sensitivity compared to uninjured knee chondrocytes ($p = 0.0006$) and injured knee chondrocytes ($p = 0.0228$) (Figure 4G). We did not observe a significant difference in chondrocyte sensitivity to shear strain between uninjured knee and injured knee ($p > 0.05$) or uninjured ankle and injured ankle ($p > 0.05$). Apoptosis data showed that uninjured knee chondrocytes displayed significantly higher sensitivity to shear strain compared to injured knee chondrocytes ($p = 0.0222$) and injured ankle chondrocytes ($p = 0.0006$) (Figure 4H). Uninjured ankle chondrocytes displayed no change in shear

strain sensitivity after injury ($p > 0.05$). Additionally injured knee chondrocytes displayed no change in sensitivity compared to injured ankle chondrocytes ($p > 0.05$). Finally, MT depolarization results showed a significant difference only between the sensitivity of uninjured knee chondrocytes and injured ankle chondrocytes ($p > 0.05$). Applying a linear correlation to the data showed shear strain was a reliable predictor of cellular damage, additionally that knee and ankle cartilage show differences in sensitivity to cell damage both before and after injury.

Discussion

In this study we successfully compared global and local level differences in injury response of knee and ankle cartilage as well as injury-driven changes in mechanical properties of the cartilage tissue from both joints. Using our custom PTOA model, we've observed that traumatic injury generates distinct spatial patterns of chondrocyte damage between knee and ankle cartilage. Additionally, traumatic injury compromises the structural integrity of ankle cartilage such that its mechanical properties decrease, whereas knee cartilage had minimal changes to its mechanical properties. Finally, we noted that chondrocytes from the knee and ankle exhibited different sensitivities to shear strain, before and after injury. These findings suggest that the mechanisms of PTOA development are different between knee and ankle cartilage.

The spatial patterns of chondrocyte damage generated in knee cartilage were primarily concentrated at the articular surface, whereas ankle cartilage demonstrated a resistance to surface zone damage. Interestingly, the results from confocal microscopy and nonlinear modeling of control and injured knee cartilage matched previously

published results.[17] In contrast, this model did not accurately capture the spatial pattern of damage in ankle cartilage. This discrepancy may be due to the fact that the thinner ankle cartilage includes deep zone tissue in the top 1 mm, in contrast to knee cartilage in which the top 1 mm contains only surface and middle zone.[3,41] Injured knee cartilage showed enhanced damage from the articular surface up to a minimum ~300 μm into the tissue before reaching a plateau, whereas injured ankle cartilage displayed minimal surface zone damage past ~100 μm. However, injured ankle cartilage damage did not reach a plateau and instead increased, showing significant damage up to 700 μm. Knee cartilage results are consistent with prior studies that show the surface layer receives most damage, acting as a protective barrier that mitigates damage propagation into the middle zone.[9,14] Meanwhile, studies on the distribution of chondrocyte death in ankle cartilage show minimal damage to chondrocytes after traumatic injury with ~8% fractional cell death around the fracture-edges, reaching only ~25% 2 days post-injury.[20]

Furthermore, as predicted by our hypothesis, we saw that traumatic injury reduced the mechanical properties of ankle cartilage significantly more than knee cartilage. While knee cartilage showed minimal change in material properties due to injury, ankle cartilage displayed a reduction in shear modulus of almost one order of magnitude at the articular surface due to injury. Post-injury the shear modulus of ankle cartilage at the surface zone was at a similar magnitude to that of knee cartilage. Past 250 μm the shear modulus of injured ankle cartilage stayed consistently lower than its uninjured counterpart while both knee cartilage groups showed increased stiffness past the surface region reaching a magnitude similar to uninjured ankle cartilage.[6,7] Prior

studies suggest that depending on the injury protocol, enough damage may be delivered to the collagen network to cause reduced shear stiffness in cartilage tissue.[42,43] These studies along with our data suggest that post-injury the collagen network of ankle cartilage is damaged to a greater degree than knee cartilage, given similar loading conditions.

Notably, we observed exists an inherent difference in sensitivity to shear strains between knee and ankle cartilage, before and after injury. Additionally, we noted that mechanical injury changes the sensitivity of chondrocytes to shear strain. Interestingly, mechanical injury decreased chondrocyte sensitivity resulting in an increased baseline of damage at low strain values and lower damage at high strain compared to controls. Hashimoto et al. previously investigated the relationship between shear strain and apoptosis and similarly found a positive correlation, however they do not offer information on how this trend varies in a depth-dependent manner.[44] We also noted that chondrocyte death and damage are proportional to local tissue strain in both impact and shear loading modalities.[9,16]

This study offers new insight into the development of ankle cartilage degeneration and a possible mechanism by which the ankle experiences disparate rates of PTOA. Mechanical injury compromises the structural integrity of the collagen network, weakening the cartilage, thus generating higher local shear strains during loading, resulting in increased cellular damage.[42] This phenomenon may be exacerbated in the ankle compared to knee due to having a stiffer surface region, resulting in an inferior ability to dissipate shear energy.[3,7] Energy dissipation has been cited as a possible mechanism by which cartilage protects itself from damage and has

been shown to correlate to cartilage thickness.[36,45] Overall, these differences would suggest that ankle cartilage may be inherently less resistant to traumatic injury compared to knee cartilage.

Additionally, differences between knee and ankle may indicate that current treatment options may have disparate outcomes for treating knee and ankle PTOA and future studies may benefit from investigating this premise. Viscosupplementation, which decreases the shear load experienced at the cartilage surface, has been shown to be an effective treatment option for treating knee PTOA by managing pain and improving joint mobility.[46] However, viscosupplementation may not be an optimal form of treating ankle PTOA due chondrocyte damage being concentrated away from the surface.[47] Treatment of ankle PTOA via therapeutics capable of penetrating into the cartilage matrix may yield better results by reaching cell populations that are engaging in catabolic processes. This may include using caspase inhibitors or anti-oxidants that can prevent apoptosis, cell death, MT depolarization, and matrix degradation.[21,48]

While this study presents exciting new information to consider, it is not without limitations. For example, cartilage samples from the knee and ankle were subjected to a similar loading protocol during confocal elastography measurements despite these joints experiencing dissimilar contact forces in vivo.[3,41] However, matching loading protocols was done to compare knee and ankle chondrocyte sensitivity to shear strain on a cell to cell basis instead of attempting to compare overall joint response to injury. Next, using neonatal cartilage may highlight an exaggerated degree of cellular damage due to being more compliant compared to

mature tissue, resulting in greater strains during deformation.[40,49] Conversely, neonatal cartilage contains more chondrocytes compared to mature tissue allowing us to more easily observe the effect of injury. Also, neonatal cartilage is a tissue source that is consistent, readily available, and used by multiple groups to study PTOA.[50] Lastly, using a non-textured glass counterface during confocal elastography measurements allows for the possibility of slipping to occur between the cartilage and the glass, resulting in an increase of frictional force generated during sliding. However, a smooth counterface was chosen to match the tribometer setup.

In conclusion, this study demonstrated that knee and ankle chondrocytes exhibit unique spatial patterns of damage and sensitivities to traumatic injury. Our results showed uninjured ankle cartilage had consistently lower cellular damage which may be attributed to possessing greater stiffness compared to knee, particularly at the surface. However, injury decreased ankle stiffness resulting in significantly greater chondrocyte damage up to 100 μm and throughout the middle zone. Additionally, ankle chondrocytes were shown to possess naturally lower sensitivity to shear strain, compared to the knee, which was further reduced because of injury. Differences in cellular response to injury may be a possible rationale for why ankle and knee injuries result in disparate rates of PTOA development.

References

1. Novakofski, K. D. *et al.* Joint-dependent response to impact and implications for post-traumatic osteoarthritis. *Osteoarthr. Cartil.* **23**, 1130–1137 (2015).
2. Riegger, J. & Brenner, R. E. Pathomechanisms of posttraumatic osteoarthritis: Chondrocyte behavior and fate in a precarious environment. *Int. J. Mol. Sci.* **21**, (2020).
3. Delco, M. L., Kennedy, J. G., Bonassar, L. J. & Fortier, L. A. Post-traumatic osteoarthritis of the ankle: A distinct clinical entity requiring new research approaches. *J. Orthop. Res.* **35**, 440–453 (2017).
4. Rolauffs, B., Williams, J. M., Grodzinsky, A. J., Kuettner, K. E. & Cole, A. A. Distinct horizontal patterns in the spatial organization of superficial zone chondrocytes of human joints. *J. Struct. Biol.* **162**, 335–344 (2008).
5. Kraeutler, M. J., Kaenkumchorn, T., Pascual-Garrido, C., Wimmer, M. A. & Chubinskaya, S. Peculiarities in Ankle Cartilage. *Cartilage* **8**, 12–18 (2017).
6. Treppo, S. *et al.* Comparison of biomechanical and biochemical properties of cartilage from human knee and ankle pairs. *J. Orthop. Res.* **18**, 739–748 (2000).
7. Henak, C. R. *et al.* Human talar and femoral cartilage have distinct mechanical properties near the articular surface. *J. Biomech.* **49**, 3320–3327 (2016).
8. Athanasiou, K. A., NIEDERAUER, G. G. & SCHENCK JR., R. C. Biomechanical Topography of Human Ankle Cartilage. *Ann. Biomed. Eng.* **23**, 697–704 (1995).
9. Bonnevie, E. D. *et al.* Microscale frictional strains determine chondrocyte fate in loaded cartilage. *J. Biomech.* **74**, 72–78 (2018).

10. Delco, M. L., Bonnevie, E. D., Szeto, H. S., Bonassar, L. J. & Fortier, L. A. Mitoprotective therapy preserves chondrocyte viability and prevents cartilage degeneration in an ex vivo model of posttraumatic osteoarthritis. *J. Orthop. Res.* (2018). doi:10.1002/jor.23882

11. Delco, M. L., Bonnevie, E. D., Bonassar, L. J. & Fortier, L. A. Mitochondrial dysfunction is an acute response of articular chondrocytes to mechanical injury. *J. Orthop. Res.* (2018). doi:10.1002/jor.23651

12. Liu, H. *et al.* Effect of chondrocyte mitochondrial dysfunction on cartilage degeneration: A possible pathway for osteoarthritis pathology at the subcellular level. *Mol. Med. Rep.* **20**, 3308–3316 (2019).

13. Bonnevie, E. D. *et al.* Characterization of tissue response to impact loads delivered using a hand-held instrument for studying articular cartilage injury. *Cartilage* **6**, 226–232 (2015).

14. Bartell, L. R., Xu, M. C., Bonassar, L. J. & Cohen, I. Local and global measurements show that damage initiation in articular cartilage is inhibited by the surface layer and has significant rate dependence. *J. Biomech.* **72**, 63–70 (2018).

15. Henao-Murillo, L., Ito, K. & van Donkelaar, C. C. Collagen Damage Location in Articular Cartilage Differs if Damage is Caused by Excessive Loading Magnitude or Rate. *Ann. Biomed. Eng.* **46**, 605–615 (2018).

16. Bartell, L. R., Fortier, L. A., Bonassar, L. J. & Cohen, I. Measuring microscale strain fields in articular cartilage during rapid impact reveals thresholds for chondrocyte death and a protective role for the superficial layer. *J. Biomech.* **48**,

3440–3446 (2015).

17. Ayala, S., Fortier, L. A., Delco, M. L., Cohen, I. & Bonassar, L. J. Cartilage articulation enhances chondrocyte injury and death after impact injury. *J. Orthop. Res.* **28**, S192–S193 (2020).

18. Sah, R. L. Y., Doong, J. Y., Grodzinsky, A. J., Plaas, A. H. K. & Sandy, J. D. Effects of tissue compression on the hyaluronate-binding properties of newly synthesized proteoglycans in cartilage explants. *Biochem. J.* **267**, 803–808 (1990).

19. Quinn, T. M., Grodzinsky, A. J., Hunziker, E. B. & Sandy, J. D. Effects of injurious compression on matrix turnover around individual cells in calf articular cartilage explants. *J. Orthop. Res.* **16**, 490–499 (1998).

20. Tochigi, Y. *et al.* Distribution and progression of chondrocyte damage in a whole-organ model of human ankle intra-articular fracture. *J. Bone Jt. Surg. - Ser. A* **93**, 533–539 (2011).

21. Pascual Garrido, C. *et al.* Anti-apoptotic treatments prevent cartilage degradation after acute trauma to human ankle cartilage. *Osteoarthr. Cartil.* **17**, 1244–1251 (2009).

22. Bartell, L. R. *et al.* Mitoprotective therapy prevents rapid, strain-dependent mitochondrial dysfunction after articular cartilage injury. *J. Orthop. Res.* 1–11 (2019). doi:10.1002/jor.24567

23. Alexander, P. G. *et al.* Development of a Spring-Loaded Impact Device to Deliver Injurious Mechanical Impacts to the Articular Cartilage Surface. *Cartilage* **4**, 52–62 (2013).

24. Noyes, F. R. & Grood, E. S. The strength of the anterior cruciate ligament in humans and rhesus monkeys: Age related and species related changes. *J. Bone Jt. Surg. - Ser. A* **58**, 1074–1082 (1976).

25. Bonnevie, E. D. *et al.* Sub-critical impact inhibits the lubricating mechanisms of articular cartilage. *J. Biomech.* **53**, 64–70 (2017).

26. Aspden, R. M., Jeffrey, J. E. & Burgin, L. V. Letter to the editor. *Osteoarthritis and Cartilage* **10**, 588–589 (2002).

27. D'Lima, D. D., Hashimoto, S., Chen, P. C., Colwell, C. W. & Lotz, M. K. Human chondrocyte apoptosis in response to mechanical injury. *Osteoarthr. Cartil.* **9**, 712–719 (2001).

28. Gleghorn, J. P., Jones, A. R. C., Flannery, C. R. & Bonassar, L. J. Boundary mode lubrication of articular cartilage by recombinant human lubricin. *J. Orthop. Res.* **27**, 771–777 (2009).

29. Bonnevie, E. D., Puetzer, J. L. & Bonassar, L. J. Enhanced boundary lubrication properties of engineered menisci by lubricin localization with insulin-like growth factor I treatment. *J. Biomech.* **47**, 2183–2188 (2014).

30. Bonnevie, E. D., Galesso, D., Secchieri, C., Cohen, I. & Bonassar, L. J. Elastoviscous transitions of articular cartilage reveal a mechanism of synergy between lubricin and hyaluronic acid. *PLoS One* **10**, 1–15 (2015).

31. Gleghorn, J. P. & Bonassar, L. J. Lubrication mode analysis of articular cartilage using Stribeck surfaces. *J. Biomech.* **41**, 1910–1918 (2008).

32. Buckley, M. R., Gleghorn, J. P., Bonassar, L. J. & Cohen, I. Mapping the depth dependence of shear properties in articular cartilage. *J. Biomech.* **41**, 2430–

2437 (2008).

33. Irwin, R. M. *et al.* Distinct tribological endotypes of pathological human synovial fluid reveal characteristic biomarkers and variation in efficacy of viscosupplementation at reducing local strains in articular cartilage. *Osteoarthr. Cartil.* **28**, 492–501 (2020).

34. Middendorf, J. M. *et al.* Mechanical properties and structure-function relationships of human chondrocyte-seeded cartilage constructs after in vitro culture. *J. Orthop. Res.* **35**, 2298–2306 (2017).

35. Silverberg, J. L., Dillavou, S., Bonassar, L. & Cohen, I. Anatomic variation of depth-dependent mechanical properties in neonatal bovine articular cartilage. *J. Orthop. Res.* **31**, 686–691 (2013).

36. Buckley, M. R., Bonassar, L. J. & Cohen, I. Localization of viscous behavior and shear energy dissipation in articular cartilage under dynamic shear loading. *J. Biomech. Eng.* **135**, 1–9 (2013).

37. Buckley, M. R., Bergou, A. J., Fouchard, J., Bonassar, L. J. & Cohen, I. High-resolution spatial mapping of shear properties in cartilage. *J. Biomech.* **43**, 796–800 (2010).

38. Silverberg, J. L. *et al.* Structure-function relations and rigidity percolation in the shear properties of articular cartilage. *Biophys. J.* **107**, 1721–1730 (2014).

39. Johannes Schindelin, Ignacio Arganda-Carreras, Erwin Frise, Verena Kaynig, Mark Longair, Tobias Pietzsch, Stephan Preibisch, Curtis Rueden, Stephan Saalfeld, Benjamin Schmid, Jean-Yves Tinevez, Daniel James White, Volker Hartenstein, Kevin Eliceiri, P. T. Fiji: an open-source platform for biological-

image analysis. *Nat. Methods* **9**, 676–682 (2012).

40. Gannon, A. R., Nagel, T., Bell, A. P., Avery, N. C. & Kelly, D. J. Postnatal changes to the mechanical properties of articular cartilage are driven by the evolution of its Collagen network. *Eur. Cells Mater.* **29**, 105–123 (2015).

41. van Dijk, C. N., Reilingh, M. L., Zengerink, M. & van Bergen, C. J. A. Osteochondral defects in the ankle: Why painful? *Knee Surgery, Sport. Traumatol. Arthrosc.* **18**, 570–580 (2010).

42. Kurz, B. *et al.* Pathomechanisms of cartilage destruction by mechanical injury. *Ann. Anat.* **187**, 473–485 (2005).

43. Zhu, W., Mow, V. C., Koob, T. J. & Eyre, D. R. Viscoelastic shear properties of articular cartilage and the effects of glycosidase treatments. *J. Orthop. Res.* **11**, 771–781 (1993).

44. Hashimoto, S. *et al.* Role of p53 in human chondrocyte apoptosis in response to shear strain. *Arthritis Rheum.* **60**, 2340–2349 (2009).

45. El-Khoury, G. Y. *et al.* Cartilage thickness in cadaveric ankles: measurement with double-contrast multi-detector row CT arthrography versus MR imaging. *Radiology* **233**, 768–773 (2004).

46. Cooper, C. *et al.* Use of Intraarticular Hyaluronic Acid in the Management of Knee Osteoarthritis in Clinical Practice. *Arthritis Care Res.* **69**, 1287–1296 (2017).

47. Waller, K. A. *et al.* Role of lubricin and boundary lubrication in the prevention of chondrocyte apoptosis. *Proc. Natl. Acad. Sci. U. S. A.* **110**, 5852–5857 (2013).

48. Zhao, K. *et al.* Cell-permeable peptide antioxidants targeted to inner mitochondrial membrane inhibit mitochondrial swelling, oxidative cell death, and reperfusion injury. *J. Biol. Chem.* **279**, 34682–34690 (2004).

49. Levin, A. S., Chen, C. T. C. & Torzilli, P. A. Effect of tissue maturity on cell viability in load-injured articular cartilage explants. *Osteoarthr. Cartil.* **13**, 488–496 (2005).

50. Torre, O. M., Das, R., Berenblum, R. E., Huang, A. H. & Iatridis, J. C. Neonatal mouse intervertebral discs heal with restored function following herniation injury. *FASEB J.* **32**, 4753–4762 (2018).

Supplemental Materials

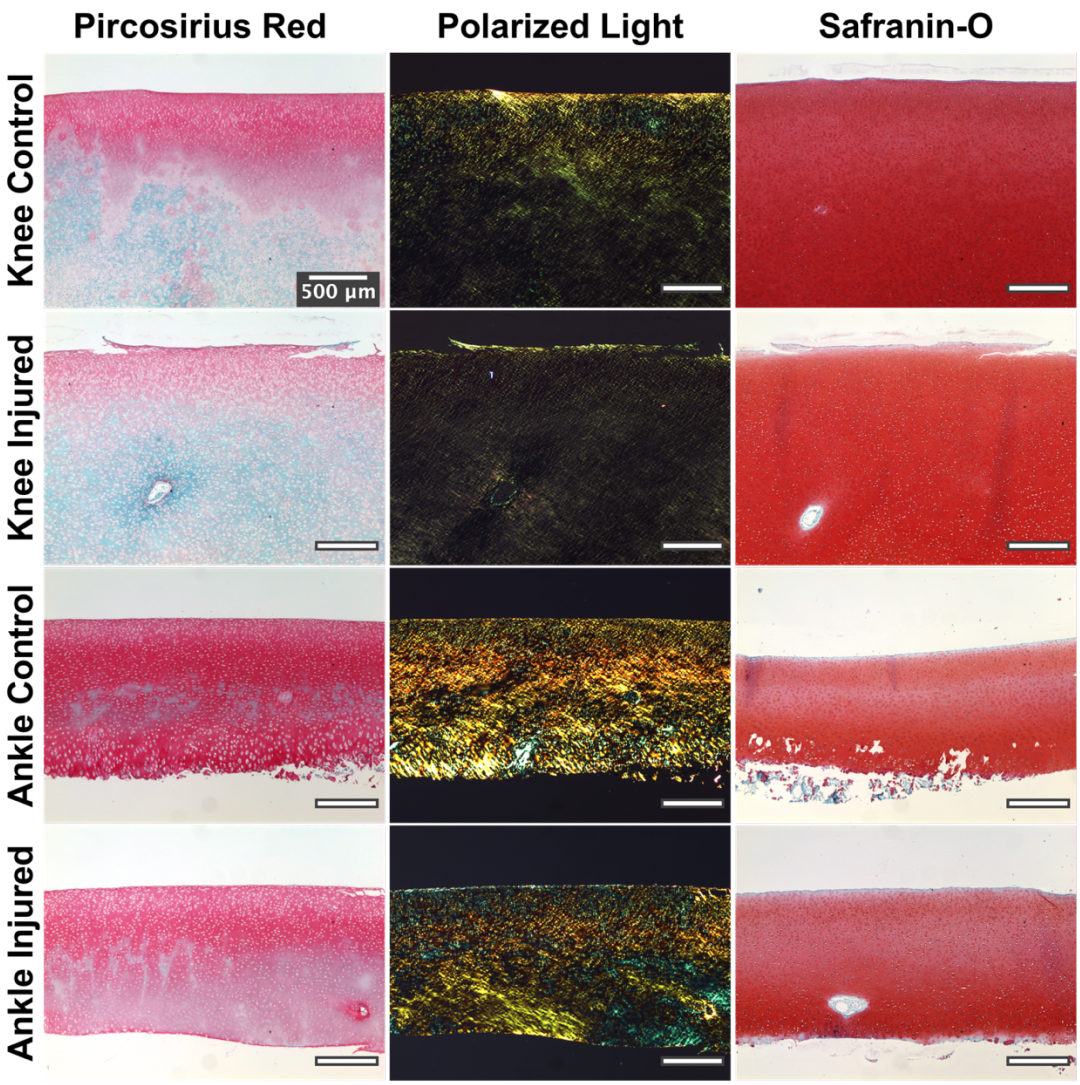

Figure 3.S1. Representative histological sections of knee and ankle cartilage both before and after injury

Picrosirius red and Safranin-O staining viewed under polarized light revealed injured cartilage samples from both the knee and the ankle showed macroscale injury in the form of cartilage fibrillation and loss of structural components (Figure 5). Picrosirius red staining shows knee cartilage has collagen localization at the tissue surface whereas ankle cartilage shows strong presence of collagen throughout the

tissue depth. While both joints show structural damage due to injury, ankle cartilage had minor fibrillation to the tissue surface compared to knee cartilage which displayed prominent tearing. Viewing under polarized light showed that ankle cartilage displayed greater collagen fiber organization throughout the tissue sample whereas knee cartilage primarily displayed collagen fiber organization near the articular surface. Additionally, traumatic injury seems to have compromised the structural integrity of both knee and ankle cartilage by reducing the overall collagen fiber organization. Safranin-O staining results show traumatic injury resulted in loss of proteoglycans near the articular surface of both ankle and knee cartilage particularly around areas of cartilage fibrillation.

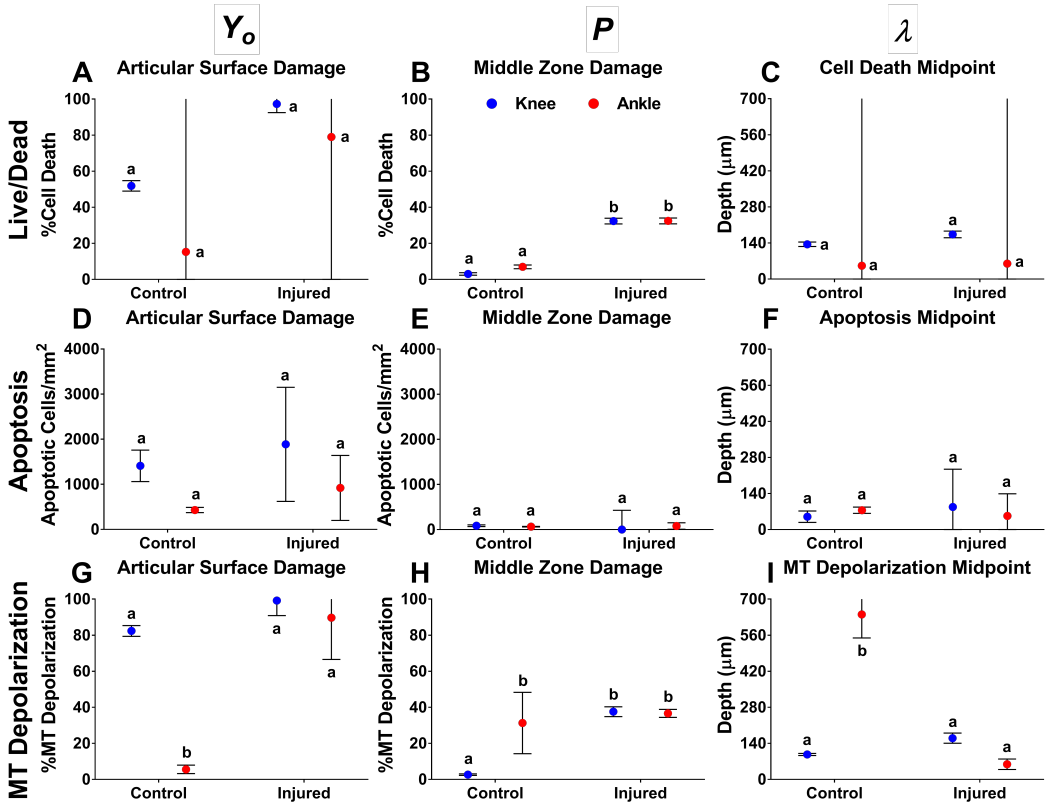

Figure 3.S2. Comparison of parameters from nonlinear model. Groups with different letters denote significant difference, n = 10-12

Articular surface damage, Y_o, for injured samples was found to be 97.26% cell death, 1886.31 apoptotic cells/mm^2, and 99.17% MT depolarization for the knee and 78.99% cell death, 920.31 apoptotic cells/mm^2, and 89.67% MT depolarization for the ankle. Conversely, articular surface damage for control samples was shown to be 51.88% cell death, 1409.39 apoptotic cells/mm^2, and 82.36% MT depolarization for the knee and 15.25% cell death, 429.70 apoptotic cells/mm^2, and 5.57% MT depolarization for the ankle (Figure 3A,D,G). Articular surface damage across groups was shown to be similar in cell death and apoptosis measurements ($p > 0.05$), however MT depolarization in control ankle cartilage was not only significantly lower than the injured group but also control and injured knee cartilage ($p < 0.0011$) (Figure 3G). We also note large standard error of mean existed within measurements of both injured and control ankle, which effects reaching significance in group comparisons.

Middle zone damage, P, seen in cell death measurements showed injured knee and ankle cartilage had a significantly greater response compared to their control counterparts ($p < 0.0001$) (Figure 3B). Next, middle zone analysis of apoptosis results showed no significant differences between the groups ($p > 0.05$) with all groups having under 100 apoptotic cells/mm^2 (Figure 3E). MT depolarization results showed both injured knee and ankle cartilage had a significantly greater response compared to control knee group ($p < 0.012$), however control ankle cartilage showed a similar magnitude of response at 31.29% ($p > 0.05$) (Figure 5H). In all three metrics of cellular response, we find that injured cartilage samples from both the knee and the ankle always had greater magnitudes of damage compared to their respective controls,

despite not always being a statistically significant difference.

The final parameter of the nonlinear model, λ, which represents the tissue depth the model transitions from the highest to lowest magnitude of cellular response showed minimal significant differences between groups for all three metrics. Cell death analysis revealed that while not significantly greater ($p > 0.05$), injured knee and ankle cartilage had deeper midpoints compared to their respective control (173.33 vs 135.09 μm, knee) (60.12 vs 52.18 μm, ankle) (Figure 5C). Apoptosis results showed minimal differences between groups concerning the midpoint of damage ($p > 0.05$) (Figure 5F). Finally, MT depolarization results showed that the control ankle group had a midpoint of damage significantly deeper into the tissue, 640.38 μm, compared to all other groups ($p < 0.0001$) (Figure 5I). Generally, we see that traumatically injuring cartilage samples, regardless of joint location, generates greater levels of chondrocyte damage compared to their intact controls which is consistent with prior studies.[17]

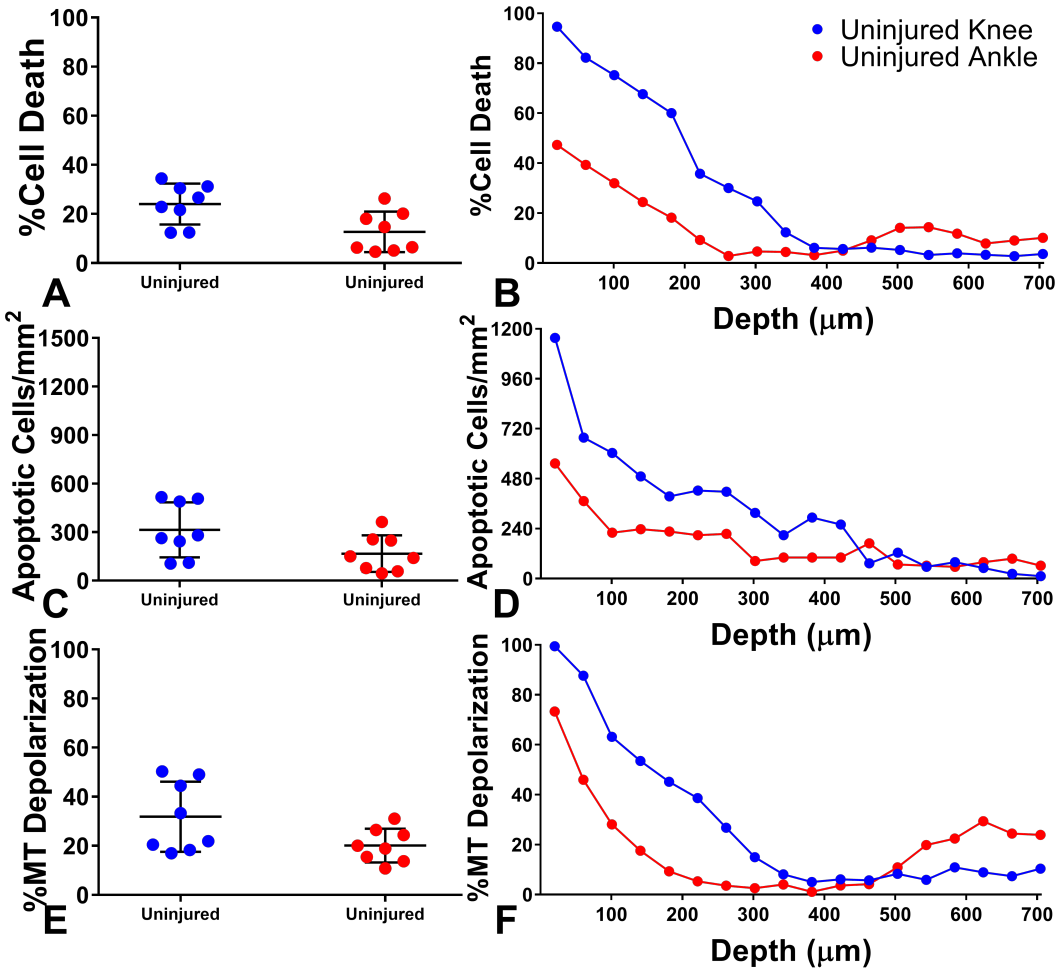

Figure 3.S3. Global and depth-dependent analysis results of samples subjected solely to shear strain through repetitive sliding. n = 8

$y(x) = (Y_o - P)*e^{-(x/\lambda)^d} + P$											
Stain/Group		N	Y_o	SEM	P	SEM	λ	SEM	d	SEM	R^2
Live/Dead	Knee Control	11	51.88	2.90	3.03	0.67	135.09	8.71	1.54	0.21	0.9836
	Ankle Control	12	15.25	1328144.27	6.97	1.58	52.18	1873194.8	4.49	1045637.31	0.2282
	Knee Injured	12	97.26	4.80	32.34	1.01	173.33	12.90	2.01	0.42	0.9625
	Ankle Injured	11	78.99	2055.84	32.45	1.61	60.12	1042.56	4.98	9248.15	0.8015
Apoptosis	Knee Control	12	1409.39	349.16	85.31	18.21	50.00	22.10	0.64	0.17	0.9847
	Ankle Control	12	429.70	58.28	63.66	6.64	75.06	12.12	1.57	0.55	0.9389
	Knee Injured	12	1886.31	1264.81	0.00	427.05	87.69	146.59	0.27	0.24	0.9564
	Ankle Injured	11	920.31	720.17	78.49	71.62	52.82	86.35	0.49	0.44	0.9239
MT Depolarization	Knee Control	12	82.36	2.98	2.66	0.42	96.85	4.10	1.33	0.10	0.9962
	Ankle Control	10	5.57	2.35	31.29	17.01	640.38	91.29	10.90	11.36	0.5301
	Knee Injured	12	99.17	8.31	37.56	2.73	160.11	19.71	2.59	1.15	0.8690
	Ankle Injured	12	89.67	23.14	36.63	2.22	58.95	20.34	2.21	3.17	0.7028

Table 3.S1. Stretched exponential model fitting results. Live/Dead and MT Depolarization are reported as percentages while Apoptosis is reported as # of cells/mm^2. SEM represents standard error of the mean and R^2 represents the correlation between the model values and experimental value.

CHAPTER 4

Depletion of Lubricating Molecules in Synovial Fluid Alters Chondrocyte Sensitivity to Shear Strain

Abstract

Articular joints facilitate motion and transfer loads to underlying bone through a combination of cartilage tissue and synovial fluid, which together generate a low friction contact surface. Traumatic injury delivered to cartilage and the surrounding joint capsule causes secretion of proinflammatory cytokines by chondrocytes and the synovium, which triggers cartilage matrix breakdown and impairs the ability of synovial fluid to lubricate the joint. Once these inflammatory processes become chronic, development of post-traumatic osteoarthritis (PTOA) becomes expected. However, the exact mechanism by which negative alterations to synovial fluid leads to PTOA pathogenesis is currently unknown. We hypothesize that removing the lubricating macromolecules from synovial fluid alters the relationship between mechanical loads and subsequent chondrocyte behavior in injured cartilage tissue. To test this hypothesis, we utilized an ex vivo model of PTOA that involves subjecting cartilage explants to a single rapid impact followed by continuous articulation within a lubricating bath of either healthy synovial fluid, synovial fluid treated with hyaluronidase, or synovial fluid treated with trypsin. This was done to remove the main macromolecules attributed with providing synovial fluid with its lubricating properties: hyaluronic acid and lubricin. Explants were then bisected and fluorescently stained to assess global and depth-dependent cell death, caspase activity, and mitochondrial depolarization. Explants were tested via confocal elastography to determine the local shear strain profile generated in each lubricant. These results show

that removing either hyaluronic acid or lubricin from synovial fluid significantly increases depth-dependent chondrocyte damage, depth-dependent shear strains, and negatively alters chondrocyte sensitivity to mechanical loads.

Ayala S, Delco ML, Cohen I, Bonassar LJ. Depletion of Lubricating Molecules in Synovial Fluid Alters Chondrocyte Sensitivity to Shear Strain. In preparation to be submitted to Biotribology. 2022.

Introduction

Healthy synovial joints facilitate movement by providing a wear resistant and low friction bearing surface via articular cartilage and synovial fluid that forms fluid film lubrication.[1] The lubricity of synovial fluid is attributed to its macromolecule components specifically: lubricin, a mucinous glycoprotein; and hyaluronic acid (HA), a high molecular weight glycosaminoglycan.[2,3] The functional role of lubricin is to adhere to the cartilage surface, forming a network that generates an antiadhesive barrier capable of preventing contact between opposing cartilage surfaces.[4] HA acts as a high viscosity lubricant that provides shock absorbing, viscoelastic, and chondroprotective properties to synovial fluid, however the specific lubricative mechanisms of HA are still largely unknown.[5–7] Together, lubricin and HA act synergistically to reduce shear stresses between cartilage surfaces, prevent chondrocyte death, and inhibit surface erosion.[2,8,9]

Joint health may become compromised following severe injury delivered to cartilage tissue, which results in inflammation and downstream catabolic changes to the synovial fluid, extracellular matrix, subchondral bone, and synovial membrane ultimately leading to post-traumatic osteoarthritis (PTOA).[10,11] Following significant trauma, joint inflammation triggers the release of cytokines and enzymes including: TNFα, IL-1β, MMPs, reactive oxygen species, aggrecanase, and hyaluronidase.[10,12–14] These biological mediators result in mitochondrial (MT) depolarization, chondrocyte apoptosis, cell death, destruction of cartilage matrix, and changes in synovial fluid quality via loss of lubricin and degradation of HA.[7,15–18] Decreased concentrations of HA and lubricin reduce synovial fluid lubricity, leading to general increases in

friction, shear strains, and chondrocyte damage during articulation.[19,20] However, changes in synovial fluid have been primarily studied in the context of idiopathic OA using uninjured cartilage tissue. Changes in synovial fluid are particularly interesting in the context of traumatic injury, as synovial inflammation has been shown to have a greater part in the pathophysiology of PTOA compared to idiopathic OA.[21] This phenomenon indicates the need to study the role of compromised synovial fluid in the development of PTOA.

Prior studies of cartilaginous injuries note levels of cellular and tissue damage are highest primarily at the site of trauma, typically the cartilage surface, then subsiding in the surrounding area.[22] These incidences can create a dangerous feedback loop starting with degradation of synovial fluid, via increased secretion of inflammatory cytokines and enzymes, leading to increased joint friction, resulting in increased shear strain during joint articulation, triggering increased chondrocyte damage, thereby generating greater inflammatory response.[8,23,24] Additionally, previous studies from our group have shown, via our ex vivo model of PTOA, that damage to the cartilage middle zone increases post-injury by subsequent articulation due to the inability of the compromised surface region to protect the tissue bulk from increased shear strains.[25,26] Yet it is unknown how the effect of degraded synovial fluid further confounds the initial traumatic injury. In the present study, we hypothesize that catabolizing the lubricating macromolecules of synovial fluid will modulate the relationship between shear strain and subsequent chondrocyte damage in traumatically injured cartilage. Therefore, our objective is to further innovate our ex vivo model of PTOA to elucidate the role of synovial inflammation in PTOA

pathogenesis by utilizing degraded synovial fluid. The results of this study will reveal the role of synovial fluid degradation in propagating damage through compromised cartilage tissue.

Materials and Methods

Cartilage preparation

Cartilage from the femoral condyle of the knee joint of six neonatal (i.e., skeletally immature) bovids (sex unknown; Gold Medal Packing) was sterilely harvested, rinsed with Dulbecco's phosphate-buffered saline (PBS) containing antibiotics (100 U/ml penicillin-streptomycin, Mediatech) and sectioned into cylindrical plugs using 6 mm diameter biopsy punches (Integra). Explants from the femoral condyle were trimmed, while keeping the articular surface intact, to 2 mm in depth. Cuts were performed using a custom jig and blades lubricated with bovine synovial fluid (Lampire) to limit chondrocyte death preceding testing.[25] Before injury, explants tested via confocal microscopy were incubated overnight in media (phenol red-free DMEM containing 1% FBS, HEPES 0.025 ml/ml, penicillin 100 U/ml, streptomycin 100 U/ml, and 2.5 mM glucose) at 37°C, 5% CO_2.

Lubricant preparations

To observe the effect of poorly lubricating synovial fluid on subsequent cartilage shear strain and chondrocyte damage during articulation, synovial fluid was enzymatically degraded with either hyaluronidase (HAase) or trypsin (Try). Hyaluronidase treatment was used to catabolize hyaluronic acid, one of the main macromolecules attributed to synovial fluid lubrication, thereby decreasing synovial fluid viscosity.[3] Whereas, trypsin was used to deplete synovial fluid of its lubricin

content, the second main macromolecules attributed to synovial fluid lubrication, thereby increasing the boundary friction coefficient between cartilage and articulating surface. Bovine synovial fluid (SF) was incubated for two hours at 37 C under constant stirring conditions with bovine testes hyaluronidase (25 μg/mL,400-1000 U/mg, Sigma Aldrich, St Louis MO) or trypsin EDTA (100 μL of 2 mg/mL, 0.25% trypsin, 0.1% EDTA, 1X, Mediatech, Manassas, VA) as previously reported.[27,28] To prevent enzymatic degradation from causing cartilage tissue degradation, both degraded lubricants were treated with a protease inhibitor cocktail (Thermo Fisher Scientific) and used for confocal elastography testing on cartilage explants.

Combined loading model of PTOA

Cartilage explants were subjected to injury using a previously described, spring-loaded impactor system.[25,29] A single cycle of unconfined compression was delivered to the articular surface of explants using a 12 mm diameter cylindrical impacting tip. All impacts were delivered, over a loading time of ~ 1 ms, at a peak stress of 17.34 ± 0.99 MPa and peak stress rate of 21.6 ± 2.45 GPa/s. Loading magnitudes of this nature have been seen in previous studies to cause failure of the anterior cruciate ligament, however this loading protocol was chosen to deliver injurious compression resulting in pathological chondrocyte death and damage without full thickness cracking.[30,31] Following traumatic injury, impacted cartilage explants were slid against a polished glass counterface (McMaster Carr) in a custom-built tribometer.[32–35] Explants were submerged in a lubricating bath of either bovine SF, PBS, SF with hyaluronidase (SF+HAase), or SF with trypsin (SF+Try), compressed to 15% axial strain, allowed to equilibrate for 60 min, then slid for 60 min at 1mm/s.[35]

This loading regimen is known to be reliable at producing cell death, apoptosis, and mitochondrial depolarization.[25,29,33,35] The results of these groups were then compared to a control group that received no form of injury or manipulation.

Confocal elastography

A setup mimicking the tribometer configuration was mounted on a 3i Marianas Spinning Disk Confocal Microscope to measure depth-dependent shear modulus and shear strains of cartilage explants.[36] Shear strains were tracked in a similar manner to previous studies that measured depth-dependent shear properties.[37] Cylindrical explants were axially bisected into hemicylinders that were stained for 1 h in 14 μg/ml 5-dichlorotriazinyl-aminofluorescein (5-DTAF, Molecular Probes, Grand Island, NY) followed by a 30 min PBS wash. Samples were then mounted via their deep zone to a tissue deformation imaging stage (TDIS) as previously described.[38,39] Samples were submerged in a lubricating bath of either bovine SF, PBS, SF+HAase, SF+Try, SF with hyaluronidase and protease inhibitors (SF+HAase&PI), or SF with trypsin and protease inhibitors (SF+Try&PI), compressed to 15% axial strain against polished glass using a micrometer stage, and allowed to stress relax for 30 min. In a similar manner to shearing performed on the tribometer, the glass slide was reciprocated against the cartilage surface using a piezoelectric positioning stage at a magnitude of 5% of sample thickness at 1 Hz. Videos were captured at 20 frames per second throughout the tissue depth to track the depth-dependent properties of the cartilage tissue. Depth-dependent shear deformations were tracked by analyzing the displacement of the tissue between frames via a custom MATLAB code. The maximum local shear strains were calculated through differentiation of the local

displacements as previously described.[40,41]

Confocal microscopy

Imaging of explants began 3 h post-injury. As described previously, cylindrical samples were axially bisected into hemicylinders and stained either for 30 min with 1 μl/ml Calcein AM and 1 μl/ml ethidium homodimer (Thermo Fisher Scientific), 30 min with CellEvent Caspase-3/7 Green (Thermo Fisher Scientific) following manufacturer instructions, or MitoTracker Green (200 nM; Thermo Fisher Scientific) for 20 min followed by addition of tetramethylrhodamine methyl ester perchlorate (10 nM; Thermo Fisher Scientific) for 30 min.[24,25] After staining, all explants were rinsed in PBS for 30 min. Cartilage explants were imaged on a Zeiss LSM880 confocal/multiphoton inverted microscope to determine the cellular response of talar and femoral condylar cartilage to rapid impact injury followed by repeated frictional shear.

Confocal images were captured and imported into ImageJ to create a composite image (550 μm wide vs 725 μm depth). Depth-dependent cellular responses were quantified using Fiji (NIH) a custom MATLAB program (MathWorks, Inc.).[42,43] Global tissue responses were reported as percent cell death, percent cells with depolarized MT, and number of caspase-positive cells normalized to the area of composite image: 0.39882 mm^2. Depth-dependent results were calculated by segmenting each image into eighteen ~40 μm bins with all bins using the same image analysis outcomes. The number of caspase-positive cells were normalized to the area of the bin, 0.022 mm^2.

Statistical analysis

One-way ANOVAs were performed to compare the global effect of poor lubricating synovial fluid on the spatial patterns of cellular response in femoral condylar cartilage while repeated measures two-way ANOVAs were used to compare depth-dependent results. Differences were considered statistically significant at $p \leq 0.05$, for both global tissue and depth-dependent results. Pairwise comparisons between groups were performed using Tukey's HSD method. Depth-dependent results were fit to a previously described stretched exponential model where the results of each stain were plotted as a function of distance away from the cartilage articular surface.[25] Goodness of fit between the data and the model was characterized by R^2 values. Two-way ANOVAs and Tukey's HSD tests were then used to compare the values of our nonlinear model between all groups for each of the three stains used. Significant differences between shear strain maps for each group were determined using a repeated measures two-way ANOVA and Tukey's HSD tests, while differences between degraded synovial fluid shear strains and their counterparts treated with protease inhibitors were determined using a standard two-way ANOVA and Tukey's HSD tests.

Depth-dependent shear strains were plotted against depth-dependent results for each cell damage metric, with coefficient of determination, represented by R^2 values, being calculated by modeling the data to a line of best fit. Differences of slopes between SF, SF+HAase, and SF+Try groups were tested using an interaction model, p-values associated with the interactions were Bonferroni adjusted and differences were considered statistically significant at $p \leq 0.05$. Nonlinear modeling, correlation plots, and statistical analyses were performed using GraphPad Prism 7 (San Diego,

CA).

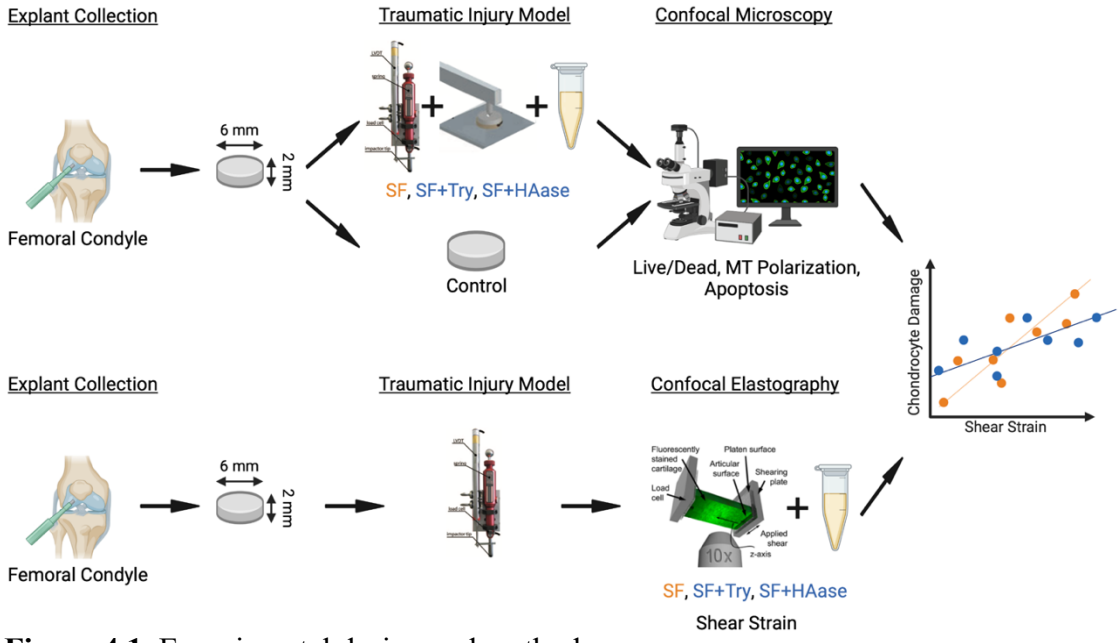

Figure 4.1. Experimental design and methods.

Results

Confocal microscopy

Global magnitudes of cell death, apoptosis, and MT depolarization for the control group (6.21%, 187 apoptotic cells/mm^2, 8.60%) was shown to be low, allowing for a reasonable assumption that additional damage displayed by treated groups is the result of the combined injury model. Bulk tissue analysis of cellular damage metrics showed significant increases in cell death ($p < 0.006$), apoptosis ($p < 0.02$), and MT depolarization ($p < 0.0002$) for SF, SF+HAase, and SF+Try each compared to control cartilage samples (Figure 2A, C, E). However, significant increases in chondrocyte damage between degraded synovial fluid groups and normal SF only existed between SF+HAase and SF in apoptosis measurements ($p = 0.0008$), 907 vs 488 apoptotic cells/mm^2 respectively (Figure 2C). All other bulk tissue

comparisons between degraded synovial fluid groups and normal SF yielded non-significant results ($p > 0.05$).

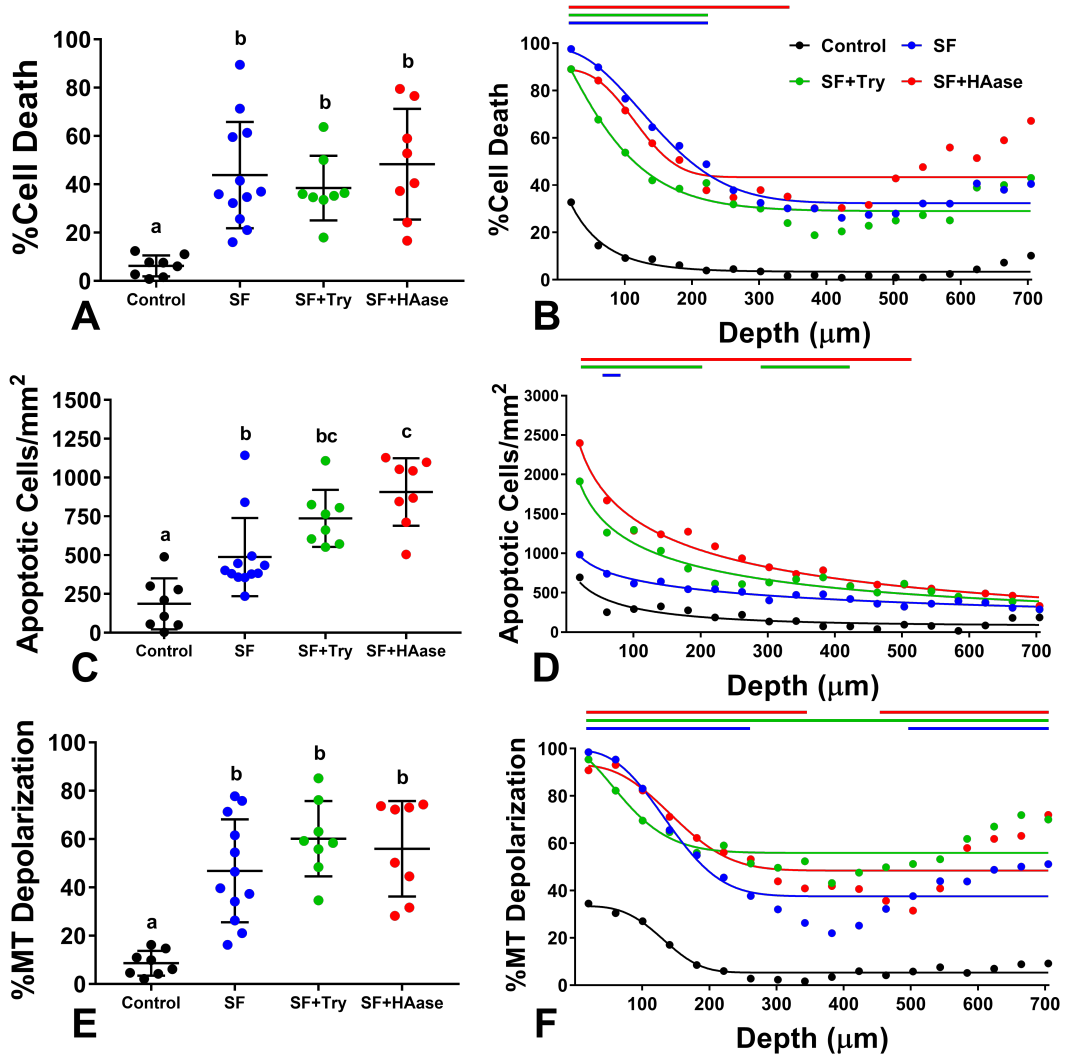

Figure 4.2. Bulk tissue and depth-dependent cellular response results with nonlinear model curve fit. Groups with different letters denote a significant difference between them, while lines show regions of tissue where a group shows significant difference between itself and the control group. n = 8-12.

Depth-dependent analysis showed that depleting the lubricating properties of synovial fluid caused significantly more damage to chondrocytes across the region of interest compared to what is expected from traumatic injury alone (Figure 2B, D, F). Sliding traumatically injured cartilage samples in non-degraded SF resulted in

significantly greater cell death, apoptosis, and MT depolarization compared to uninjured controls at the cartilage surface up to ~300 μm, while in the middle zone only MT depolarization significantly increased specifically from ~500 μm to 700 μm ($p < 0.05$). However, both SF+HAase and SF+Try caused additional regions of cartilage tissue to experience significantly greater chondrocyte damage compared to uninjured controls. SF+HAase resulted in greater cell death up to 340 μm (minimum of 35.18%), while SF+Try (minimum of 40.91%) and SF (minimum of 48.84%) resulted in greater cell death up to only 220 μm ($p < 0.0143$) (Figure 2B). We observed no significant differences in cell death, at any region of the cartilage, between samples slid in degraded SF and those slid in standard SF or between SF+HAase and SF+Try ($p > 0.05$). Caspase activity measurements revealed that SF+HAase and SF+Try resulted in significantly greater chondrocyte apoptosis, compared to uninjured controls, from the cartilage surface up to 500 μm ($p < 0.0386$) (Figure 2D). Levels of apoptosis in this region ranged from 1912 to 604 apoptotic cells/mm^2 for the SF+HAase group, and 2398 to 502 apoptotic cells/mm^2 for the SF+Try group. Conversely, injured cartilage samples slid in SF produced caspase activity greater than controls only at one site, 60 μm ($p < 0.0264$), with every other region showing chondrocyte apoptosis at a similar level to control samples ($p > 0.05$). Across the region where degraded synovial fluid showed significantly higher apoptosis, the magnitude of apoptosis ranged only from 985 to 323 apoptotic cells/mm^2. Additionally, SF+HAase and SF+Try groups generated greater levels of chondrocyte apoptosis compared to SF from the articular surface up to 200 μm and 100 μm ($p < 0.0143$) respectively. Lastly, the magnitude of MT depolarization in the

SF group was significantly greater than controls from 0 to 260 μm and 500 to 700 μm ($p < 0.0449$) (Figure 4F). Surface zone depolarization ranged from 98.47% to 37.67% and the middle zone depolarization ranged from 37.63% to 51.14%, showing an increasing trend within the middle zone. However, SF+HAase showed significantly enhanced MT depolarization from 0 to 380 μm (93.13% to 41.88%) and 460 to 700 μm (35.64% to 71.96%) ($p < 0.0465$) while SF+Try showed enhanced depolarization across the entire region of interest (minimum of 43.14%) ($p < 0.016$), both compared to control group. Similarly, SF+HAase and SF+Try groups both showed showing an increasing trend of MT depolarization within the cartilage middle zone. No significant intergroup differences in MT depolarization were observed between SF, SF+HAase, and SF+Try ($p > 0.05$).

$y(x) = (Y_o - P)*e^{-(x/\lambda)^{\wedge}d} + P$											
Stain/Group		N	Yo	SEM	P	SEM	λ	SEM	d	SEM	R^2
Live/Dead	Control	8	47.17	21.34	3.37	0.86	50.00	36.73	0.93	0.59	0.8951
	SF	12	97.26	4.80	32.34	1.58	173.33	12.90	2.01	0.42	0.9625
	SF+Try	8	97.76	18.27	29.01	2.50	98.75	30.94	1.22	0.60	0.8587
	SF+HAase	8	88.99	10.81	43.35	3.17	133.39	27.82	2.79	2.28	0.6837
Apoptosis	Control	8	1086.82	1181.25	79.90	78.87	50.00	105.18	0.56	0.67	0.8143
	SF	12	1886.31	1264.81	0.00	427.05	87.69	146.59	0.27	0.24	0.9564
	SF+Try	8	3804.50	4423.25	98.70	709.02	50.00	132.45	0.35	0.47	0.9503
	SF+HAase	8	4338.08	1415.33	0.00	191.64	77.13	60.30	0.37	0.12	0.9775
MT Depolarization	Control	8	33.39	1.95	5.31	0.65	146.17	8.41	3.39	0.92	0.9566
	SF	12	99.17	8.31	37.56	2.73	160.11	19.71	2.59	1.15	0.8690
	SF+Try	8	98.24	14.55	55.90	2.45	95.88	33.70	1.67	1.38	0.6719
	SF+HAase	8	92.90	9.94	48.45	3.45	170.55	34.88	2.60	1.93	0.7018

Table 4.1. Results of nonlinear model curve fit of confocal microscopy data. Live/Dead and MT Depolarization are reported as percentages while Apoptosis is reported as # of cells/mm^2.

Depth-dependent microscopy data was fit to the nonlinear function, $y(x) = P+(Y_o - P)*e^{-(x/\lambda)^{\wedge}d}$, to predict average levels of chondrocyte damage for a given group

as a function of depth. Group comparisons of the parameters of our nonlinear model can be observed in Figure 3 and numerical results can be seen in Table 1. The magnitude of damage at the articular surface, represented by Y_o, showed no significant differences between any groups in the case of apoptosis ($p > 0.05$). However, the magnitude of cell death and MT depolarization at the articular surface for SF, SF+HAase, and SF+Try were all significantly greater than that of the control group ($p < 0.0497$). The amount of cell death seen at the surface zone between these groups ranged from 88.99% to 97.76%, while the control group was at 47.17%. There were no significant differences between non-control groups in Y_o for any of the three metrics of chondrocyte damage ($p > 0.05$). The magnitude of damage at the middle zone, P, showed multiple significant differences between groups in cell death and MT depolarization measurements. For cell death, not only were SF, SF+HAase, and SF+Try all significantly greater than the control group ($p < 0.0001$), but SF+HAase was seen to be significantly greater than SF ($p = 0.0001$). SF+HAase also possessed a significantly higher P value than SF+Try ($p = 0.0004$). The value of P, in the case of cell death, for controls, SF, SF+HAase, and SF+Try groups were: 3.37%, 32.34%, 29.01%, and 43.35% respectively. For MT depolarization, while we once again see SF, SF+HAase, and SF+Try were significantly greater than the control group ($p < 0.05$), in this case both SF+HAase, and SF+Try possessed significantly greater middle zone damage compared to SF ($p < 0.025$). The value of P for MT depolarization was 5.31% for controls, 37.56% for SF, 48.45 % for SF+HAase, and 55.9% for SF+Try. We note no significant differences between any groups in P for apoptosis measurements ($p > 0.05$). Finally, the midpoint location between the greatest and

lowest magnitudes of damage, λ, showed minimal significant differences between groups. The only significant difference seen was in cell death where SF had a midpoint location deeper in the tissue only compared to the control group (p = 0.0079).

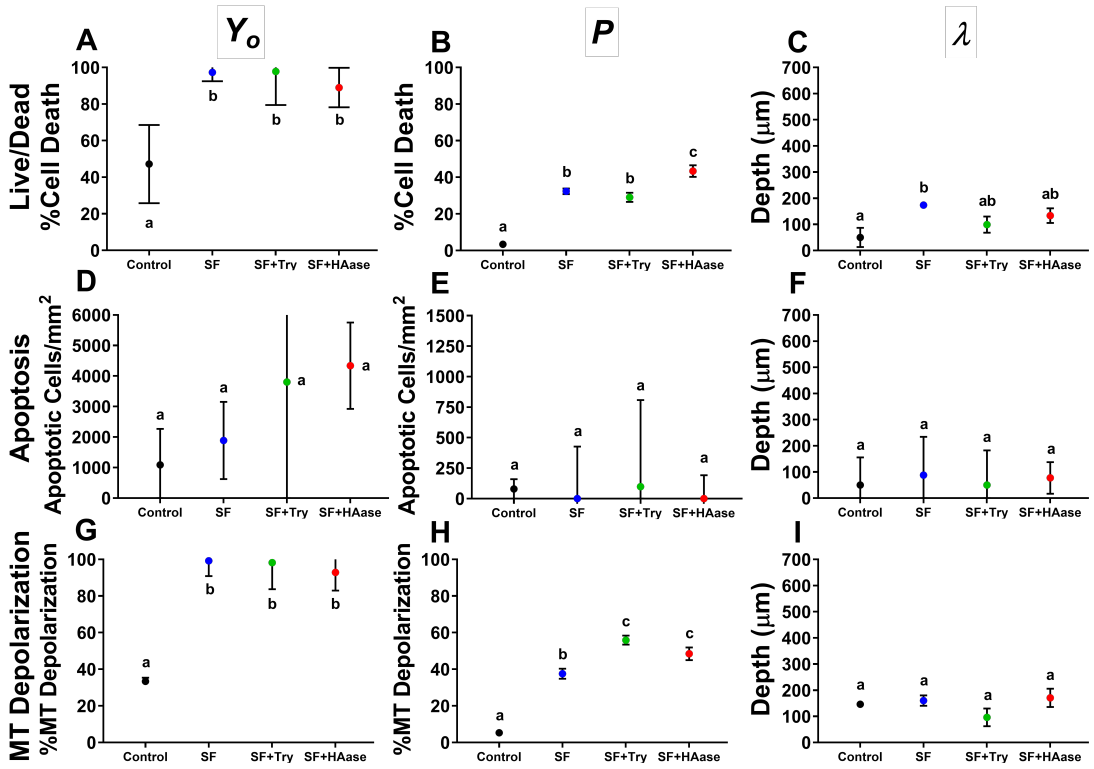

Figure 4.3. Comparison of parameters from nonlinear model. Groups with different letters denote significant difference, n = 8-12.

Confocal elastography

Using less viscous and less lubricious synovial fluid produced significantly greater shear strains, particularly at the cartilage surface (Figure 4). Injured cartilage samples that were slid in PBS, SF+HAase, and SF+Try resulted in shear strains at the cartilage surface that were 36% - 68% greater than the SF group (p < 0.0029). This trend continued for PBS, SF+HAase, and SF+Try up to a depth of 155 μm (p < 0.05), after which each group showed one other region of significantly greater shear strains

compared to SF. PBS showed greater shear strains from 375 to 400 μm ($p < 0.0176$), SF+HAase from 370 to 405 μm ($p < 0.0477$), SF+Try from 385 to 405 μm ($p < 0.0449$), all compared to SF. Within this region the average shear strains from PBS, SF+HAase, and SF+Try groups was ~5%, while the shear strain of the SF group was ~1.2%. A graph comparing shear strains of degraded synovial fluid and their counterparts treated with protease inhibitors can be seen in Supplemental Figure 1. These results show neither SF+HAase&PI nor SF+Try&PI showed significant differences in shear strain compared to their counterpart at any location across the region of interest ($p > 0.05$), indicating the presence of HAase or Try in SF did not damage the cartilage tissue during testing. Comparison of depth-dependent shear modulus between all groups can be seen in Supplemental Figure 2, however intergroup comparisons between all groups yielded no significant differences between groups at any location across the tissue span ($p > 0.05$).

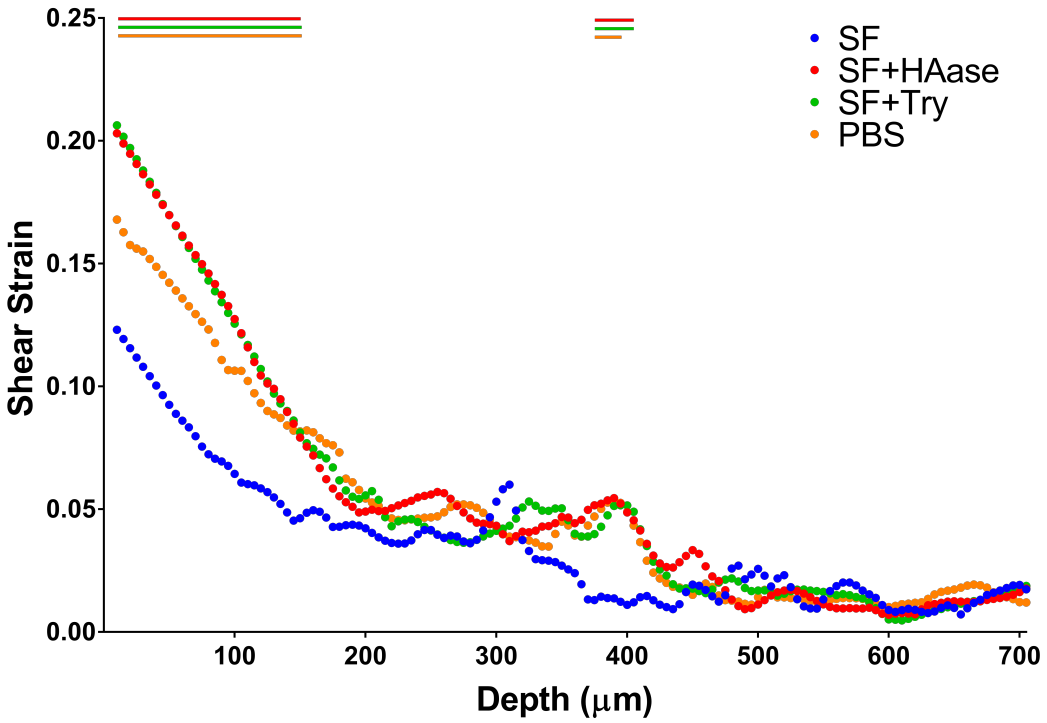

Figure 4.4. Depth-dependent shear strains for lubricant groups used in study, lines above indicate areas of significant difference between SF group and the group indicated by line color. n = 8.

Chondrocyte damage vs shear strain

After performing confocal elastography and microscopy analysis, the entire region of interest now possesses a magnitude of local cell death, apoptosis, MT depolarization, and shear strain. Each cellular injury metric may be plotted against shear strain data to generate plots that show magnitude of damage for a given level of mechanical load, thereby displaying the sensitivity of chondrocytes to shear strain. Chondrocytes sensitivity to shear strain was represented as the slope of the linear trendline for each group. Correlation plots revealed shear strain was a strong predictor of chondrocyte fate, regardless of which lubricant was used. Detail on the results of linear regression analysis, for all datasets, can be seen in Table 2.

y(x) = mx + b									
Stain/Group		N_x	N_y	m	SEM	b	SEM	R^2	Slope Comparison
Live/Dead	Pooled Data	8	8/12	300.00	42.22	30.41	2.81	0.4926	-
	SF	8	12	712.20	82.11	20.69	3.69	0.8246	a
	SF+Try	8	8	286.70	43.39	22.20	3.26	0.7318	b
	SF+HAase	8	8	231.20	62.25	38.14	4.69	0.4629	b
	SF	8	8	712.20	82.11	20.69	3.69	0.8246	a
	Degraded SF	8	8	259.90	42.82	30.11	3.22	0.5200	b
Apoptosis	Pooled Data	8	8/12	8402.00	496.80	304.90	33.11	0.8426	-
	SF	8	12	5745.00	604.80	282.80	27.20	0.8494	a
	SF+Try	8	8	7375.00	449.00	336.70	33.69	0.9440	ab
	SF+HAase	8	8	9338.00	748.50	394.10	56.39	0.9068	b
	SF	8	12	5745.00	604.80	282.80	27.20	0.8494	a
	Degraded SF	8	8	8362.00	530.60	365.40	39.90	0.8796	b
MT Depolarization	Pooled Data	8	8/12	281.90	40.79	42.49	2.72	0.4787	-
	SF	8	12	663.90	114.40	25.97	5.15	0.6778	a
	SF+Try	8	8	173.70	45.46	51.48	34.12	0.4771	b
	SF+HAase	8	8	263.60	57.89	43.27	4.36	0.4643	b
	SF	8	12	663.90	114.40	25.97	5.15	0.6778	a
	Degraded SF	8	8	218.20	36.92	47.41	2.78	0.5068	b

Table 4.2. Results from fitting shear strain vs chondrocyte fate data to linear regression model. Live/Dead and MT Depolarization are reported as percentages while Apoptosis is reported as # of cells/mm^2. SEM represents standard error of the mean and R^2 represents the correlation between the linear regression and experimental values. Rows that shared colors had slopes compared via two-way ANOVA.

The relationship between chondrocyte damage and shear strain displayed strong R^2 values ranging between 0.4787 to 0.8426 for pooled data (Figure 5A,B,C). For cell death, apoptosis, and MT depolarization measurements the sensitivities of chondrocytes to shear strain for all datasets pooled together were 300%, 8402 apoptotic cells/mm^2, and 281.90% respectively. Separating the data by lubricant group revealed that removing the lubricating macromolecules of synovial fluid alters the sensitivity of chondrocytes to shear strain (Figure 5D,E,F). The sensitivities of the SF group for cell death, apoptosis, and MT depolarization plots were 712.20%, 5745 apoptotic cells/mm^2, and 663.90% respectively. When compared against SF+HAase, the SF group showed sensitives that were significantly higher for cell death (p =

0.0006) and MT depolarization (p = 0.0189) and significantly lower for apoptosis (p = 0.0102). Compared against SF+Try, we again saw that SF had significantly higher cell death (p = 0.0003) and MT depolarization (p = 0.0006) sensitivity, however there was no significant difference in the case of apoptosis (p = 0.1791). R^2 values for all three lubricants for each chondrocyte fate metric ranged between 0.4629 to 0.9440, again showing a high degree of correlation between shear strain and cell damage. When SF data is compared to degraded synovial data (SF+HAase and SF+Try pooled together) we see similar trends occur (Figure G,H,I). Degraded SF showed sensitivities for cell death, apoptosis, and MT depolarization that were 259.90%, 8362 apoptotic cells/mm^2, and 218.20%, which showed significant differences compared to the normal SF group (p = 0.0002 for cell death, p = 0.0497 for apoptosis, p = 0.0002 for MT depolarization).

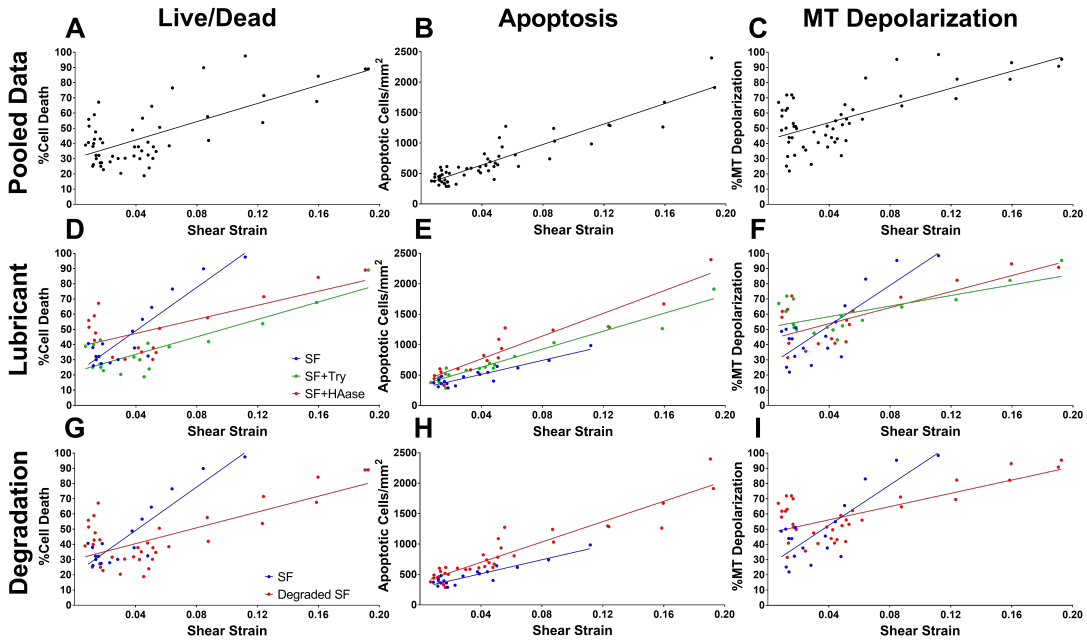

Figure 4.5. Correlation plots of local shear strain against magnitude of cellular responses with all data pooled together (top row), followed by grouped by lubricant used (middle row), and by degraded vs normal SF (bottom row). Statistical analysis

between groups in middle and bottom rows are performed by comparing slopes of linear trendlines fit to each group. Significant differences appear as intersections between lines of different groups, whereas nonsignificant comparisons result in parallel lines. y axis n = 8-12, x axis n = 8.

Discussion

In this body of work, we have shown that removal of the lubricating components of synovial fluid, specifically HA and lubricin, resulted in increased shear strains during cartilage articulation, leading to enhanced chondrocyte damage. We note that modulating the quality of synovial fluid resulted in significant changes in the spatial patterns of chondrocyte damage compared to healthy tissue, and even compared to traumatically injured cartilage. This result was seen regardless of whether HA or lubricin was removed from synovial fluid, indicating that both macromolecules are essential to ensure maximal protection of cartilage tissue. Furthermore, enzymatic degradation of the lubricating macromolecules in synovial fluid altered the relationship between shear strain and cellular injury. Ultimately, these results suggest that the role of synovial inflammation in the context of PTOA is to propagate cellular injury into deeper regions of cartilage tissue, which would normally be shielded by healthy synovial fluid.

Decreasing the lubricating quality of synovial fluid resulted in greater chondrocyte damage throughout the middle zone of cartilage tissue and minimal change to the damage at the surface region. Studies have shown that in uninjured cartilage tissue, poor quality lubricants generate higher friction and shear strains during articulation causing greater cellular damage near the articular surface.[7,23,24] However, our PTOA model has been shown to result in the death and damage of an

overwhelming majority of chondrocytes up to a minimum of 200 μm from the surface.[25] Increased shear strains at the surface caused by poor lubricating synovial fluid resulted in minimal additional surface zone chondrocyte damage, because impact injury had already compromised this region. Instead, removing HA and lubricin from synovial fluid appeared to decrease fluid lubrication such that depth-dependent shear strain increased, leading to increased damage propagation into deeper regions of the cartilage tissue. In addition to the mechanical role of synovial fluid in maintaining joint health, it is important to note potential biological mechanisms by which degraded synovial fluid may facilitate propagation of cellular damage in cartilage. For example, there is evidence to suggest that catabolism of high molecular weight HA into smaller oligomers triggers increased production of reactive oxygen species, pro-inflammatory cytokines, and hyaluronidase by macrophages, synoviocytes, and chondrocytes.[44–47] Focal defects generated during trauma may allow a pathway for low molecular weight HA that exists within the synovium to spread to middle zone chondrocytes they could not normally reach. Furthermore, lubricin also possess chondroprotective qualities and its removal is associated with enhanced apoptosis, degradative enzyme production, and decreased lubricin secretion by chondrocytes.[48–50]

Removal of HA and lubricin from synovial fluid caused significant changes in the sensitivity of chondrocytes to shear strain as manifested in cell death, apoptosis, and MT depolarization. Decreasing the lubricating properties of SF resulted in shear strains almost twice as high from baseline injury at the articular surface. This caused linear trend lines to have lower sensitivities, reflected by slope, in the case of percent cell death and percent MT depolarization and higher sensitivity for apoptosis. These

results are consistent with previous studies that suggest osteoarthritic changes cause chondrocytes to become more susceptible to inflammatory cytokines, reactive oxygen species, and mechanical stimuli.[51–53] These findings reinforce the notion of a positive feedback loop of PTOA progression where traumatic injury compromises cartilage tissue such that there is an increase of mechanical load and inflammatory cytokines that cause destruction of both chondrocytes and cartilage tissue, thereby triggering greater mechanical loads and increased release of inflammatory cytokines until the disease progresses to its end-stage.[54–56]

While this study provides exciting new insight on the role of synovial fluid in the manifestation of PTOA, it is not without its limitations. These limitations include an inability to examine long term effects of degrading synovial fluid. The biological mechanisms by which synovial fluid interacts with chondrocytes and the surrounding matrix may not be fully captured over the timescale that cartilage explants were exposed to the lubricants used in this study.[57–59] Despite this, analyzing the effects of synovial fluid degradation from a mechanics perspective was largely able to explain the changes in chondrocyte response between lubricant groups. Additionally, enzymatic degradation of lubricin and HA resulted in complete removal of these macromolecules which may not reflect the quality of synovial fluid in the subacute-acute timescale of PTOA pathogenesis.[12,60] However, the decision to completely remove lubricin and HA was to model a worst-case scenario in the spectrum of synovial fluid concentration of these two macromolecules.

In conclusion, the results of this study suggest that while the dominant effect in the manifestation of PTOA pathogenesis is the initial trauma generated during injury,

removal of lubricin and HA synovial inflammation raises the magnitudes of shear strains and chondrocyte damage generated during articulation. This insight may suggest that synovial inflammation may be particularly threatening within the context of PTOA progression, compared to that of idiopathic OA. Further, these conclusions suggests that therapeutic application of lubricants may be an important strategy for treating PTOA. Finally, we observed minimal differences between synovial fluid with catabolized lubricin or HA, indicating that these macromolecules act together to achieve optimal joint lubrication and functionality. Through the work of this study, we have been able to advance our ex vivo model of PTOA by considering synovial inflammation and long term this model may serve as a platform to test the efficacy disease modifying treatments.

References

1. Desrochers J, Amrein MW, Matyas JR. 2013. Microscale surface friction of articular cartilage in early osteoarthritis. Journal of the Mechanical Behavior of Biomedical Materials 25:11–22.
2. Jay GD. 2009. Characterization of a bovine synovial fluid lubricating factor. I. Chemical, Surface activity and lubricating properties. http://dx.doi.org/10.3109/03008209209014228 28(1–2):71–88 [cited 2022 Jun 28] Available from: https://www.tandfonline.com/doi/abs/10.3109/03008209209014228.
3. Balazs EA, Watson D, Duff IF, Roseman S. 1967. Hyaluronic acid in synovial fluid. I. Molecular parameters of hyaluronic acid in normal and arthritic human fluids. Arthritis & Rheumatism 10(4):357–376 [cited 2022 Jun 28] Available from: https://onlinelibrary.wiley.com/doi/full/10.1002/art.1780100407.
4. Jay GD, Torres JR, Rhee DK, et al. 2007. Association between friction and wear in diarthrodial joints lacking lubricin. Arthritis Rheum 56(11):3662–3669 [cited 2022 Jun 29] Available from: https://pubmed.ncbi.nlm.nih.gov/17968947/.
5. Gupta RC, Lall R, Srivastava A, Sinha A. 2019. Hyaluronic Acid: Molecular Mechanisms and Therapeutic Trajectory. Frontiers in Veterinary Science 6(JUN):192 [cited 2022 Jun 28] Available from: /pmc/articles/PMC6603175/.
6. Tamer TM. 2013. Hyaluronan and synovial joint: function, distribution and healing. Interdisciplinary Toxicology 6(3):111 [cited 2022 Jun 13] Available from: /pmc/articles/PMC3967437/.

7. Bonnevie ED, Galesso D, Secchieri C, Bonassar LJ. 2018. Degradation alters the lubrication of articular cartilage by high viscosity, hyaluronic acid-based lubricants. Journal of Orthopaedic Research 36(5):1456–1464 [cited 2022 Jun 29].

8. Waller KA, Zhang LX, Elsaid KA, et al. 2013. Role of lubricin and boundary lubrication in the prevention of chondrocyte apoptosis. Proc Natl Acad Sci U S A 110(15):5852–5857.

9. Jones ARC, Gleghorn JP, Hughes CE, et al. 2007. Binding and localization of recombinant Lubricin to articular cartilage surfaces. Journal of Orthopaedic Research 25(3):283–292 [cited 2022 Jun 28].

10. Martel-Pelletier J, Barr AJ, Cicuttini FM, et al. 2016. Osteoarthritis. [cited 2022 Jun 14] Available from: www.nature.com/nrdp.

11. Ulrich-Vinther M, Maloney MD, Schwarz EM, et al. 2003. Articular cartilage biology. J Am Acad Orthop Surg 11(6):421–430.

12. Catterall JB, Stabler T v., Flannery CR, Kraus VB. 2010. Changes in serum and synovial fluid biomarkers after acute injury (NCT00332254). Arthritis Research and Therapy 12(6):1–9 [cited 2022 Jun 16] Available from: https://arthritis-research.biomedcentral.com/articles/10.1186/ar3216.

13. de Lange-Brokaar BJE, Ioan-Facsinay A, van Osch GJVM, et al. 2012. Synovial inflammation, immune cells and their cytokines in osteoarthritis: A review. Osteoarthritis and Cartilage 20(12):1484–1499 [cited 2022 Jun 18].

14. Delco ML, Bonnevie ED, Bonassar LJ, Fortier LA. 2018. Mitochondrial dysfunction is an acute response of articular chondrocytes to mechanical

injury. Journal of Orthopaedic Research .

15. Punzi L, Galozzi P, Luisetto R, et al. 2016. Post-traumatic arthritis: overview on pathogenic mechanisms and role of inflammation. RMD Open 2(2) [cited 2022 Jul 5] Available from: https://pubmed.ncbi.nlm.nih.gov/27651925/.

16. Bartell LR, Fortier LA, Bonassar LJ, et al. 2019. Mitoprotective therapy prevents rapid, strain-dependent mitochondrial dysfunction after articular cartilage injury. Journal of Orthopaedic Research (December):1–11 Available from: http://dx.doi.org/10.1002/jor.24567.

17. Stevens AL, Wishnok JS, White FM, et al. 2009. Mechanical injury and cytokines cause loss of cartilage integrity and upregulate proteins associated with catabolism, immunity, inflammation, and repair. Molecular and Cellular Proteomics 8(7):1475–1489 [cited 2022 Jun 15].

18. Elsaid KA, Fleming BC, Oksendahl HL, et al. 2008. Decreased Lubricin Concentrations and Markers of Joint Inflammation in Synovial Fluids from Patients with Anterior Cruciate Ligament Injury. Arthritis Rheum 58(6):1707 [cited 2022 Jul 5] Available from: /pmc/articles/PMC2789974/.

19. Kosinska MK, Ludwig TE, Liebisch G, et al. 2015. Articular Joint Lubricants during Osteoarthritis and Rheumatoid Arthritis Display Altered Levels and Molecular Species. PLoS One 10(5) [cited 2022 Jul 6] Available from: https://pubmed.ncbi.nlm.nih.gov/25933137/.

20. Temple-Wong MM, Ren S, Quach P, et al. 2016. Hyaluronan concentration and size distribution in human knee synovial fluid: variations with age and cartilage degeneration. Arthritis Research & Therapy 18(1) [cited 2022 Jul 6]

Available from: /pmc/articles/PMC4721052/.

21. Thomas NP, Wu WJ, Fleming BC, et al. 2017. Synovial inflammation plays a greater role in post-traumatic osteoarthritis compared to idiopathic osteoarthritis in the Hartley guinea pig knee. BMC Musculoskelet Disord 18(1) [cited 2022 Jul 5] Available from: https://pubmed.ncbi.nlm.nih.gov/29284451/.

22. Tochigi Y, Buckwalter JA, Martin JA, et al. 2011. Distribution and progression of chondrocyte damage in a whole-organ model of human ankle intra-articular fracture. Journal of Bone and Joint Surgery - Series A 93(6):533–539.

23. Irwin RM, Feeney E, Secchieri C, et al. 2020. Distinct tribological endotypes of pathological human synovial fluid reveal characteristic biomarkers and variation in efficacy of viscosupplementation at reducing local strains in articular cartilage. Osteoarthritis and Cartilage 28(4):492–501 Available from: https://doi.org/10.1016/j.joca.2020.02.029.

24. Bonnevie ED, Delco ML, Bartell LR, et al. 2018. Microscale frictional strains determine chondrocyte fate in loaded cartilage. Journal of Biomechanics 74:72–78.

25. Ayala S, Fortier LA, Delco ML, et al. 2020. Cartilage articulation enhances chondrocyte injury and death after impact injury. Journal of Orthopaedic Research 28(December):S192–S193 Available from: https://pubmed.ncbi.nlm.nih.gov/33274781/.

26. Bartell LR, Xu MC, Bonassar LJ, Cohen I. 2018. Local and global measurements show that damage initiation in articular cartilage is inhibited by the surface layer and has significant rate dependence. Journal of Biomechanics

72:63–70.

27. Linn FC. 1968. LUBRICATION OF ANIMAL JOINTS II THE MECHANISM*. Pergamon Press. 193–205 p.

28. Jay GD, Torres JR, Warman ML, et al. 2007. The role of lubricin in the mechanical behavior of synovial fluid. Proc Natl Acad Sci U S A 104(15):6194–6199 [cited 2022 Jun 27] Available from: www.pnas.orgcgidoi10.1073pnas.0608558104.

29. Bonnevie ED, Delco ML, Fortier LA, et al. 2015. Characterization of tissue response to impact loads delivered using a hand-held instrument for studying articular cartilage injury. Cartilage 6(4):226–232.

30. Noyes FR, Grood ES. 1976. The strength of the anterior cruciate ligament in humans and rhesus monkeys: Age related and species related changes. Journal of Bone and Joint Surgery - Series A 58(8):1074–1082.

31. Bonnevie ED, Delco ML, Galesso D, et al. 2017. Sub-critical impact inhibits the lubricating mechanisms of articular cartilage. Journal of Biomechanics 53:64–70.

32. Gleghorn JP, Jones ARC, Flannery CR, Bonassar LJ. 2009. Boundary mode lubrication of articular cartilage by recombinant human lubricin. Journal of Orthopaedic Research 27(6):771–777.

33. Gleghorn JP, Bonassar LJ. 2008. Lubrication mode analysis of articular cartilage using Stribeck surfaces. Journal of Biomechanics 41(9):1910–1918.

34. Bonnevie ED, Puetzer JL, Bonassar LJ. 2014. Enhanced boundary lubrication properties of engineered menisci by lubricin localization with insulin-like

growth factor I treatment. Journal of Biomechanics 47(9):2183–2188.

35. Bonnevie ED, Galesso D, Secchieri C, et al. 2015. Elastoviscous transitions of articular cartilage reveal a mechanism of synergy between lubricin and hyaluronic acid. PLoS ONE 10(11):1–15.

36. Buckley MR, Gleghorn JP, Bonassar LJ, Cohen I. 2008. Mapping the depth dependence of shear properties in articular cartilage. Journal of Biomechanics 41(11):2430–2437.

37. Middendorf JM, Griffin DJ, Shortkroff S, et al. 2017. Mechanical properties and structure-function relationships of human chondrocyte-seeded cartilage constructs after in vitro culture. Journal of Orthopaedic Research 35(10):2298–2306.

38. Silverberg JL, Dillavou S, Bonassar L, Cohen I. 2013. Anatomic variation of depth-dependent mechanical properties in neonatal bovine articular cartilage. Journal of Orthopaedic Research 31(5):686–691.

39. Buckley MR, Bonassar LJ, Cohen I. 2013. Localization of viscous behavior and shear energy dissipation in articular cartilage under dynamic shear loading. Journal of Biomechanical Engineering 135(3):1–9.

40. Buckley MR, Bergou AJ, Fouchard J, et al. 2010. High-resolution spatial mapping of shear properties in cartilage. Journal of Biomechanics 43(4):796–800 Available from: http://dx.doi.org/10.1016/j.jbiomech.2009.10.012.

41. Silverberg JL, Barrett AR, Das M, et al. 2014. Structure-function relations and rigidity percolation in the shear properties of articular cartilage. Biophysical Journal 107(7):1721–1730 Available from:

http://dx.doi.org/10.1016/j.bpj.2014.08.011.

42. Bartell LR, Fortier LA, Bonassar LJ, Cohen I. 2015. Measuring microscale strain fields in articular cartilage during rapid impact reveals thresholds for chondrocyte death and a protective role for the superficial layer. Journal of Biomechanics 48(12):3440–3446 Available from: http://dx.doi.org/10.1016/j.jbiomech.2015.05.035.

43. Johannes Schindelin, Ignacio Arganda-Carreras, Erwin Frise, Verena Kaynig, Mark Longair, Tobias Pietzsch, Stephan Preibisch, Curtis Rueden, Stephan Saalfeld, Benjamin Schmid, Jean-Yves Tinevez, Daniel James White, Volker Hartenstein, Kevin Eliceiri PT. 2012. Fiji: an open-source platform for biological-image analysis. Nature Methods 9:676–682.

44. Rayahin JE, Buhrman JS, Zhang Y, et al. 2015. High and low molecular weight hyaluronic acid differentially influence macrophage activation. ACS Biomater Sci Eng 1(7):481 [cited 2022 Jul 18] Available from: /pmc/articles/PMC4533115/.

45. McKee CM, Penno MB, Cowman M, et al. 1996. Hyaluronan (HA) fragments induce chemokine gene expression in alveolar macrophages. The role of HA size and CD44. The Journal of Clinical Investigation 98(10):2403–2413 [cited 2022 Jul 18].

46. Euppayo T, Siengdee P, Buddhachat K, et al. 2015. Effects of low molecular weight hyaluronan combined with carprofen on canine osteoarthritis articular chondrocytes and cartilage explants in vitro. In Vitro Cellular and Developmental Biology - Animal 51(8):857–865 [cited 2022 Jul 18] Available

from: https://link.springer.com/article/10.1007/s11626-015-9908-9.

47. Wang CT, Lin YT, Chiang BL, et al. 2006. High molecular weight hyaluronic acid down-regulates the gene expression of osteoarthritis-associated cytokines and enzymes in fibroblast-like synoviocytes from patients with early osteoarthritis. Osteoarthritis Cartilage 14(12):1237–1247 [cited 2022 Jul 18] Available from: https://pubmed.ncbi.nlm.nih.gov/16806998/.

48. Elsaid KA, Zhang L, Waller K, et al. 2012. The impact of forced joint exercise on lubricin biosynthesis from articular cartilage following ACL transection and intra-articular lubricin's effect in exercised joints following ACL transection. Osteoarthritis and Cartilage 20(8):940–948 [cited 2022 Jul 19].

49. Jay GD, Waller KA. 2014. The biology of Lubricin: Near frictionless joint motion. Matrix Biology 39:17–24 [cited 2022 Jul 19].

50. Jones ARC, Flannery CR. 2007. Bioregulation of lubricin expression by growth factors and cytokines. European Cells and Materials 13:40–45 [cited 2022 Jul 19].

51. Lee W, Nims RJ, Savadipour A, et al. 2021. Inflammatory signaling sensitizes Piezo1 mechanotransduction in articular chondrocytes as a pathogenic feed-forward mechanism in osteoarthritis. Proc Natl Acad Sci U S A 118(13):e2001611118 [cited 2022 Jul 19] Available from: https://www.pnas.org/doi/abs/10.1073/pnas.2001611118.

52. Zhao Z, Li Y, Wang M, et al. 2020. Mechanotransduction pathways in the regulation of cartilage chondrocyte homoeostasis. Journal of Cellular and Molecular Medicine 24(10):5408 [cited 2022 Jul 19] Available from:

/pmc/articles/PMC7214151/.

53. Collins JA, Moots RJ, Winstanley R, et al. 2013. Oxygen and pH-sensitivity of human osteoarthritic chondrocytes in 3-D alginate bead culture system. Osteoarthritis and Cartilage 21(11):1790 [cited 2022 Jul 19] Available from: /pmc/articles/PMC3807787/.

54. Anderson DD, Chubinskaya S, Guilak F, et al. 2011. Post-traumatic osteoarthritis: Improved understanding and opportunities for early intervention. Journal of Orthopaedic Research 29(6):802–809 [cited 2022 Jun 14] Available from: https://onlinelibrary.wiley.com/doi/full/10.1002/jor.21359.

55. Woodell-May JE, Sommerfeld SD. 2020. Role of Inflammation and the Immune System in the Progression of Osteoarthritis. Journal of Orthopaedic Research 38(2):253–257 [cited 2022 Jun 16] Available from: https://onlinelibrary.wiley.com/doi/full/10.1002/jor.24457.

56. Whittaker JL, Woodhouse LJ, Nettel-Aguirre A, Emery CA. 2015. Outcomes associated with early post-traumatic osteoarthritis and other negative health consequences 3-10 years following knee joint injury in youth sport. Osteoarthritis and Cartilage 23(7):1122–1129 Available from: http://dx.doi.org/10.1016/j.joca.2015.02.021.

57. Lieberthal J, Sambamurthy N, Scanzello CR. 2015. Inflammation in joint injury and post-traumatic osteoarthritis. Osteoarthritis and Cartilage 23(11):1825–1834 [cited 2022 Jun 14].

58. Khella CM, Asgarian R, Horvath JM, et al. 2021. An Evidence-Based Systematic Review of Human Knee Post-Traumatic Osteoarthritis (PTOA):

Timeline of Clinical Presentation and Disease Markers, Comparison of Knee Joint PTOA Models and Early Disease Implications. International Journal of Molecular Sciences 22(4):1–48 [cited 2022 Jul 19] Available from: /pmc/articles/PMC7922905/.

59. Watt FE, Paterson E, Freidin A, et al. 2016. Acute Molecular Changes in Synovial Fluid Following Human Knee Injury: Association With Early Clinical Outcomes. Arthritis and Rheumatology 68(9):2129–2140 [cited 2022 Jul 19] Available from: https://pubmed.ncbi.nlm.nih.gov/26991527/.

60. Lopa S, Leijs MJC, Moretti M, et al. 2015. Arthritic and non-arthritic synovial fluids modulate IL10 and IL1RA gene expression in differentially activated primary human monocytes. Osteoarthritis and Cartilage 23(11):1853–1857 [cited 2022 Jul 18] Available from: http://www.oarsijournal.com/article/S1063458415012078/fulltext.

Supplemental Materials

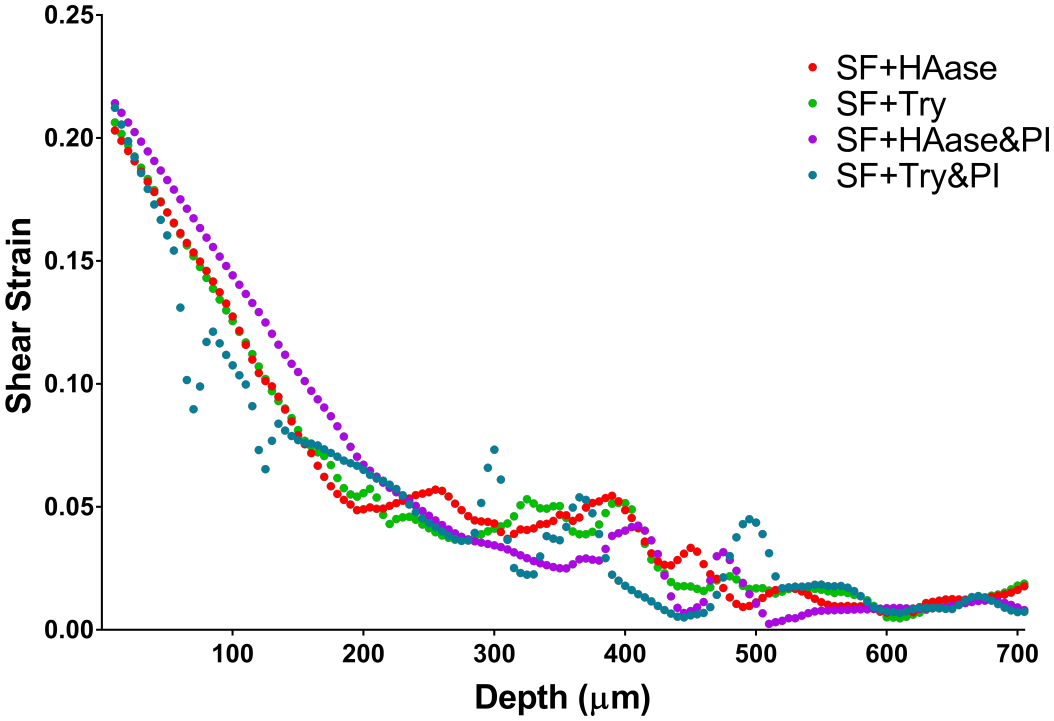

Figure 4.S1. Shear strain of cartilage samples slid in synovial fluid both with and without protease inhibitors (PI) after enzymatic degradation. n = 8 for groups without PI and n = 3 for groups with PI

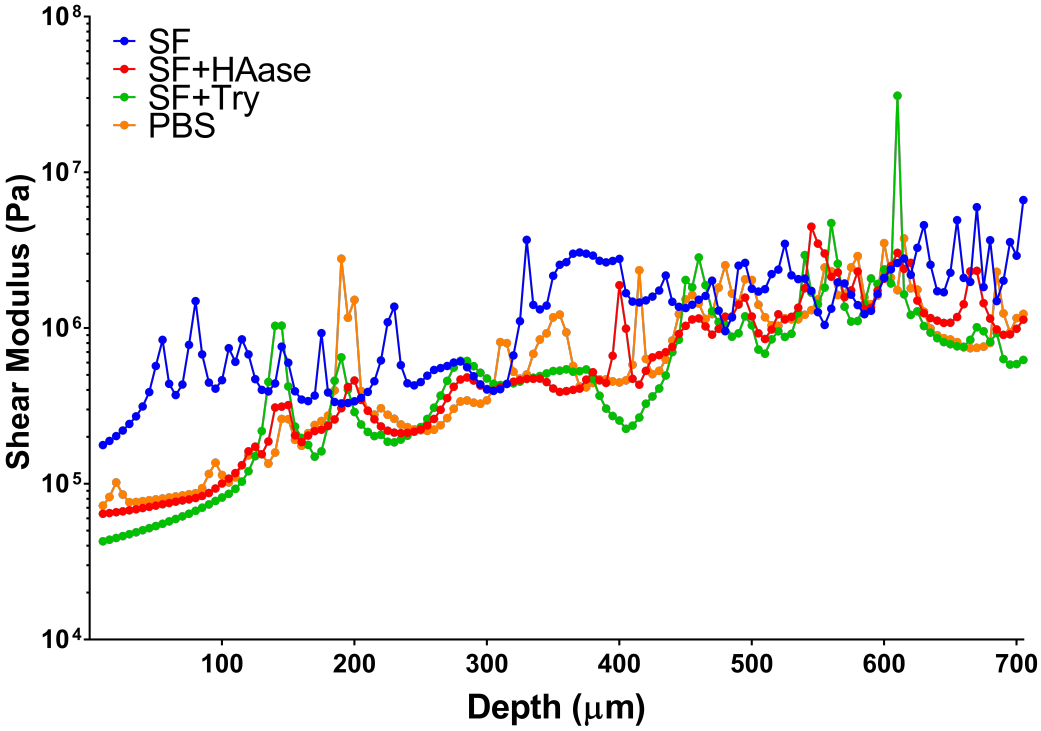

Figure 4.S2. Depth-dependent shear modulus of cartilage samples. n = 8.

CHAPTER 5

Conclusions and Future Directions

Conclusions

The primary goal of this thesis project was to generate an ex vivo model of PTOA that could more closely mimic the environment of a synovial joint early after trauma. The first step in this achieving this goal was to evaluate the effects of impact injury combined with continuous articulation, to simulate both rapid compression and shear loading, on chondrocyte health (Chapter 2). Secondly, we integrated mechanical testing techniques into our assessment of injured cartilage tissue to evaluate changes in mechanical properties and chondrocyte sensitivity to loading (Chapter 3). Finally, we incorporated the effects of synovial fluid inflammation into our custom PTOA model by using synovial fluid deprived of its primary lubricating macromolecules (Chapter 4). By competition these projects we have created an ex vivo PTOA model that more closely simulates an injured articular joint, which will serve as a platform for future research endeavors.

In Chapter 2, we investigated the effects of multiple modalities of loading, impact injury, continuous shear strain, and both loading modalities combined, on the spatial patterns of chondrocyte response in cartilage tissue. Shear loading, in the form of repetitive sliding, caused significant cell death, caspase activity, and MT depolarization that was limited to the surface region of cartilage tissue. This finding is consistent with prior studies which concluded that the function of the surface region is to serve as a compliant boundary layer to restrict damage propagation from the bulk of the tissue.[1–3] Next, we showed that impact injury caused chondrocyte damage not only

in the surface region, but residual damage within the middle zone as well. However, the novel findings of this experiment were that combined loading generated significantly greater global and depth-dependent chondrocyte damage, specifically MT depolarization, compared to either type of loading alone. Additionally, depth-dependent analysis showed that combined loading caused synergistic chondrocyte damage within the middle zone of the cartilage tissue. These findings are likely due to structurally compromised cartilage being unable to support mechanical loads that were once tolerable, behaving similarly to cartilage tissue when the surface has been removed.[4] These results imply that joint immobilization post-injury is necessary to avoid additional damage to cartilage, while it is in a weakened state. Prior studies have shown that preoperative rehabilitation therapy before surgical intervention has positive effects on long-term patient outcomes, however, it is currently unknown when the optimal timing for patient prehabilitation is.[5] Future studies may benefit from attempting to answer what the appropriate timeline for cartilage loading is post-injury.

In Chapter 3, we expanded our findings from Chapter 2 using mechanical testing techniques to determine how changes in cartilage mechanical properties cause downstream chondrocyte damage. Our results revealed that femoral condylar and talar cartilage display unique spatial patterns of cellular damage in response to traumatic injury. Measurements of chondrocyte sensitivity of uninjured cartilage showed that cartilage from the femoral condyle and talus have unique sensitivity in mechanical stimuli. We also demonstrated that femoral condylar cartilage showed insignificant changes in depth-dependent shear modulus or shear strain after injury, while talar cartilage displayed significantly greater shear strains at the surface. Furthermore,

injury related changes in mechanical properties of talar cartilage resulted in significant changes in chondrocyte sensitivity but minimal changes for the femoral condyle. These findings seem counter intuitive at first due to histological evaluation showing greater surface fracturing in condylar cartilage tissue post-injury, whereas talar cartilage showed minimal surface disruption. However, talar cartilage has been shown to possess a shear modulus at the cartilage surface that is an order of magnitude greater compared to the femoral condyle.[6,7] Being that stiffness is inversely proportional to energy dissipation, a less compliant surface region results in talar cartilage being less capable of dissipating energy compared to the condyle.[8,9] A stiffer surface region results in higher amounts of energy being propagated through the talar cartilage tissue during injury. These results show that the mechanism by which PTOA manifests is not identical for all joints, some may be more likely to develop PTOA than others. One major advantage that our PTOA model has is the capability to test cartilage tissue from any joint in the body, so long as an explant of at least 1 mm can be obtained. An exciting future project may involve investigating chondrocyte sensitivity in cartilage from joints that are commonly affected by PTOA, such as the hips and elbows, and observe how they differ from one another.

In Chapter 4, we observed how removal of the lubricating macromolecules of synovial fluid further aggravates cartilage injury and ultimately leads to PTOA development. By removing lubricin and HA from synovial fluid we observed significant increases in cartilage shear strain, particularly at the cartilage surface, and greater levels of chondrocyte damage within the middle zone. We also note that depleting the lubricating qualities of synovial fluid resulted in significant changes to

chondrocyte sensitivity to shear strain. Changes in chondrocyte sensitivity can be largely explained by significant increases in depth-dependent shear strain, however there may also be biological changes at play. For example, low molecular weight HA and removal of lubricin from has been shown to trigger production of pro-inflammatory cytokines, increase oxidative stress, enhance chondrocyte apoptosis.[10–14] To combat further disease progression, several biological mediators can be employed in future experiments to assess their efficacy in halting PTOA manifestation. The PTOA model developed in this thesis presents an interesting new approach to studying the efficacy of possible disease modifying drugs. The techniques we've developed allow us to use chondrocyte health and cartilage mechanical properties as reliable quantitative indicators of cartilage health compared to qualitative assessments such as histology that are popularly used.[15]

In conclusion, each of these chapters emphasize the necessity to study cartilage behavior depth-dependently rather than relying on global analyses that reduce cartilage tissue to a homogenous structure. This inference is evidenced throughout this body of work which shows the spatial patterns of cellular response between the surface and middle zone of cartilage are significantly different. These differences in injury response are in part due to differences in mechanical properties, biochemical content, and cellular organization between distinct regions of cartilage tissue.

Future Directions

Optimal Timing of Cartilage Loading Post-Injury. As mentioned before, the timeline for osteochondral injury healing is still not well established. Evidence

from this thesis shows that continuous passive motion too soon after injury promotes further damage to the cartilage tissue. However, studies have shown that CPM and range of motion exercises in the weeks following surgical intervention can improve patient outcomes.[16] These findings imply that sometime after the cartilage healing process has begun, chondrocytes will respond to mechanical stimuli with an upregulation anabolic cytokines.[17] Unfortunately, simulating the cartilage healing process will be complicated due to our PTOA model using cartilage explants, which are isolated from the body's immune response pathways. However, a technique that could be used to circumvent this obstacle would be exposing injured cartilage to anabolic cytokines such as the TGF-βs, IL-4, and IL-5.[18,19] These biological mediators have been shown to promote cartilage healing via inhibiting chondrocyte apoptosis and promoting cartilage repair. Work from our group has also demonstrated that TGF-β1 can stimulate production of extracellular matrix components such as glycosaminoglycan and collagen fibers, which may adequately recapitulate the in vivo cartilage healing process.[20,21] These studies have already identified concentrations of TGF-β1 that generate positive outcomes in tissue engineered constructs, which provide a starting point for new experiments to begin. By treating traumatically injured cartilage explants with these cytokines at varying time points after injury, we can observe how much time is needed before cartilage health has been significantly recovered. After this time point has been identified, additional bouts of cyclic shear loading can be applied to observe if chondrocytes are once again agitated or minimally disturbed.

Additional Joint Locations. While the ankle and knee joints are most afflicted

by PTOA, the disease can also manifest in other locations such as the shoulder, hip, and even temporomandibular joint.[22,23] Chapter 4 of this thesis has provided evidence that mechanisms behind PTOA pathogenesis is not the same between joints, therefore we can use our model to investigate PTOA in a site-specific manner. While other groups have investigated the mechanical properties and response to injury of various joints in a global manner, our group possesses technology, such as the tissue deformation imaging stage, that allows us to study these phenomena depth-dependently.[24,25] As shown throughout this thesis, examining PTOA development depth-dependently provides us a finer resolution to detect changes in cartilage tissue that would easily be overlooked were we to only look globally. Using the analysis techniques already outlined, we would be able to determine the spatial patterns of cellular response, depth-dependent mechanical properties, and chondrocyte sensitivity for each joint that was tested. Following these experiments, we would be able to make comparisons between each joint location to see which are most sensitive to injury and what commonalities exist between them.

Testing PTOA Disease Modifying Drugs. Currently, there do not exist any clinically used pharmacological interventions that arrest of modulate PTOA pathogenesis. While clinical trials have yielded disappointing results thus far, our model can serve as a consistent, readily available, and inexpensive platform to test new therapeutics. Models in which drugs are tested on isolated cells are too simplistic to infer how they would act in patients, however animal models present issues with costs, maintenance, and group sizes.[26–28] The ex vivo model presented in this thesis provides results that are more physiologically relevant than 2D cell culture and more

accessible than animal models are. Furthermore, no other in vitro/ex vivo model incorporates multiple loading modalities, depth-dependent analysis, mechanical testing, and changes in synovial fluid quality into their design. The next step is to identify novel therapeutics that may bring about substantial changes in the disease course, however there are multiple biological pathways that can be targeted for therapeutic relief. Treatments that target synovitis include IL-1 receptor antagonist and TNF inhibitors, which can act on the chondrocytes to arrest synovial inflammation.[29] Antioxidants are another class of therapeutics that have been shown to possess cell- and chondroprotective features by relieving oxidative stress. [30]. Some of these drugs include SS-31, a peptide that has been shown to restore damaged mitochondria to its native conformation thereby restoring its bioenergetics, and rotenone, an electron transport chain inhibitor that suppresses release of superoxide from mitochondria.[31–33] Finally, there are chondroanabolic agents such as bone morphogenic proteins, insulin-like growth factor-1, and SOX9 that seek to stimulate chondrogenesis and repair within damaged tissue.[30] Each of these therapeutics can be tested, alone or in combination, to assess optimal concentrations, timelines of administration, exposure durations.

Concluding Remarks

In summary, the goal of this dissertation was to generate an ex vivo model of PTOA that could more closely mimic the environment of an injured synovial joint. This goal was accomplished by incorporating multiple elements that are responsible for disease progression rather than using initial injury alone. This work demonstrated

that cartilage tissue post-injury experiences significant changes in its cellular behavior and mechanical properties that drive further damage. Additionally, we showed that not all cartilage is equal with joints having different inherent resistances to PTOA development. Ultimately, this dissertation has furthered our understanding of PTOA pathogenesis and provides a template for future work to investigate treatment strategies for clinical application.

References

1. Desrochers J, Amrein MW, Matyas JR. 2013. Microscale surface friction of articular cartilage in early osteoarthritis. Journal of the Mechanical Behavior of Biomedical Materials 25:11–22.
2. Jasin HE. 1995. Structure and function of the articular cartilage surface. Scandinavian Journal of Rheumatology 24(S101):51–55 [cited 2022 Jun 12].
3. Bonnevie ED, Delco ML, Bartell LR, et al. 2018. Microscale frictional strains determine chondrocyte fate in loaded cartilage. Journal of Biomechanics 74:72–78.
4. Bartell LR, Xu MC, Bonassar LJ, Cohen I. 2018. Local and global measurements show that damage initiation in articular cartilage is inhibited by the surface layer and has significant rate dependence. Journal of Biomechanics 72:63–70.
5. Failla MJ, Logerstedt DS, Grindem H, et al. 2016. Does Extended Preoperative Rehabilitation Influence Outcomes 2 Years after ACL Reconstruction? A Comparative Effectiveness Study between the MOON and Delaware-Oslo ACL Cohorts: American Journal of Sports Medicine 44(10):2608–2614.
6. Henak CR, Ross KA, Bonnevie ED, et al. 2016. Human talar and femoral cartilage have distinct mechanical properties near the articular surface. Journal of Biomechanics 49(14):3320–3327.
7. Delco ML, Kennedy JG, Bonassar LJ, Fortier LA. 2017. Post-traumatic osteoarthritis of the ankle: A distinct clinical entity requiring new research approaches. Journal of Orthopaedic Research 35(3):440–453.

8. Buckley MR, Bonassar LJ, Cohen I. 2013. Localization of viscous behavior and shear energy dissipation in articular cartilage under dynamic shear loading. Journal of Biomechanical Engineering 135(3):1–9.

9. Silverberg JL, Dillavou S, Bonassar L, Cohen I. 2013. Anatomic variation of depth-dependent mechanical properties in neonatal bovine articular cartilage. Journal of Orthopaedic Research 31(5):686–691.

10. Rayahin JE, Buhrman JS, Zhang Y, et al. 2015. High and low molecular weight hyaluronic acid differentially influence macrophage activation. ACS Biomater Sci Eng 1(7):481 [cited 2022 Jul 18] Available from: /pmc/articles/PMC4533115/.

11. McKee CM, Penno MB, Cowman M, et al. 1996. Hyaluronan (HA) fragments induce chemokine gene expression in alveolar macrophages. The role of HA size and CD44. The Journal of Clinical Investigation 98(10):2403–2413 [cited 2022 Jul 18].

12. Wang CT, Lin YT, Chiang BL, et al. 2006. High molecular weight hyaluronic acid down-regulates the gene expression of osteoarthritis-associated cytokines and enzymes in fibroblast-like synoviocytes from patients with early osteoarthritis. Osteoarthritis Cartilage 14(12):1237–1247 [cited 2022 Jul 18] Available from: https://pubmed.ncbi.nlm.nih.gov/16806998/.

13. Jay GD, Waller KA. 2014. The biology of Lubricin: Near frictionless joint motion. Matrix Biology 39:17–24 [cited 2022 Jul 19].

14. Jones ARC, Flannery CR. 2007. Bioregulation of lubricin expression by growth factors and cytokines. European Cells and Materials 13:40–45 [cited

2022 Jul 19].

15. Elsaid KA, Zhang L, Waller K, et al. 2012. The impact of forced joint exercise on lubricin biosynthesis from articular cartilage following ACL transection and intra-articular lubricin's effect in exercised joints following ACL transection. Osteoarthritis and Cartilage 20(8):940–948 [cited 2022 Jul 19].

16. Tyler TF, Lung JY. 2012. Rehabilitation following osteochondral injury to the knee. Current Reviews in Musculoskeletal Medicine 5(1):72–81.

17. Wong M, Carter DR. 2003. Articular cartilage functional histomorphology and mechanobiology: A research perspective. Bone 33(1):1–13 [cited 2022 Jun 13].

18. Gasser O, Schifferli JA. 2004. Activated polymorphonuclear neutrophils disseminate anti-inflammatory microparticles by ectocytosis. Blood 104(8):2543–2548 [cited 2022 Jun 18].

19. Alahdal M, Zhang H, Huang R, et al. [date unknown]. Potential efficacy of dendritic cell immunomodulation in the treatment of osteoarthritis. [cited 2022 Jun 18] Available from: https://academic.oup.com/rheumatology/article/60/2/507/6010470.

20. Kim J, Boys AJ, Estroff LA, Bonassar LJ. 2021. Combining TGF-β1 and Mechanical Anchoring to Enhance Collagen Fiber Formation and Alignment in Tissue-Engineered Menisci. ACS Biomaterials Science and Engineering 7(4):1608–1620 [cited 2022 Jul 23].

21. Pham TM, Frich LH, Lambertsen KL, et al. 2021. Elevation of Inflammatory Cytokines and Proteins after Intra-Articular Ankle Fracture: A Cross-Sectional

Study of 47 Ankle Fracture Patients. Mediators of Inflammation 2021 [cited 2022 Jul 23] Available from: /pmc/articles/PMC7811423/.

22. Bhatti FUR, Karydis A, Lee BS, et al. 2021. Understanding Early-Stage Posttraumatic Osteoarthritis for Future Prospects of Diagnosis: from Knee to Temporomandibular Joint. Curr Osteoporos Rep 19(2):166–174 [cited 2022 Jul 23] Available from: https://pubmed.ncbi.nlm.nih.gov/33523424/.

23. Punzi L, Galozzi P, Luisetto R, et al. 2016. Post-traumatic arthritis: overview on pathogenic mechanisms and role of inflammation. RMD Open 2(2):279 [cited 2022 Jul 23] Available from: /pmc/articles/PMC5013366/.

24. Reuther KE, Sarver JJ, Schultz SM, et al. 2012. Glenoid Cartilage Mechanical Properties Decrease after Rotator Cuff Tears in a Rat Model. Journal of Orthopaedic Research 30(9):1435 [cited 2022 Jul 23] Available from: /pmc/articles/PMC3374903/.

25. Guo JB, Liang T, Che YJ, et al. 2020. Structure and mechanical properties of high-weight-bearing and low-weight-bearing areas of hip cartilage at the micro- And nano-levels. BMC Musculoskeletal Disorders 21(1):1–9 [cited 2022 Jul 23] Available from: https://bmcmusculoskeletdisord.biomedcentral.com/articles/10.1186/s12891-020-03468-y.

26. Mitchell W, Ng E, Tamucci J, et al. 2019. Molecular Mechanism of Action of Mitochondrial Therapeutic SS-31 (Elamipretide): Membrane Interactions and Effects on Surface Electrostatics.31.

27. Hartung T. 2008. Thoughts on limitations of animal models. Parkinsonism &

Related Disorders 14(SUPPL.2):S81–S83 [cited 2022 Jul 23].

28. Simon F, Oberhuber A, Schelzig H. 2015. Advantages and Disadvantages of Different Animal Models for Studying Ischemia/Reperfusion Injury of the Spinal Cord. European Journal of Vascular and Endovascular Surgery 49(6):744 [cited 2022 Jul 23] Available from: http://www.ejves.com/article/S1078588415001938/fulltext.

29. Oo WM, Hunter DJ. 2022. Repurposed and investigational disease-modifying drugs in osteoarthritis (DMOADs). Ther Adv Musculoskelet Dis 14:1759720X2210902 [cited 2022 Jul 23] Available from: https://pubmed.ncbi.nlm.nih.gov/35619876/.

30. Riegger J, Brenner RE. 2020. Pathomechanisms of posttraumatic osteoarthritis: Chondrocyte behavior and fate in a precarious environment. International Journal of Molecular Sciences 21(5).

31. Bartell LR, Fortier LA, Bonassar LJ, et al. 2019. Mitoprotective therapy prevents rapid, strain-dependent mitochondrial dysfunction after articular cartilage injury. Journal of Orthopaedic Research (December):1–11 Available from: http://dx.doi.org/10.1002/jor.24567.

32. Delco ML, Bonnevie ED, Szeto HS, et al. 2018. Mitoprotective therapy preserves chondrocyte viability and prevents cartilage degeneration in an ex vivo model of posttraumatic osteoarthritis. Journal of Orthopaedic Research .

33. Goodwin W, McCabe D, Sauter E, et al. 2010. Rotenone prevents impact-induced chondrocyte death. J Orthop Res 28(8):1057–1063 [cited 2022 Jul 23] Available from: https://pubmed.ncbi.nlm.nih.gov/20108345/.